

# **Statistical thermodynamics of ordered intermetallic compounds containing point defects**

Von der Fakultät Chemie der Universität Stuttgart  
zur Erlangung der Würde eines Doktors der  
Naturwissenschaften (Dr. rer. nat) genehmigte Abhandlung

Vorgelegt von  
**Jutta Breuer**  
aus Münster/ Westf.

Hauptberichter: Prof. Dr. Ir. E.J. Mittemeijer  
Mitberichter: Prof. Dr. H.-E. Schaefer

Tag der mündlichen Prüfung: 4. Juli 2001

Institut für Metallkunde der Universität Stuttgart  
Max-Planck-Institut für Metallforschung Stuttgart

2001



# *Abstract*

The relationship between point defect properties and thermodynamic data of ordered intermetallic compounds can be described quantitatively by statistical thermodynamic models of the Bragg-Williams type. From thermodynamic data as functions of the composition and, if available of the temperature, enthalpy and entropy parameters can be calculated that characterize the interaction between pairs of atoms.

In the present work it is shown that the B2-phases NiAl, CoAl and (Ni,Co)Al can be described by the triple defect model based on such kind of model.

Compared with other statistical thermodynamic methods (Wagner-Schottky approach, ab initio electron theory based approach) the Bragg-Williams formalism is an easy applicable method that- proper use supposed- leads to accurate predictions concerning thermodynamic as well as defect properties.

The enthalpy of formation of the binary phase B2-Fe<sub>1-x</sub>Al<sub>x</sub> and the ternary phase B2-(Ni,Fe)<sub>1-x</sub>Al<sub>x</sub> were measured by isoperibolic solution calorimetry at 1073 K with an accuracy of about 1%. The enthalpy of formation of B2-FeAl is most negative for the composition Fe<sub>0.50</sub>Al<sub>0.50</sub> ( $-36.29 \text{ kJ/mol}$ ). Compounds with Al contents less than about 40 at.% show a deviation from a linear dependence of the enthalpy of formation with composition that prevails for Al contents larger than 40 at.% Upon replacing Fe by Ni while maintaining a constant Al content, the enthalpy of formation of B2- (Fe,Ni)Al compounds becomes more negative. With decreasing Al content and for a constant Fe/Ni ratio the enthalpy of formation of the ternary phase becomes less negative.



# Table of Contents

<b>1</b>	<b>Intermetallic compounds: thermodynamics and point defects</b>	<b>1</b>
1.1	Introduction . . . . .	3
1.2	Defects in intermetallic phases . . . . .	5
1.3	Thermodynamic models . . . . .	6
1.4	Experimental . . . . .	6
<b>2</b>	<b>Thermodynamics of B2 intermetallic compounds with triple defects: a Bragg-Williams model for (Ni,Co)Al</b>	<b>7</b>
2.1	Introduction . . . . .	9
2.2	Thermodynamic Model . . . . .	10
2.3	Application to B2-(Ni,Co)Al . . . . .	18
2.4	Results and Discussion . . . . .	21
2.5	Conclusions . . . . .	31
<b>3</b>	<b>Thermodynamics of constitutional and thermal point defects in B2-Ni<sub>1-x</sub>Al<sub>x</sub></b>	<b>33</b>
3.1	Introduction . . . . .	35
3.2	Models for point defect formation in B2 intermetallic compounds . . . . .	36
3.3	Results . . . . .	39
3.4	Conclusions . . . . .	49
3.A	Appendix: Algorithm for fitting the model equations . . . . .	51
<b>4</b>	<b>Thermodynamics of ordering in intermetallics –A new life for pair interaction models?–</b>	<b>55</b>
4.1	Introduction . . . . .	57
4.2	Theory . . . . .	58
4.3	Applications of the Bragg-Williams method . . . . .	66
4.4	Comparison: Wagner-Schottky, Bragg-Williams and ab-initio methods . . . . .	72
4.5	Conclusions . . . . .	73
<b>5</b>	<b>Enthalpy of formation of B2-Fe<sub>1-x</sub>Al<sub>x</sub> and B2-(Ni,Fe)<sub>1-x</sub>Al<sub>x</sub></b>	<b>75</b>
5.1	Introduction . . . . .	77
5.2	Experimental . . . . .	77
5.3	Results and Discussion . . . . .	79
5.4	Conclusions . . . . .	88
<b>6</b>	<b>Kurzfassung der Dissertation in deutscher Sprache</b>	<b>91</b>
	<b>References</b>	<b>105</b>
	<b>Curriculum Vitae</b>	<b>111</b>



---

*Intermetallic compounds:  
thermodynamics and point defects*

**Abstract:** Thermodynamic quantities are important properties for the prediction of the stability of intermetallic compounds. The internal structure of the ordered alloys is determined largely by the types and concentrations of the point defects present in the structure. This chapter provides a brief introduction into the scope of the present work. The crystal structures of the compounds studied are presented. Statistical thermodynamic models of the Bragg-Williams type are introduced as a method for quantifying relationships between thermodynamic properties and defects of intermetallic compounds.





## 1.1 Introduction

Thermodynamic properties of materials such as intermetallic phases are closely related to their internal structures; from which one may calculate the thermodynamic properties using methods of statistical thermodynamics. The preciseness of this type of calculation depends on the understanding of the alloy constitution and the relative complexity of the alloy systems [1]. In view of the practical needs for alloy thermodynamic data in predicting the stabilities of these alloys under a given environment or the appearance of intermediate phases in binary and multicomponent alloy systems, it is important to develop theoretical models on the basis of alloy structures for calculating the thermodynamic properties as a function of the composition and temperature. The primary objective of the present work is to contribute to such efforts, i.e. to investigate the relationship between thermodynamic properties and the internal structure of the alloys.

When two metallic elements are brought together, they tend to form random solid solutions at high temperatures due to the contribution of the entropy term. The higher the temperature, the more important the entropy contribution is since  $G = H - TS$ , where  $G$ ,  $H$  and  $S$  are the Gibbs free energy, enthalpy and entropy, respectively, while  $T$  is the absolute temperature. Although both  $H$  and  $S$  increase with temperature, the product  $TS$  increases more rapidly. In fact, the stabilities of many intermediate phases at high temperatures are often dominated by the entropy term. With decreasing temperature, many solid solutions separate into two phases when there is repulsion between unlike atoms, i.e. endothermic enthalpy of formation. On the other hand, many other solid solutions become ordered at low temperatures and are often referred to in the literature as superlattice alloys when there is strong attraction between unlike atoms, i.e. exothermic enthalpy of formation. As temperature approaches absolute zero, perfect order of such solid solutions becomes possible since the enthalpy term controls the stability of this phase under this condition.

Three of the most common superlattices occurring in binary intermetallic phases are the B2 type (or CsCl type), the L1<sub>0</sub> type (or AuCuI type) and the L1<sub>2</sub> type (or Au<sub>3</sub>CuI type). As shown in Figure 1.1 (a), the disordered structure of the B2-type consists of two identical lattice points, one at the corner position and the second at the body-centered position. On the average, each lattice point represents 50 % of an A and 50 % of a B atom. The structure has the symmetry of a body-centered cubic A2 type lattice. On the other hand the ordered structure as shown in Figure 1.1 (b) also has two atoms per unit cell with one kind (say, B atom) occupying the body-centered position and the other (say, A atom) occupying the corner position. The symmetry is no longer of body-centered cubic but one of simple cubic with each lattice point associated with two different atoms (B2 type). The structure may also be considered as consisting of two simple cubic sublattices interpenetrating each other. The relationship of the L1<sub>2</sub> type (ordered) to the A1 type (disordered) structure as shown in Figs. 1.1 (c) and (d) is

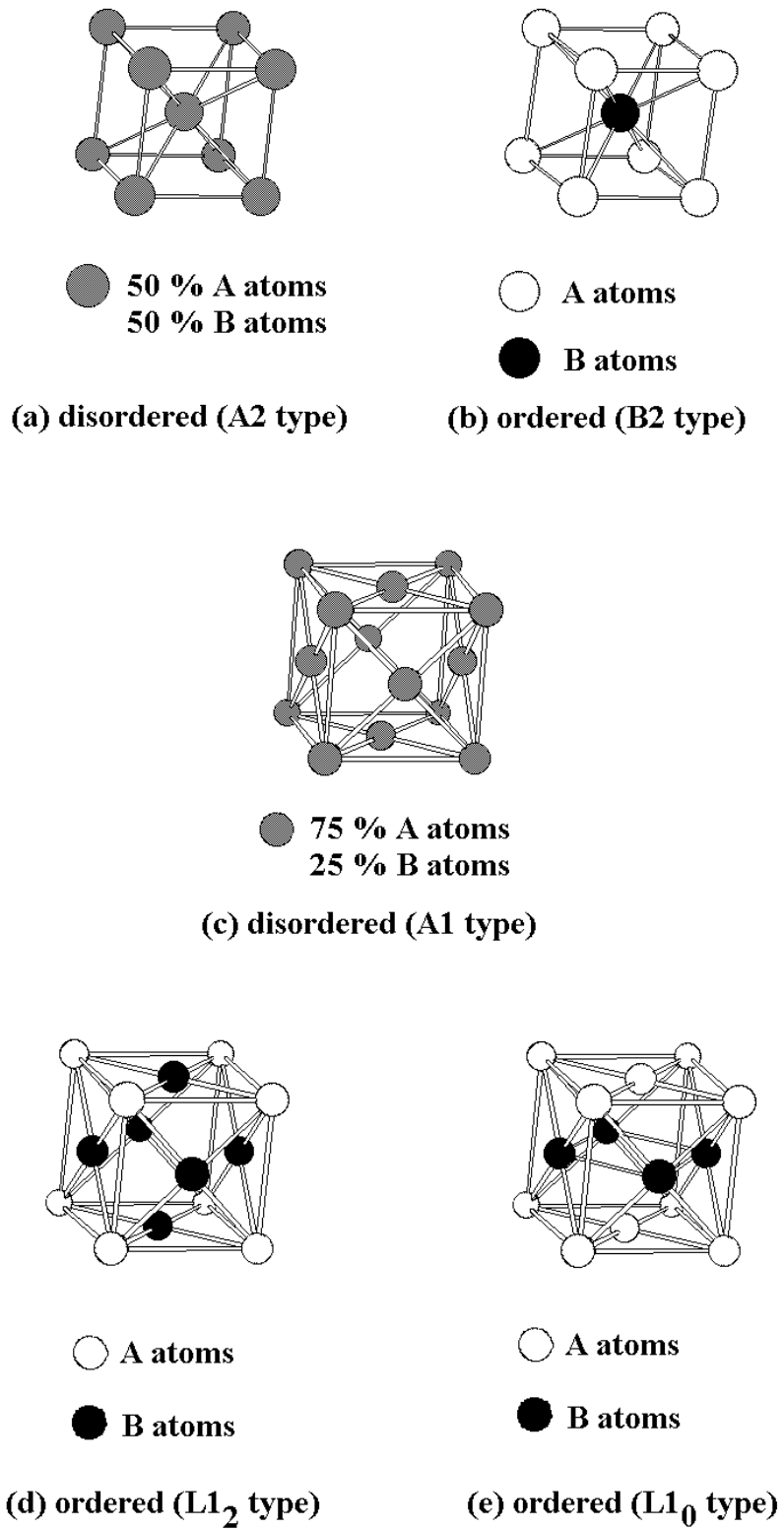


Figure 1.1: Structures of three common superlattices in binary intermetallic phases and their corresponding disordered structures.

similar to that of B2 type to the A2 type. The only difference is in the latter case; the ratio of A atoms to B atoms is 3:1 instead of 1:1. Accordingly, in the disordered state (A1 type), each lattice point on the average represents 75 % of an A atom and 25 % of a B atom, retaining the symmetry of a face-centered cubic lattice. On the other hand, in the ordered state, all A atoms are located on the corner positions while all B atoms are located on the face-centered positions. The symmetry again becomes one of simple cubic having four atoms associated with each lattice point. The face-centered tetragonal L1<sub>0</sub> type (AuCuI type) superlattice as shown in Figure 1.1 (e) is also related to the A1 type lattice. However, in this case the ratio of A to B atoms is 1:1 with the two different kinds of atoms occupying the alternate (001) layers, resulting in a tetragonal distortion of the lattice.

From the foregoing discussion, it is obvious that perfectly ordered structures are possible only at the simple atomic ratios of 1:1 or 3:1 for the three superlattices considered. Deviations from the simple atomic ratios will result in the formation of lattice disorder introduced by point defect formation.

## 1.2 Defects in intermetallic phases

The overall amount of defects is the sum of the numbers of defects caused by any finite temperature and by the deviation from the stoichiometric composition. Although these are two different variations from the perfectly ordered structure, the defects created are comprised of the same defect types. Considering a binary intermetallic phase, A<sub>1</sub>B<sub>1/2</sub>, where the A atoms regularly occupy the  $\alpha$  sublattice and the B atoms regularly occupy the  $\beta$  sublattice, six mechanisms of defect formation may occur:

1. substitution of B atoms on the  $\alpha$  sublattice (so called B antistructure atoms)
2. substitution of A atoms on the  $\beta$  sublattice (so called A antistructure atoms)
3. creation of vacancies on the  $\alpha$  sublattice
4. creation of vacancies on the  $\beta$  sublattice
5. formation of A atom interstitials
6. formation of B atom interstitials.

There is no direct evidence that interstitials are present in intermetallic compounds, so the formation of interstitials (mechanisms 5 and 6) can be dismissed for the intermetallic compounds considered.

Compared with pure metals the defect formation in intermetallic compounds is much more complex. Since the overall ordered structure, i.e. the homogeneity is retained to high temperatures at even large deviations from the stoichiometric composition, defects formed out of more than one of the mechanisms listed above are introduced. This was noticed first by WASILEWSKI [2] and can easily be understood (see

e.g. [3]): consider as an example the ordered stoichiometric B2-compound AB and suppose for the moment that vacancies can exclusively be created on the  $\alpha$  sublattice. Then, as a result, a surface layer exclusively built by A atoms would be generated and the bulk material would consist of material with a smaller A concentration, i.e. the homogeneity of the compound would be destroyed. In principle, the homogeneity could be maintained by generating an equal number of vacancies on the  $\beta$  sublattice. This would then create "pairs" of A and B atoms at the surface. If the formation of vacancies on the  $\beta$  sublattice is- because of physical reasons (e.g. atom size difference)-unlikely, the homogeneity of the compound may be maintained by the introduction of A antistructure atoms on the  $\beta$  sublattice. This leads to the formation of so-called triple defects, since from simple statistics one can conclude that one A antistructure atom on the  $\beta$  sublattice has to be balanced by two vacancies on the  $\alpha$  sublattice, thus "the triple defect" is created [2]. Applying experimental as well as theoretical methods involved in the determination of defect concentrations in intermetallic compounds one has to be aware of the discussed complexity of the defects found in the compounds. Otherwise, misinterpretations of the obtained results cannot be avoided [3].

### 1.3 Thermodynamic models

In 1931, WAGNER AND SCHOTTKY formulated the basic thermodynamic framework for deriving thermodynamic relationships for ordered alloys at finite temperature and/or non-stoichiometric compositions in terms of lattice disorder [4] based on the consideration of the single species (i.e. atoms or vacancies) found in the alloys. The other classical study in this context was published by BRAGG AND WILLIAMS in 1934 who considered the interactions between pairs of species for the formulation of the thermodynamic model [5]. Employing a combination of the ab initio electron theory with statistical mechanics, the calculation of defect properties in intermetallic compounds became possible in recent years (see, e.g [6]).

The present study is devoted to the utilization of Bragg-Williams type models. The proposed treatment and the obtained results will be described in considerable details in the individual section (see Chapters 2, 3 and 4).

### 1.4 Experimental

An important input parameter for the model calculations performed in the present study are enthalpy of formation data of high accuracy. For the phases B2-FeAl and B2-(Fe,Ni)Al the enthalpy of formation as function of the composition were measured with an isoperibolic differential solution calorimeter in this work (see Chapter 5).

# *Thermodynamics of B2 intermetallic compounds with triple defects: a Bragg-Williams model for (Ni,Co)Al*

*J. Breuer, F. Sommer and E. J. Mittemeijer*

**Abstract:** Applying the Bragg-Williams approximation, a pair interaction model has been developed for describing the composition and temperature dependence of thermodynamic properties of ternary intermetallic B2 phases. Taking the activities and the integral enthalpies of formation as input data, values for the enthalpy and the entropy of bonds between atoms have been obtained. An analytical expression has been derived for the dependence of the concentration of point defects (vacancies and antistructure atoms) on composition and temperature. The model has been applied successfully to the available experimental data for the Ni-Al, Co-Al and Ni-Co-Al systems. It has been shown that the values calculated accordingly for the effective enthalpy (and entropy) of formation of vacancies agree well with those from experimental observations and theoretical ab initio calculations.



## 2.1 Introduction

A number of models have been proposed for calculating the thermodynamic properties of intermetallics as a function of composition and temperature (e.g. see [7] and references therein). Models based on pair-interactions of atoms, for example according to the Wagner-Schottky [4, 8] or the Bragg-Williams [5] approaches, provide such explicit or implicit descriptions for these thermodynamic properties. By fitting these expressions to experimental data values for the model parameters, i.e. the pair-interaction parameters, can be determined. In this way conclusions can be drawn concerning, for example, the occurrence of certain types of defects in the compounds considered [9].

Among the intermetallic compounds, alloys with B2 (CsCl) crystal structure, as holds for aluminides of transition metals (e.g. nickel, iron and cobalt), have attracted considerable interest because of their possible utilization in high temperature applications [10]. For B2-NiAl and B2-CoAl experimental data have been reported for the dependence on composition of the activities as well as the integral enthalpies of formation [11–14]. Yet, until now, usually only activities and *partial* enthalpies of formation normalized with respect to the values at stoichiometric composition were employed for the model calculations of the Bragg-Williams type for binary B2 compounds [7, 15]. Recently integral enthalpies of formation for ternary B2-compounds (Ni,Co)Al have been determined by our group [16]. Hence, both development and testing of statistical thermodynamical models for ternary B2 compounds has now become feasible. Departing from the previous work [7, 15, 17], here a statistical thermodynamic model is presented that (i) describes the composition dependence of thermodynamic properties of binary and, in particular, ternary B2 ordered compounds and (ii) allows direct and *simultaneous* fitting to experimental values of both the activity and the *integral* enthalpy of formation.

The present work focusses on ordered compounds of the B2 structure exhibiting so-called triple defects. Also in contrast with previous work [7, 15], here the interaction between next-nearest neighbour pairs and the vibrational entropy are incorporated in the model, that is presented in Section 2.2. Starting with the binary phases B2-NiAl and B2-CoAl, the thereby obtained values for the *binary* pair-interaction parameters are adopted in the calculations for the *ternary* system and the pair-interaction parameters specific for the ternary compounds are determined subsequently (Section 2.3). Finally, the model description is compared with available experimental data and the calculation of the composition and temperature dependence of the defect concentrations are discussed in Section 2.4.

## 2.2 Thermodynamic Model

### 2.2.1 The defect structure

Intermetallic compounds of the B2-type (CsCl) crystal structure occur in several binary systems at about equiatomic composition. In this B2 structure of the  $A_{1-x}B_x$  compound, one of the elements, say A, occupies the body-centered position of the cubic unit cell (all such sites constitute the  $\alpha$  sublattice) whereas the other element, B, occupies the corner positions (all such sites constitute the  $\beta$  sublattice). A perfectly ordered structure with all lattice sites occupied can be achieved only at the stoichiometric composition and at absolute zero. At 0 K a deviation in composition from the stoichiometric composition, while maintaining the B2-type crystal structure, is associated with the introduction of structure defects: constitutional defects. Structure defects can also be thermally activated while maintaining the composition: thermal defects. The same type of defect can be of constitutional or thermal nature. Usually, the concentration of the constitutional defects is much larger than that of the thermal defects.

Two types of point defects are relevant to ordered compounds: antistructure atoms and vacancies (see, e.g. [8]). Two common types of defect structures are the antistructure defect type and the triple defect type. In so-called antistructure defect compounds the governing defects are antistructure atoms, e.g. in the present case A atoms on the  $\beta$  sublattice and/or B atoms on the  $\alpha$  sublattice. Antistructure defect compounds form if the different atoms have approximately the same size. In so-called triple defect compounds the governing defects are antistructure atoms on the one sublattice (e.g. A atoms on the  $\beta$  sublattice) and vacancies on the other sublattice (e.g. vacancies on the  $\alpha$  sublattice). In the present case the B atoms may not occur as antistructure atoms because they are larger than the A atoms. Thus an excess of A atoms involves the presence of antistructure A atoms, and an excess of B atoms involves the presence of vacancies on the  $\alpha$  sublattice. In the B2 structure equal numbers of sites are required for the  $\alpha$  and  $\beta$  sublattices. Therefore, as compared to the perfect B2 compound, the occurrence of one A antistructure atom on an additional  $\beta$  sublattice site has to be balanced by the introduction of two A vacancies (one at the  $\alpha$  sublattice site left by the A atom now on the  $\beta$  sublattice and one generated as an additional, balancing  $\alpha$  sublattice site): such a combination of defects that maintains the composition is called triple defect which is a thermal defect [2].

In nature, also ternary B2 phases occur. A ternary B2 compound  $(A,C)_{1-x}B_x$  consists of, ideally, A and C atoms on the  $\alpha$  sublattice and B atoms on the  $\beta$  sublattice. The defect structure of ternary B2 compounds is the same as for the binary case discussed above: to compensate deviations from the stoichiometric composition  $(A,C)_{1/2}B_{1/2}$  constitutional defects occur and thermally activated defects exist as well.



### 2.2.2 Definitions and basic assumptions

Considering a ternary B2 compound,  $(A,C)_{1-x}B_x$ , the following definitions and assumptions are used (see also Ref. [17]).

1. The total numbers of A, B and C atoms in the crystal are  $N_A$ ,  $N_B$  and  $N_C$ , respectively.  $N$  denotes the constant total number of atoms (here one mole of atoms is considered, so  $N = \text{Avogadro's number}$ ):  $N \equiv N_A + N_B + N_C$ .
2. The only defects considered are A and C atoms on the  $\beta$  sublattice (numbers:  $N_A^\beta$ ,  $N_C^\beta$ ) and vacancies on the  $\alpha$  sublattice (number:  $N_\square^\alpha$ ). The number of vacancies on the  $\beta$  sublattice ( $N_\square^\beta$ ) and the number of B atoms on the  $\alpha$  sublattice ( $N_B^\alpha$ ) are taken to be zero:  $N_\square^\beta = 0$ ,  $N_B^\alpha = 0$ .
3. The total concentration of vacancies is defined as  $z \equiv N_\square/N = N_\square^\alpha/N$ .
4. The crystal consists of an equal number of  $\alpha$  and  $\beta$  sublattice sites. In the ideal crystal (stoichiometric composition at 0K) all A and C atoms occupy all  $\alpha$  sublattice sites while all B atoms occupy all  $\beta$  sublattice sites. The total number of sites  $N_S$ ,  $N_S = N + N_\square$ , is variable.
5. The probability of forming antistructure defects is the same for A and C atoms.
6. The overall composition of the ternary system is specified by two composition variables  $\chi = N_B/N - \frac{1}{2}$  and  $y = N_A/(N_A + N_C)$ .
7. For small deviations from the stoichiometric composition the concentration of defects is small. The defects are randomly distributed and do not interact. Therefore, enthalpy and entropy contributions containing  $z$  and/or  $\chi$  in the second or higher power are neglected. The approximation  $1/(1+z) \approx 1-z$  is used.

The numbers of atoms and vacancies on the  $\alpha$  and  $\beta$  sublattices can be expressed in terms of  $N$ ,  $y$ ,  $z$  and  $\chi$ ; see the expressions gathered in Table 2.1.

Table 2.1: Numbers of atoms and vacancies on the  $\alpha$ - and  $\beta$ -sublattice.

	$\alpha$ -sites	$\beta$ -sites	total number of sites
A atoms	$N_A^\alpha = \frac{N}{2}y(1-z)$	$N_A^\beta = \frac{N}{2}y(z-2\chi)$	$N_A = \frac{N}{2}y(1-2\chi)$
C atoms	$N_C^\alpha = \frac{N}{2}(1-y)(1-z)$	$N_C^\beta = \frac{N}{2}(1-y)(z-2\chi)$	$N_C = \frac{N}{2}(1-y)(1-2\chi)$
B atoms	$N_B^\alpha = 0$	$N_B^\beta = \frac{N}{2}(1+2\chi)$	$N_B = \frac{N}{2}(1+2\chi)$
Vacancies	$N_\square^\alpha = \frac{N}{2}(2z)$	$N_\square^\beta = 0$	$N_\square = \frac{N}{2}(2z)$
Total sites	$N^\alpha = \frac{N_S}{2} = \frac{N}{2}(1+z)$	$N^\beta = \frac{N_S}{2} = \frac{N}{2}(1+z)$	$N_S = N(1+z)$

### 2.2.3 Gibbs energy

To formulate an expression for the Gibbs energy  $G$ , the concept of the canonical ensemble, where the pressure  $p$ , the temperature  $T$  and the number of atoms are kept constant in the treatment of equilibrium, is used. In the current approach the number of atoms (including vacancies as "atoms") is not fixed (see [4] and basic assumption (4)). Yet, this approach yields almost identical results to the results obtained from the use of the formalism of a grand canonical ensemble where the volume  $V$ ,  $T$  and the chemical potentials of the constituent atoms are kept constant (see e.g. [18, 19]).

On the basis of the Bragg-Williams approximation, the interaction of (only) pairs of atoms is considered (a vacancy is considered as an "atom"). The interaction enthalpy and the vibrational entropy of each type of bond between pairs of atoms is assumed to be independent of composition and temperature.

For the enthalpy term, nearest- and next-nearest-neighbour interactions are considered. The general expression for the total enthalpy then is

$$H = \sum_{ij} n_{ij} h_{ij} + \sum_{ij} n'_{ij} h'_{ij}, \quad (2.1)$$

where  $n_{ij}$  is the number of nearest-neighbour pairs  $i - j$  and  $h_{ij}$  is the corresponding interaction enthalpy ( $i$  and  $j$  can be A, B or C atoms, or vacancies  $\square$ ), and the analogous terms for the next-nearest-neighbour pairs are represented by  $n'_{ij}$  and  $h'_{ij}$ . On the basis of the relations given in Table 2.1 for the numbers of atoms and vacancies on the  $\alpha$  and  $\beta$  sublattices and taking into consideration the coordination numbers  $Z = 8$  for the nearest-neighbour pairs and  $Z' = 6$  for the next-nearest-neighbour pairs in the B2 structure, the following expression is obtained for the enthalpy  $H$ :

$$\begin{aligned} H = & 4N[y^2(z - 2\chi)h_{AA} + (1 - y)^2(z - 2\chi)h_{CC} + \\ & + y(1 - 2z + 2\chi)h_{AB} + 2y(1 - y)(z - 2\chi)h_{AC} + \\ & + (1 - y)(1 - 2z + 2\chi)h_{BC} + 2zh_{B\square}] + \\ & + 3N[y^2(1 - 3z)h'_{AA} + (1 - z + 4\chi)h'_{BB} + (1 - y)^2(1 - 3z)h'_{CC} + \\ & + y(z - 2\chi)h'_{AB} + y(1 - y)(1 - 3z)h'_{AC} + (1 - y)(z - 2\chi)h'_{BC} + \\ & + 2zyh'_{A\square} + 2z(1 - y)h'_{C\square}] \end{aligned} \quad (2.2)$$

The entropy consists of the configurational entropy  $S^c$  and the vibrational entropy  $S^v$ :

$$S = S^c + S^v \quad (2.3)$$

For the configurational entropy,  $S^c$ , a random distribution of each species on each sublattice is assumed. On the basis of the relations given in Table 2.1 for the numbers of atoms and vacancies on the  $\alpha$  and  $\beta$  sublattices, and applying Stirling's approximation

to the Boltzmann equation for the entropy, it is obtained:

$$\begin{aligned}
S^c = & \frac{R}{2} [2(1+z) \ln(1+z) - y(1-z) \ln(y(1-z)) + \\
& - (1-y)(1-z) \ln((1-y)(1-z)) + \\
& - y(z-2\chi) \ln(y(z-2\chi)) - (1-y)(z-2\chi) \ln((1-y)(z-2\chi)) + \\
& - (1+2\chi) \ln(1+2\chi) - 2z \ln(2z)], \tag{2.4}
\end{aligned}$$

where  $R = Nk$ , with  $k$  as Boltzmann's constant. Analogous to the enthalpy (see above), the total vibrational entropy is written as

$$S^v = \sum_{ij} n_{ij} s_{ij} + \sum_{ij} n'_{ij} s'_{ij}, \tag{2.5}$$

where the entropy parameters for the nearest- and next-nearest-neighbour interactions are denoted by  $s_{ij}$  and  $s'_{ij}$ , respectively. Accordingly, an expression analogous to Eq. (2.2) holds for  $S^v$ .

## 2.2.4 Equilibrium

Thermodynamic equilibrium at constant temperature and pressure requires the Gibbs energy  $G$  to be minimal. Thus the equilibrium defect concentrations at a specific temperature, pressure and overall composition can be obtained by minimizing  $G$  with respect to the defect concentration, e.g. the vacancy concentration  $z$ :

$$\left. \frac{\partial G}{\partial z} \right|_{T,p,\chi,y} = 0 \tag{2.6}$$

After substitution of the above derived expressions for  $H$  (Eq. (2.2)) and  $S$  (Eqs. (2.4) and (2.5)) in the Gibbs-Helmholtz relationship  $G = H - TS$  and applying the minimization condition according to Eq. (2.6) one obtains:

$$\begin{aligned}
& 4N[y^2 h_{AA} + (1-y)^2 h_{CC} - 2y h_{AB} + 2y(1-y) h_{AC} - 2(1-y) h_{BC} + \\
& \quad + 2h_{\square B}] + \\
& + 3N[-3y^2 h'_{AA} - h'_{BB} - 3(1-y)^2 h'_{CC} + \\
& \quad + y h'_{AB} - 3y(1-y) h'_{AC} + (1-y) h'_{BC} + 2y h'_{A\square} + 2(1-y) h'_{C\square}] + \\
& - 4NT[y^2 s_{AA} + (1-y)^2 s_{CC} - 2y s_{AB} + 2y(1-y) s_{AC} - 2(1-y) s_{BC} + \\
& \quad + 2s_{\square B}] + \\
& - 3NT[-3y^2 s'_{AA} - s'_{BB} - 3(1-y)^2 s'_{CC} + \\
& \quad + y s'_{AB} - 3y(1-y) s'_{AC} + (1-y) s'_{BC} + 2y s'_{A\square} + 2(1-y) s'_{C\square}] \\
& = \frac{RT}{2} \ln \frac{(1+z)^2(1-z)}{(z-2\chi)(2z)^2}, \tag{2.7a}
\end{aligned}$$

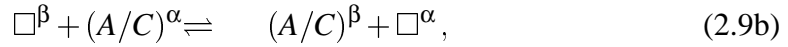
which in short notation can be given as

$$4N[h] + 3N[h'] - 4NT[s] - 3NT[s'] = \frac{RT}{2} \ln \frac{(1+z)^2(1-z)}{(z-2\chi)(2z)^2}, \quad (2.7b)$$

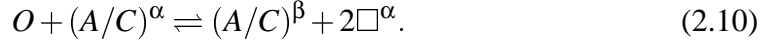
where  $h$ ,  $h'$ ,  $s$  and  $s'$  represent the terms between brackets in Eq. (2.7a). Using the expressions given in Table 2.1 Eq. (2.7b) may be rewritten as

$$\begin{aligned} \frac{\left(\frac{N_{\square}^{\alpha}}{N^{\alpha}}\right)^2 \left(\frac{N_{A+C}^{\beta}}{N^{\beta}}\right)}{\left(\frac{N_{A+C}^{\alpha}}{N^{\alpha}}\right)} &= \frac{(z-2\chi)(2z)^2}{(1+z)^2(1-z)} \\ &= \exp\left(-\frac{1}{kT}(8[h] + 6[h']) + \frac{1}{k}(8[s] + 6[s'])\right) \end{aligned} \quad (2.8)$$

The term in the denominator of the left-hand side of Eq. (2.8) represents the concentration of the 'normal' (i.e. not antistructure) A/C atoms; the first and second term in the numerator are the concentrations of vacancies and antistructure A/C atoms, respectively. The same results can be obtained by application of the mass action law for the sum of the two defect reactions (cf. [20]):



where the notation  $(A/C)^{\alpha}$  represents an A or C atom on the  $\alpha$  sublattice, etc. Equilibrium (2.9a) describes the formation of two vacancies, e.g. at the surface. In triple-defect type B2 intermetallic compounds the vacancy on the  $\beta$  sublattice is unstable and it will "react" with a neighbouring A or C atom to form an antistructure A or C atom and a vacancy on the  $\alpha$  sublattice (see equilibrium (2.9b)). The overall defect reaction, that is the formation of a triple defect, is given by the sum of equilibria (2.9a) and (2.9b):



Now, apparently, the equilibrium constant  $K$  of equilibrium (2.10) is given by the left-hand side of Eq. (2.8). Then using van't Hoff's equation,  $kT \ln K = -\Delta G$ , where  $\Delta G$  denotes the difference in Gibbs energy between products and reactants, inspection of Eq. (2.8) leads to the conclusion that

$$h_t \equiv 8[h] + 6[h'] \quad (2.11a)$$

can be interpreted as the enthalpy of formation of one triple defect and that

$$s_t \equiv 8[s] + 6[s'] \quad (2.11b)$$

can be interpreted as the entropy of formation of one triple defect.

The expressions for  $h_t$  and  $s_t$  can be further rewritten in terms of *differences* of the energy and entropy parameters as shown for a binary B2 compound exhibiting triple defects considering next nearest neighbour interactions [9]. Therefore,  $h_t$  and  $s_t$  are independent of the reference state of the parameters  $h_{ij}$ ,  $h'_{ij}$ ,  $s_{ij}$  and  $s'_{ij}$ .

## 2.2.5 Composition and temperature dependences of the defect concentrations

The model allows the description of the variation of the defect concentrations with composition and temperature. The condition for thermodynamic equilibrium (Eq. (2.7b)) provides an implicit expression for the vacancy concentration  $z$ . The equation can be numerically solved with respect to  $z$  for known parameters  $h_{ij}$ ,  $h'_{ij}$ ,  $s_{ij}$  and  $s'_{ij}$  (see section 4.3). For special cases (the stoichiometric compound and for small  $|\chi|$ ), the right-hand side of Eq. (2.7b) can be approximated yielding explicit expressions for  $z$  (see what follows).

### 2.2.5.1 Stoichiometric compounds

For equiatomic compositions (where  $\chi = 0$  and  $z \ll 1$ ) the right hand side of Eq. (2.7b) can be approximated by

$$\frac{RT}{2} \ln \frac{(1+z)^2(1-z)}{(z-2\chi)(2z)^2} \approx \frac{RT}{2} \ln \frac{1}{4z^3}. \quad (2.12)$$

Applying this approximation to the condition for the thermodynamic equilibrium (Eq. (2.7b)) and solving for  $z$  at  $\chi = 0$  yields:

$$z|_{p,\chi=0} = \exp\left(\frac{s_{\square}^{\chi=0}}{k}\right) \exp\left(\frac{-h_{\square}^{\chi=0}}{kT}\right), \quad (2.13)$$

where

$$h_{\square}^{\chi=0} = \frac{8}{3}[h] + \frac{6}{3}[h'] = \frac{1}{3}h_t \quad (2.14a)$$

and

$$s_{\square}^{\chi=0} = \frac{8}{3}[s] + \frac{6}{3}[s'] - \frac{2}{3}k \ln 2 = \frac{1}{3}s_t - \frac{2}{3}k \ln 2. \quad (2.14b)$$

The quantities  $h_{\square}^{\chi=0}$  and  $s_{\square}^{\chi=0}$  can be conceived as an effective enthalpy and an effective entropy of formation of one vacancy. The notion "effective" is used since in contrast to pure metals in intermetallic compounds vacancies cannot be created as the only defects (cf. Eq. (2.10) and its discussion). Note that for the stoichiometric composition ( $\chi = 0$ ) the occurring vacancies can only be of thermal nature.

### 2.2.5.2 A/C-rich compounds

For A/C-rich alloys ( $\chi < 0$ ), since the vacancy concentration is small ( $z \ll 1$ ), the following approximation holds:

$$\frac{RT}{2} \ln \frac{(1+z)^2(1-z)}{(z-2\chi)(2z)^2} \approx \frac{RT}{2} \ln \frac{1}{-2\chi(2z)^2}. \quad (2.15)$$

Inserting Eq. (2.15) into Eq. (2.7b) one obtains for  $z$

$$z = \exp\left(\frac{s_{\square}^{\chi < 0}}{k}\right) \exp\left(\frac{-h_{\square}^{\chi < 0}}{kT}\right) \quad (2.16)$$

with

$$h_{\square}^{\chi < 0} = \frac{8}{2}[h] + \frac{6}{2}[h'] = \frac{3}{2}h_{\square}^{\chi=0} = \frac{1}{2}h_t \quad (2.17a)$$

and

$$s_{\square}^{\chi < 0} = \frac{8}{2}[s] + \frac{6}{2}[s'] + k \ln\left(\frac{1}{2} \sqrt{-\frac{1}{2\chi}}\right) = \frac{1}{2}s_t + k \ln\left(\frac{1}{2} \sqrt{-\frac{1}{2\chi}}\right). \quad (2.17b)$$

Analogous to the discussion of Eqs. (2.14a) and (2.14b) above,  $h_{\square}^{\chi < 0}$  and  $s_{\square}^{\chi < 0}$  can be conceived as an effective enthalpy and an effective entropy of formation of one vacancy. Note that for A/C-rich alloys ( $\chi < 0$ ) the occurring vacancies can only be of thermal nature.

### 2.2.5.3 B-rich compounds

For B-rich alloys ( $\chi > 0$ ) the condition  $z \ll 1$  is not generally valid. As compared to the case  $\chi < 0$ , the concentration of antistructure atoms is small and it follows  $z \approx 2\chi$  (because  $z - 2\chi = 0$  for  $\chi = 0.5$ , cf. expressions for the concentration of antistructure atoms in Table 2.1), which gives

$$\frac{RT}{2} \ln \frac{(1+z)^2(1-z)}{(z-2\chi)(2z)^2} \approx \frac{RT}{2} \ln \frac{(1+2\chi)^2(1-2\chi)}{(z-2\chi)(4\chi)^2}. \quad (2.18)$$

Inserting Eq. (2.18) into Eq. (2.7b) the following expression for  $z$  results

$$z = \frac{(1+2\chi)^2(1-2\chi)}{(4\chi)^2} \cdot \exp\left(-\frac{2}{RT}(4N[h] + 3N[h'] - 4NT[s] - 3NT[s'])\right) + 2\chi. \quad (2.19)$$

Note that for B-rich alloys ( $\chi > 0$ ) at  $T > 0$  K the occurring vacancies are partly of thermal and partly of constitutional nature. The additional term  $2\chi$  in Eq. (2.19) represents the fraction of constitutional vacancies. Considering only the thermally activated vacancies, the concentration of such vacancies for B-rich compounds is (cf. Eq. (2.19))

$$z = \exp\left(\frac{s_{\square}^{\chi > 0}}{k}\right) \exp\left(\frac{-h_{\square}^{\chi > 0}}{kT}\right) \quad (2.20)$$

where

$$h_{\square}^{\chi > 0} = 8[h] + 6[h'] = 3h_{\square}^{\chi=0} = h_t \quad (2.21a)$$

and

$$\begin{aligned} s_{\square}^{\chi>0} &= 8[s] + 6[s'] + k \ln\left(\frac{(1+2\chi)^2(1-2\chi)}{(4\chi)^2}\right) \\ &= s_t + k \ln\left(\frac{(1+2\chi)^2(1-2\chi)}{(4\chi)^2}\right). \end{aligned} \quad (2.21b)$$

The quantities  $h_{\square}^{\chi>0}$  and  $s_{\square}^{\chi>0}$  can be conceived as an effective enthalpy and an effective entropy of formation of one thermal vacancy (cf. discussion of Eqs. (2.14a), (2.14b) and (2.17a), (2.17b)).

## 2.2.6 Activities

It is possible to describe the activities of all components in terms of the present model. In the literature activity data have been reported mostly for component B. Therefore, in the following, an equation is derived for the evaluation of the thermodynamic activity of component B. For the ternary (A,C)<sub>1-x</sub>B<sub>x</sub> alloy it holds for the activity of component B,  $a_B$ , expressed in terms of the composition variables  $\chi$  and  $y$  [17]

$$RT \ln a_B = G + \left(\frac{1}{2} - \chi\right) \frac{dG}{d\chi} \Big|_y - G_B^0, \quad (2.22)$$

where  $G_B^0$  is the Gibbs energy of pure B in its reference state (cf. Section 2.2.7). Inserting the expression for the Gibbs energy (using  $H$  and  $S$  as given in Section 2.3) it follows

$$\begin{aligned} \ln a_B &= \frac{4}{kT} [y^2(z-1)h_{AA} + (1-y)^2(z-1)h_{CC} + 2y(1-z)h_{AB} + \\ &\quad + 2y(1-y)(z-1)h_{AC} + 2(1-y)(1-z)h_{BC} + 2zh_{B\square}] + \\ &\quad + \frac{3}{kT} [y^2(1-3z)h'_{AA} + (3-z)h'_{BB} + (1-y)^2(1-3z)h'_{CC} + \\ &\quad + y(z-1)h'_{AB} + y(1-y)(1-3z)h'_{AC} + \\ &\quad + (1-y)(z-1)h'_{BC} + 2yzh'_{A\square} + 2(1-y)zh'_{C\square}] + \\ &\quad - \frac{1}{2} [2(1+z) \ln(1+z) + (z-1) \ln(1-z) + (1-z) \ln(z-2\chi) + \\ &\quad - 2 \ln(1+2\chi) - 2z \ln(2z)] + \\ &\quad - \frac{4}{k} [y^2(z-1)s_{AA} + (1-y)^2(z-1)s_{CC} + 2y(1-z)s_{AB} + \\ &\quad + 2y(1-y)(z-1)s_{AC} + 2(1-y)(1-z)s_{BC} + 2zs_{B\square}] + \\ &\quad - \frac{3}{k} [y^2(1-3z)s'_{AA} + (3-z)s'_{BB} + (1-y)^2(1-3z)s'_{CC} + \\ &\quad + y(z-1)s'_{AB} + y(1-y)(1-3z)s'_{AC} + \\ &\quad + (1-y)(z-1)s'_{BC} + 2yzs'_{A\square} + 2(1-y)zs'_{C\square}] - \frac{NG_B^0}{kT}. \end{aligned} \quad (2.23)$$

## 2.2.7 Relation to experimental values

The relation between the total enthalpy  $H$  (see Eq. (2.2)) and the enthalpy of formation  $\Delta H$ , that can be experimentally determined (e.g. by solution calorimetry), is given by

$$\Delta H = H - [y(\frac{1}{2} - \chi)H_A + (\chi + \frac{1}{2})H_B + (1 - y)(\frac{1}{2} - \chi)H_C], \quad (2.24)$$

where  $H_i$  ( $i=A,B,C$ ) are the enthalpies per mole of the pure elements at the same temperature and pressure as pertaining to  $H$  and  $\Delta H$ . For the activity (see Eq. (2.23)), the reference state  $G_B^0$  has to be the same as the reference state for  $H_B$  (Eq. (2.24)).

Given a set of measured integral enthalpies of formation,  $\Delta H$ , and a set of measured activities  $a_B$ , both as a function of composition and at the same constant temperature and with respect to the same reference state, values for the enthalpy and entropy parameters ( $h_{ij}$ ,  $h'_{ij}$ ,  $s_{ij}$  and  $s'_{ij}$ ) can be determined from Eqs. (2.24) (after substitution of Eq. (2.2)) and (2.23) and the equilibrium condition (Eq. (2.7a)). Of course the reference state pertaining to these parameters then is the reference state taken for the experimental input data of  $a_B$  and  $\Delta H$ . The proposed and applied numerical procedure is given in Section 2.3.2.

## 2.3 Application to B2-(Ni,Co)Al

Ni and Co are chemically alike, have similar atomic volume and in the binary system Ni-Co a solid solution exists over the entire composition range between the two elements. This suggests that assumption (5) of section 2.2 holds: the amounts of nickel and cobalt as antistructure atoms on the Al sublattice in  $(\text{Ni,Co})_{1-x}\text{Al}_x$  are equal. This is also supported by a neutron diffraction study [21] pertaining to about the pseudobinary NiAl-CoAl section of the Ni-Co-Al phase diagram with an Al concentration of 50 at% which indicated that Ni and Co are randomly distributed on the  $\alpha$  sublattice.

### 2.3.1 Experimental data

All experimental data about the enthalpy of formation  $\Delta H$  and the activity  $a_{Al}$  ( $= a_B$ ) for B2-NiAl, B2-CoAl and B2-(Ni,Co)Al were used in the evaluation.

Values for the activity of aluminium,  $a_{Al}$ , in B2-NiAl were reported in [12]. For the present evaluation these data were recalculated such that they pertain to 1273 K by using the partial enthalpy values calculated from the integral enthalpy values [11] and applying the differential Gibbs-Helmholtz relationship. The correction for the systematic error in the values for the composition of the alloys in the original work [12], as noted by several authors (see e.g. [11, 15]), was executed. The thus obtained data are shown in Figure 2.1(a).

Values for the activity of aluminium in B2-CoAl were reported in [14]; the data at 1273 K are shown in Figure 2.2(a). The reference state for both sets of activity data



is liquid aluminium at 1273 K and normal pressure. The corresponding value for  $G_B^0$  for liquid aluminium at 1273 K and normal pressure (see Eqs. (2.22) and (2.23)) was taken from the SGTE table [22].

Values for the enthalpy of formation for the two binary B2-phases were reported as a function of composition at 1100 K in Refs. [11] and [13]. Using the same technique and apparatus (an isoperibolic heat-flow differential solution calorimeter), the enthalpy of formation of the B2-phase in  $(\text{Ni,Co})_{1-x}\text{Al}_x$  (for  $x_{\text{Al}}=0.42$  and  $x_{\text{Al}}=0.50$ ; at both Al contents with variable Ni (and thus Co) content, and for  $\text{Ni}_{0.30}\text{Co}_{0.15}\text{Al}_{0.55}$ ) at 1073 K was determined as well [16]. Although it was claimed in Ref. [11], [13] and [16] that the measurements were performed with the very high accuracy of about  $\pm 1\%$ , there are inconsistencies in the data reported. The enthalpy of formation of  $\text{Ni}_{0.50}\text{Al}_{0.50}$  as reported in Ref. [16] is  $0.95 \text{ kJ/mol}$  less negative than the value reported in Ref. [11]. For  $\text{Ni}_{0.45}\text{Al}_{0.55}$  a similar difference of  $0.77 \text{ kJ/mol}$  occurs [23]. In the present study the enthalpy values of the binary systems as well as those of the ternary system were used for the calculations. To counteract the above mentioned ambiguity in the experimental input data the values reported in Ref. [11] were corrected according to the average of the deviations as indicated by the data in Refs. [11] and [16], i.e.  $+0.86 \text{ kJ/mol}$  was added to every value of the enthalpy of formation of B2-NiAl reported in Ref. [11]. Likewise, for the Co-Al system,  $-0.355 \text{ kJ/mol}$  was added to every value of the enthalpy of formation of B2-CoAl reported in Ref. [13]. The discussed discrepancies in the enthalpy of formation values for both binary phases cannot be explained by the slightly different measuring temperatures at which they were obtained. A pronounced variation with temperature of the enthalpy values is not expected, as indicated by the difference in  $c_p$  (heat capacity at normal pressure) values for, e.g., B2-NiAl [24] and the pure elements [22]. This difference is about  $-6 \text{ J/(molK)}$ , and thus the difference in measuring temperature yields a difference in the enthalpy values of only about  $0.162 \text{ kJ/mol}$ . This is distinctly smaller than the values of the applied corrections (see above), and within the experimental error for the value of the enthalpy of formation. Therefore the enthalpy of formation data reported in [16] and the corrected data for B2-NiAl and B2-CoAl were taken as if measured at 1273 K (the temperature for which the  $a_{\text{Al}}$  data hold).

The values for the enthalpies of the pure elements at 1273 K and normal pressure were taken from the SGTE table [22]. Activity data for the ternary B2-phase  $(\text{Ni,Co})_{1-x}\text{Al}_x$  are not available.

## 2.3.2 Algorithm

### 2.3.2.1 Binary phases

First (simultaneous) fitting of the enthalpy and activity data of the binary phases B2-NiAl ( $y = 1$ ) and B2-CoAl ( $y = 0$ ) is performed. For the enthalpy curves Eqs. (2.2),

(2.24) and Eq. (2.7a) and for the activity curves Eq. (2.23) and Eq. (2.7a), respectively, have to be fulfilled simultaneously. Starting with an array of chosen values for the vacancy concentration  $z$  and a first guess for the parameters  $h_{ij}$ ,  $h'_{ij}$ ,  $s_{ij}$  and  $s'_{ij}$ , application of Eq. (2.7a) leads to an array of  $\chi$  values. The density of the calculated  $\chi$  values is very large as compared to the experimental  $\chi$  values. Then, selecting the  $z$  values pertaining to the experimental  $\chi$  values, values for the enthalpy of formation (Eqs. (2.2), (2.24)) and the activity (Eq. (2.23)) can be calculated. The differences between experimental and calculated values (for the  $\chi$  values equal to the experimental ones) lead to new estimates for the parameters  $h_{ij}$ ,  $h'_{ij}$ ,  $s_{ij}$  and  $s'_{ij}$ . The numerical procedure for finding the least squares difference between calculated and experimental data is based on the downhill simplex method [25].

### 2.3.2.2 Ternary phase

The routine for fitting the enthalpies of formation of the ternary phase (activity data are not available) is different from that for the binary phases since the available experimental data were measured for constant fraction of Al rather than for constant  $y$  (in section 2.3.2.1  $y = 0$  or  $y = 1$ ). Starting with an array of chosen values for the vacancy concentration  $z$  and a first guess for the additional (as compared to the binary case) parameters  $h_{AC}$ ,  $h'_{AC}$ ,  $s_{AC}$  and  $s'_{AC}$ , one has to solve, for a known value of  $\chi$  (which is set by the experimental data) Eq. (2.7a) for  $y$ . Then the procedure of comparing the sets of calculated enthalpy values and experimentally determined enthalpy values and finding values for  $h_{AC}$ ,  $h'_{AC}$ ,  $s_{AC}$  and  $s'_{AC}$  which provide the least squares difference is performed as described for the binary case.

Note that this procedure could have been applied to the binary case as well. However, it was not adopted for the binary case because of the following numerical problem that arises in the fitting and which has to be dealt with for the ternary phases as considered here ( $y \neq \text{constant}$ ). Since Eq. (2.7a) is quadratic in  $y$ , the solution for  $y$  might not be unique (i.e. if two positive roots with  $0 \leq y \leq 1$  are obtained) if the starting values for the parameters are far from the true ones. Therefore, in order to obtain acceptable first guess values for  $h_{AC}$ ,  $h'_{AC}$ ,  $s_{AC}$  and  $s'_{AC}$ , an initial fitting was performed as follows: starting with an array of chosen values for  $y$  ( $0 \leq y \leq 1$ ) and a first guess for the parameters,  $z$  values were calculated from Eq. (2.7a) using one of the approximations given by Eqs. (2.12), (2.15) and (2.18) (the choice of either Eq. (2.12), Eq. (2.15) or Eq. (2.18) is based on the value of  $\chi$ , cf. section 2.5). Because of these approximations this leads to a single value for  $z$ . Then values for the enthalpy of formation can be calculated from Eqs. (2.2) and (2.24). Optimal values for  $h_{AC}$ ,  $h'_{AC}$ ,  $s_{AC}$  and  $s'_{AC}$  are then determined by fitting. The thus obtained values for the parameters are then used in the definitive fitting as first guess values for the parameters in the procedure described above using the not approximated Eq. (2.7a).

## 2.4 Results and Discussion

### 2.4.1 Thermodynamics of NiAl and CoAl

The results of the simultaneous fitting of the enthalpy of formation and the activity of aluminium for  $\text{Ni}_{1-x}\text{Al}_x$  and  $\text{Co}_{1-x}\text{Al}_x$  are shown in Figures 2.1 and 2.2, respectively.

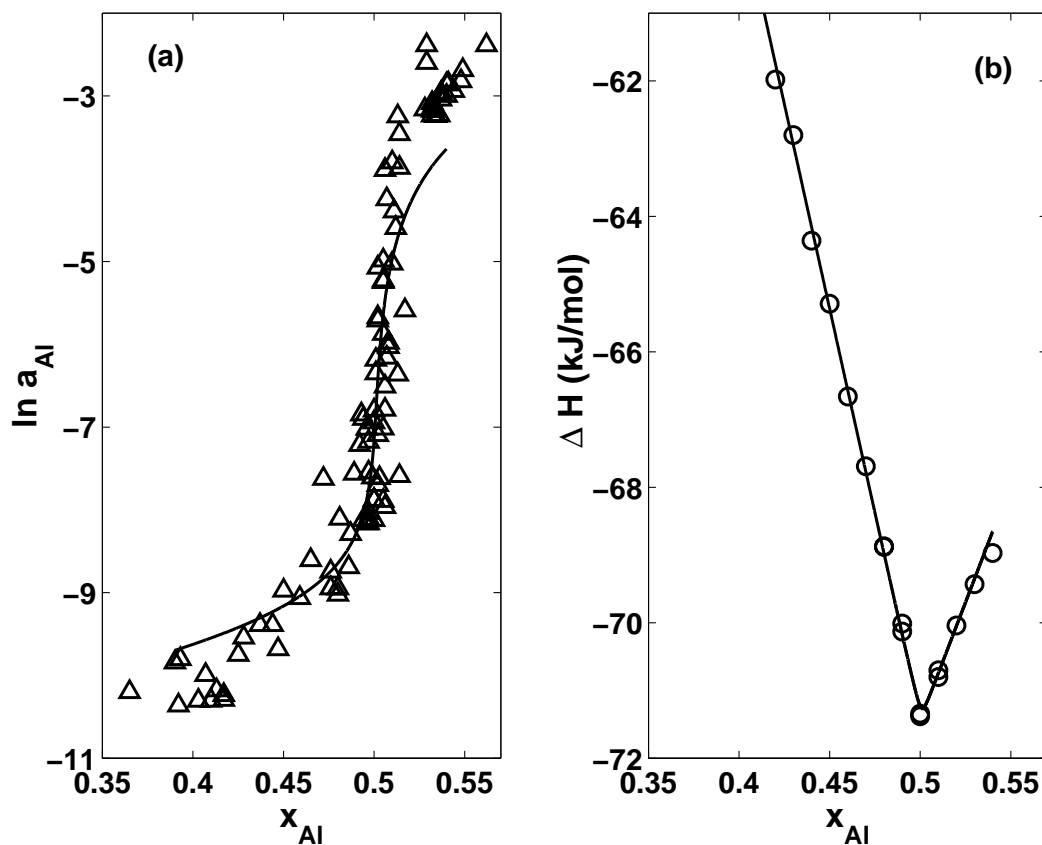


Figure 2.1:  $\text{Ni}_{1-x}\text{Al}_x$  ( $T=1273\text{ K}$ ): (a) Natural logarithm of Al-activity as function of the atomic fraction Al,  $\triangle$  rectified data from [12], — calculated with the parameters from Tables 2.2 and 2.3, (b) Enthalpy of formation as function of the atomic fraction Al,  $\circ$  corrected data from [11], — calculated with the parameters from Tables 2.2 and 2.3.

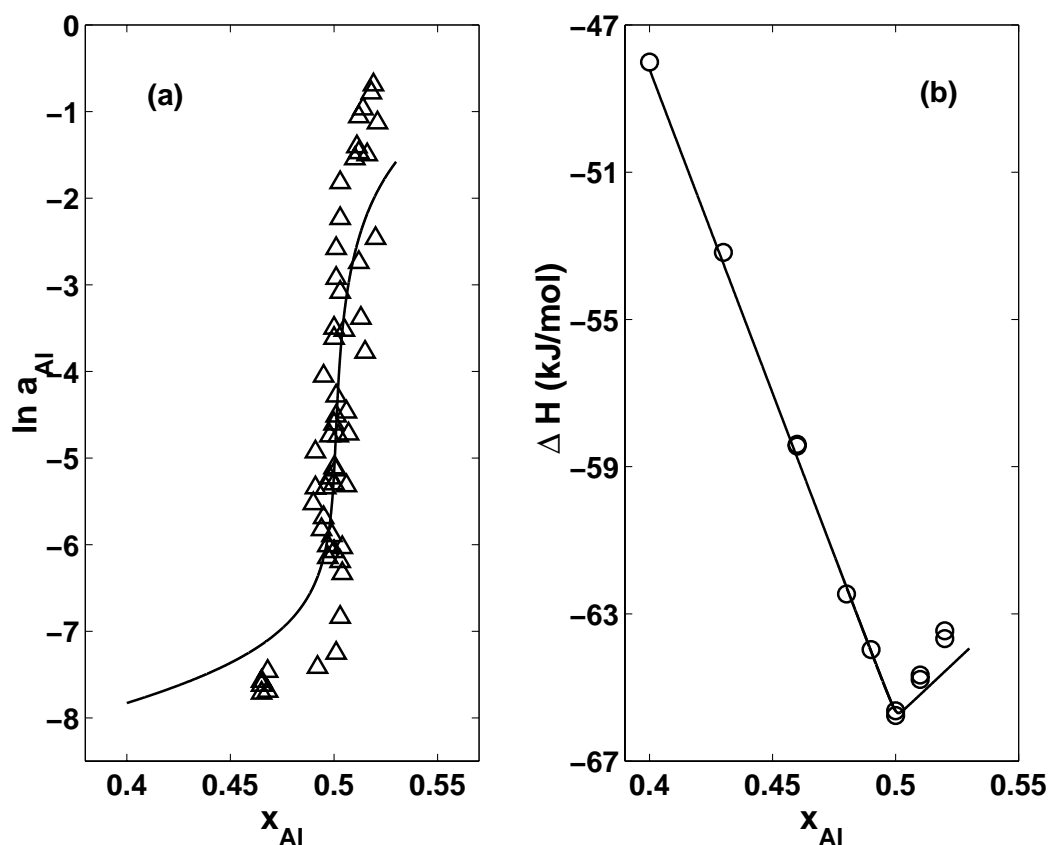


Figure 2.2:  $\text{Co}_{1-x}\text{Al}_x$  ( $T=1273$  K): (a) Natural logarithm of Al-activity as function of the atomic fraction Al,  $\Delta$  data from [14], — calculated with the parameters from Tables 2.2 and 2.3, (b) Enthalpy of formation as function of the atomic fraction Al,  $\circ$  corrected data from [13], — calculated with the parameters from Tables 2.2 and 2.3.

It was found that the enthalpy of formation and the aluminium activity can be described adequately taking into account the interaction of only nearest neighbour pairs of species for both B2-NiAl and B2-CoAl: the absolute values of the parameters for the interactions of next nearest neighbour pairs of species turned out to be small ( $Nh'_{ij} < 5 \cdot 10^{-4}$  J). The resulting values for the enthalpy parameters are shown in Table 2.2\*.

\* It is noted here that the enthalpy parameters  $h_{XAl}$  ( $X=\text{Ni}$  or  $X=\text{Co}$ ) are related to the absolute values of the enthalpy of formation of the stoichiometric compounds  $\text{Ni}_{1/2}\text{Al}_{1/2}$  and  $\text{Co}_{1/2}\text{Al}_{1/2}$ , respectively, and the enthalpy parameters  $h_{XX}$  and  $h_{\square Al}$  are related to the slopes of the enthalpy of formation vs. composition curves for  $x_{Al} < 1/2$  and  $x_{Al} > 1/2$ , respectively.

Table 2.2: Enthalpy parameters (in  $kJ/mol$ ), obtained from the simultaneous fitting of the enthalpy and activity curves of NiAl and CoAl.

	$Nh_{XX}$	$Nh_{XAl}$	$Nh_{\square Al}$
X=Ni	3.278	-9.902	0.386
X=Co	11.589	-8.480	0.659

The values obtained for the entropy parameters are given in Table 2.3<sup>†</sup>. The other entropy parameters (for next nearest neighbour interaction) have absolute values smaller than  $0.3 J/K$ .

Table 2.3: Entropy parameters (in  $J/K$ ), obtained from the simultaneous fitting of the enthalpy and activity curves of NiAl and CoAl.

	$s_{XX}$	$s_{XAl}$	$s_{\square Al}$
X=Ni	-4.451	5.585	8.373
X=Co	0.320	3.958	6.165

Enthalpy parameters of negative value contribute to the stability of the compound, whereas entropy parameters of negative value lead to destabilization. It is noted that the parameter describing the bond enthalpy of Al and a vacancy,  $h_{\square Al}$ , and the analogous parameter for the entropy,  $s_{\square Al}$ , have different values for B2-NiAl and B2-CoAl. This can be understood recognizing that the Al atom and the vacancy are surrounded by nearest neighbour Ni atoms in the case of B2-NiAl, and nearest neighbour Co atoms in the case of B2-CoAl. These different surroundings influence the absolute value of the energy of the Al-vacancy bond, while the nature of the interactions is identical for B2-NiAl and B2-CoAl.

## 2.4.2 Thermodynamics of $(Ni,Co)_{1-x}Al_x$

For the ternary phase  $(Ni,Co)_{1-x}Al_x$  those enthalpy and entropy parameters which were obtained by fitting thermodynamic properties of the binary phases NiAl and CoAl were adopted. To describe the enthalpy and entropy contributions of the interaction of vacancies and Al atoms,  $h_{Al\square}$  and  $s_{Al\square}$  respectively, a linear relationship was assumed between the corresponding values found for NiAl and CoAl (see discussion at the end of

<sup>†</sup> It is noted here that the entropy parameters  $s_{XAl}$  (X=Ni or X=Co) are related to the absolute values of the thermodynamic activity of the stoichiometric compounds  $Ni_{1/2}Al_{1/2}$  and  $Co_{1/2}Al_{1/2}$ , respectively, and the entropy parameters  $s_{XX}$  and  $s_{\square Al}$  are related to the curvature of the activity vs. composition curves for  $x_{Al} < 1/2$  and  $x_{Al} > 1/2$ , respectively.

section 4.1). To achieve a satisfying fit of the model to simultaneously the experimental data of the enthalpy of formation for both  $(\text{Ni},\text{Co})_{0.50}\text{Al}_{0.50}$  and  $(\text{Ni},\text{Co})_{0.58}\text{Al}_{0.42}$ , the parameters  $h_{\text{NiCo}}$  and  $h'_{\text{NiCo}}$  were found to be non-negligible. In this way the curves shown in Figure 2.3 were obtained; the corresponding values for the interaction parameters (additional to those for the binary systems) have been gathered in Table 2.4.

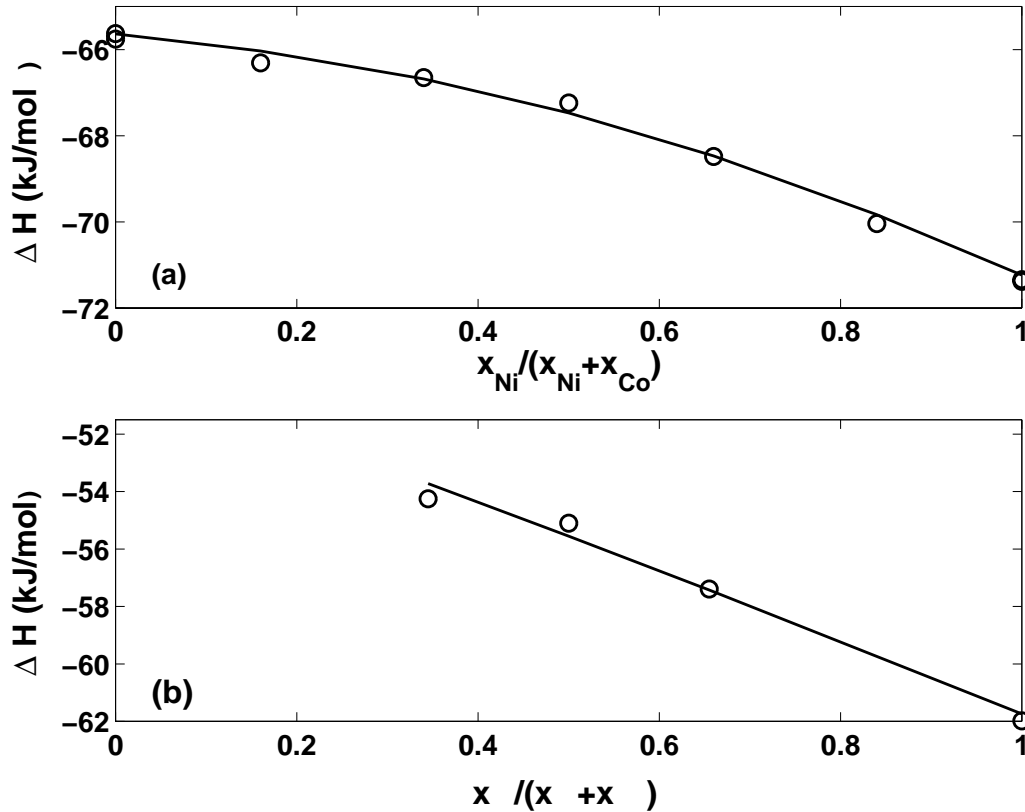


Figure 2.3:  $(\text{Ni},\text{Co})_{1-x}\text{Al}_x$  ( $T=1273$  K). Enthalpy of formation as function of  $y = x_{\text{Ni}}/(x_{\text{Ni}} + x_{\text{Co}})$ : (a)  $x_{\text{Al}}=0.50$ , (b)  $x_{\text{Al}}=0.42$ .  $\circ$  data from [16], — calculated with the parameters from Tables 2.2, 2.3 and 2.4.

Table 2.4: Enthalpy parameters (in  $\text{kJ/mol}$ ), obtained from simultaneous fitting of the enthalpy curves of  $(\text{Ni},\text{Co})_{0.50}\text{Al}_{0.50}$  and  $(\text{Ni},\text{Co})_{0.58}\text{Al}_{0.42}$ .

$Nh_{\text{NiCo}}$	$Nh'_{\text{NiCo}}$
5.722	0.943

Note that while fitting the enthalpy curves for the ternary system the entropy terms for the interaction between Ni and Co atoms cannot be determined accurately because

the sensitivity of the ternary enthalpy values for the ternary entropy parameters (as a consequence of the equilibrium condition Eq. (2.7a)) is not very distinct. The entropy parameters  $s_{NiCo}$  and  $s'_{NiCo}$  were taken as zero for fitting the enthalpy values of the ternary phase. However, the calculation of the aluminium activity curves for the ternary phase on the basis of the determined parameters revealed that at least one entropy parameter describing the interaction between Ni and Co is non-negligible in order to provide a satisfactory description of the concentration dependence of the aluminium activity: taking a value of  $-4 J/K$  for the parameter  $s_{NiCo}$ , which is- in analogy to the enthalpy parameters- expected to be the more important one, a variation of the activity of Al with composition in the ternary phase  $(Ni_{0.50},Co_{0.50})_{1-x}Al_x$  is obtained that is bounded by the corresponding curves for the binary phases; see Figure 2.4. More exact values for the ternary entropy parameters have to be obtained by fitting to (now not available) experimental values for the activities in B2-(Ni,Co)Al.

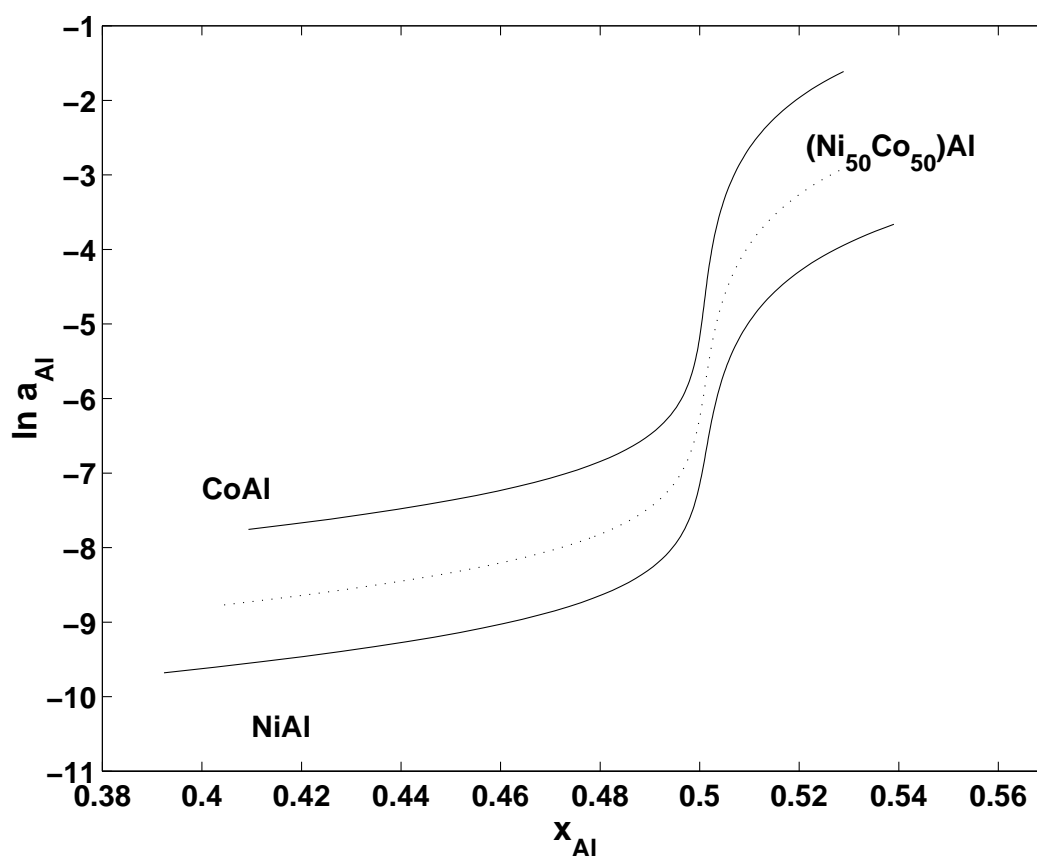


Figure 2.4: Natural logarithm of Al-activity as function of atomic fraction Al ( $T=1273$  K). Curves (full lines) for  $Ni_{1-x}Al_x$  and  $Co_{1-x}Al_x$  as in Figs. 2.1 and 2.2; curve (dashed line) calculated for  $(Ni_{0.50}Co_{0.50})_{1-x}Al_x$  using  $s_{NiCo} = -4 J/K$  (see text).

Clearly, the ternary phases containing 50 at% Al and 42 at% Al, respectively, show good agreement between experimental and calculated enthalpy of formation values (Figure 2.3). However, on the basis of the same model it was impossible to achieve satisfactory agreement between experimental and calculated values for the enthalpy of formation of  $\text{Ni}_{0.30}\text{Co}_{0.15}\text{Al}_{0.55}$ . This Al-rich phase is still within the homogeneity range of the B2 structure [26] and therefore heterogeneity is unlikely to be the cause for the discrepancy. It might be suggested that in this Al-rich alloy the amount of vacancies is that large that they can no longer be considered as distributed randomly and non-interacting. Or a different defect structure may occur in Al-rich B2-NiAl alloys: the present model only accounts for vacancies on the Ni/Co sublattice as defects in the Al-rich phases, whereas X-ray diffractometry of B2-NiAl revealed the presence of Al-antistructure atoms (about 6% for  $\text{Ni}_{0.45}\text{Al}_{0.55}$ ) [27].

The treatment given here for structure defects in ordered binary and ternary phases of B2 structure considers only vacancies on the  $\alpha$  sublattice and antistructure atoms on the  $\beta$  sublattice as possible structure defects. For the stoichiometric composition,  $(\text{A,C})_{1/2}\text{B}_{1/2}$  this implies that the ratio of vacancies and antistructure atoms equals two (at  $T > 0$  K), i.e. only so-called triple defects (cf. Section 2.1) can occur at  $T > 0$  K. For non-stoichiometric compositions at 0 K either antistructure atoms (on the  $\beta$  sublattice) or vacancies (on the  $\alpha$  sublattice) occur, i.e., also in this case, there are no triple defects at 0 K. For non-stoichiometric compositions at  $T > 0$  K, in addition, triple defects are generated. It has been suggested very recently [28] that B2-NiAl and B2-CoAl would be no triple defect phases in the above sense. Because of the good fit of the model presented here, based on triple defects, to the experimental data for these phases (see Figures 2.1 and 2.2), at this stage it appears unnecessary to apply an even more complicated model, that, for example, allows for the presence of vacancies on the  $\alpha$  sublattice and antistructure atoms on both sublattices [28]. Furthermore, it will be shown elsewhere [29] that the current model describes all available experimental properties, i.e. defect concentrations as well as thermodynamic properties, as least as good as the more complicated model of [28].

### 2.4.3 Composition and temperature dependence of defect concentrations

The knowledge acquired of the enthalpy and entropy parameters (Tables 2.2-2.4) makes it possible to calculate the concentration of vacancies and antisite atoms. The calculated vacancy concentrations as a function of the Ni:Co ratio ( $y$ ) for various temperatures are shown in Figure 2.5.



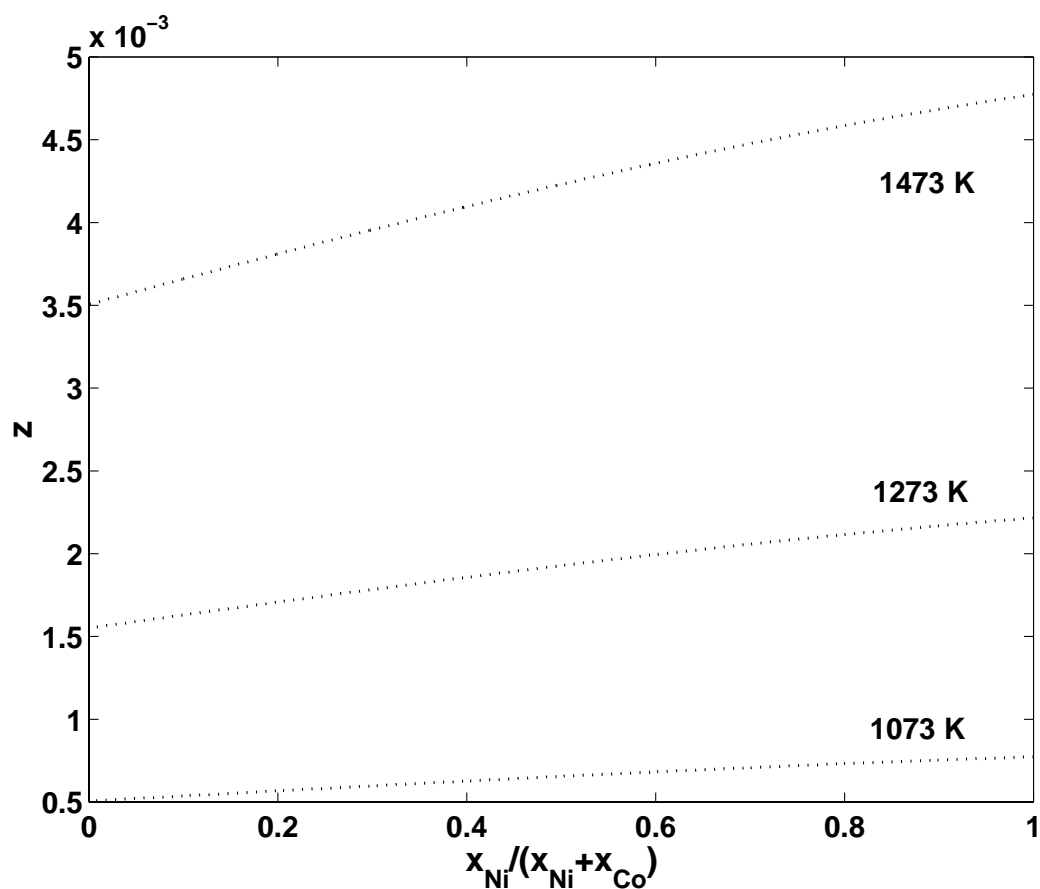


Figure 2.5: "Atomic" fraction of thermal vacancies in  $(Ni,Co)_{0.5}Al_{0.5}$  as function of  $y = x_{Ni} / (x_{Ni} + x_{Co})$ , as calculated from the present model for  $T=1073$  K,  $1273$  K and  $1473$  K using  $s_{NiCo} = -4$  J/K (see text).

The calculated concentration of thermal vacancies is shown as a function of temperature for the stoichiometric compounds NiAl and CoAl in Figure 2.6, together with available experimental data, determined via dilatometric measurements and measurements of the lattice parameter and density.

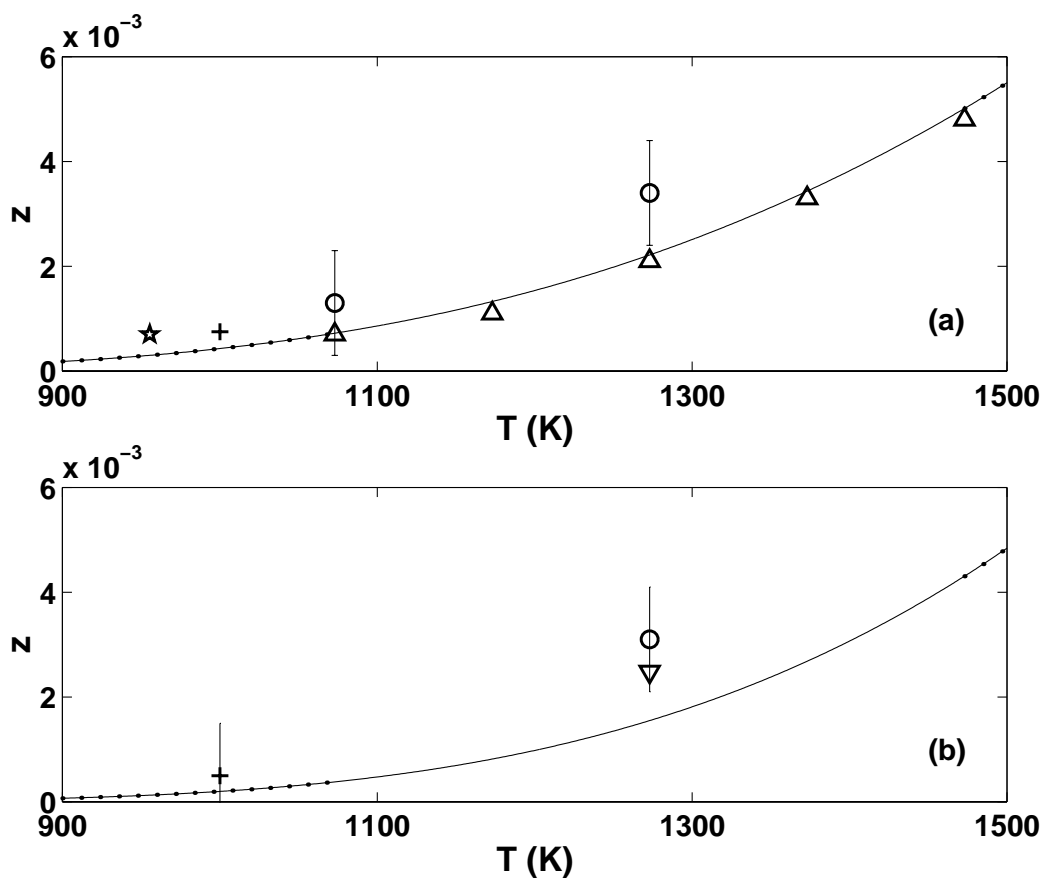


Figure 2.6: "Atomic" fraction of thermal vacancies as a function of temperature: (a)  $\text{Ni}_{0.50}\text{Al}_{0.50}$ , experimental data:  $\circ$  [30],  $\triangle$  [31],  $+$  [32],  $*$  [33] (b)  $\text{Co}_{0.50}\text{Al}_{0.50}$ , experimental data:  $\circ$  [30],  $+$  [34],  $\nabla$  [35]; error bars as given by the authors.

A good agreement between the model predictions and the experimental results occurs. In this context it should be recognized that the present model yields a value of  $1.55 \cdot 10^{-3}$  for the vacancy concentration in stoichiometric  $\text{CoAl}$  at  $T=1273$  K (see Table 2.5). This is a factor of 10 larger than the value predicted by a previous model [7, 15]. This large difference is ascribed to the unjustified neglect of the vibrational entropy in the previous model.

The entropy and enthalpy of formation of triple defects can be determined (Eqs. (2.11a) and (2.11b)) and values for the effective enthalpy and effective entropy of formation of thermal vacancies can be calculated using Eqs. (2.14a,b), (2.17a,b) and (2.21a,b). The results obtained for the stoichiometric composition ( $\chi = 0$ ) have been gathered in Table 2.5.

Table 2.5: Calculated vacancy concentrations at  $T=1273$  K and calculated enthalpy and entropy of formation of vacancies in B2 phases  $(\text{Ni},\text{Co})_{0.50}\text{Al}_{0.50}$  using the parameters from Tables 2.2 and 2.4 and  $s_{\text{NiCo}} = -4$  J/K.

Phase	$z$ (T=1273 K)	$h_{\square}^{\chi=0}$ [eV]	$s_{\square}^{\chi=0}$ [k]
NiAl	$2.22 \cdot 10^{-3}$	0.66	-0.0041
$(\text{Ni}_{0.42}\text{Co}_{0.08})\text{Al}$	$2.14 \cdot 10^{-3}$	0.67	-0.0033
$(\text{Ni}_{0.33}\text{Co}_{0.17})\text{Al}$	$2.03 \cdot 10^{-3}$	0.68	0.0005
$(\text{Ni}_{0.25}\text{Co}_{0.25})\text{Al}$	$1.93 \cdot 10^{-3}$	0.70	0.0067
$(\text{Ni}_{0.17}\text{Co}_{0.33})\text{Al}$	$1.81 \cdot 10^{-3}$	0.73	0.0154
$(\text{Ni}_{0.08}\text{Co}_{0.42})\text{Al}$	$1.68 \cdot 10^{-3}$	0.78	0.0282
CoAl	$1.55 \cdot 10^{-3}$	0.83	0.0420

A continuous change of the enthalpy and entropy values for thermal vacancy formation occurs from pure NiAl to pure CoAl (Table 2.5). The values obtained for the effective enthalpy of formation of thermal vacancies for the pure, binary phases B2-NiAl and B2-CoAl agree well with the values reported in literature [30–35]. The only experimental value of 0.68 eV for the effective enthalpy of formation of thermal vacancies in stoichiometric B2-NiAl, determined from differential thermal-expansion measurements [31], is in excellent agreement with the data calculated from the present model (0.66 eV, see Table 2.5). Also results of theoretical calculations, e.g. ab initio calculations ([36] and [37]), show reasonable agreement: 0.74 eV and 1.29 eV for stoichiometric B2-NiAl and B2-CoAl, respectively (results from this model: 0.66 eV and 0.83 eV, respectively).

For non-stoichiometric phases, the effective enthalpy and entropy of formation of thermal vacancies can be obtained from the enthalpy and entropy parameters by using the approximated equations given in section 2.5 (i.e. Eqs. (2.17a,b) and (2.21a,b)). These approximations yield values for the enthalpy of formation of vacancies in B2-NiAl of 0.99 eV ( $\chi < 0$ ) and 1.98 eV ( $\chi > 0$ ), respectively. From the ab initio calculations [36], the corresponding values are 1.11 eV and 2.22 eV, respectively. The approximations used in deriving Eqs. (2.17a,b) and (2.21a,b) can be avoided, because the effective enthalpy and entropy of formation of thermal vacancies can also be obtained by numerically solving Eq. (2.7a) for  $z(T)$  and expressing  $z(T)$  as:

$$z(T) = \exp\left(\frac{s_{\square}}{k}\right) \exp\left(-\frac{h_{\square}}{kT}\right). \quad (2.25)$$

Note that for Al-rich compounds, the term  $2\chi$  that accounts for constitutional vacancies has to be subtracted (cf. discussion below Eq. (2.19)). The results obtained for B2-NiAl are shown in Figure 2.7. The results for the effective enthalpy of formation of

thermal vacancies correspond for  $\chi \leq 0.01$  and  $\chi \geq 0.01$  to the results of the approximated equations given in section 2.5 (see above). The entropy of formation shows a pronounced composition dependence.

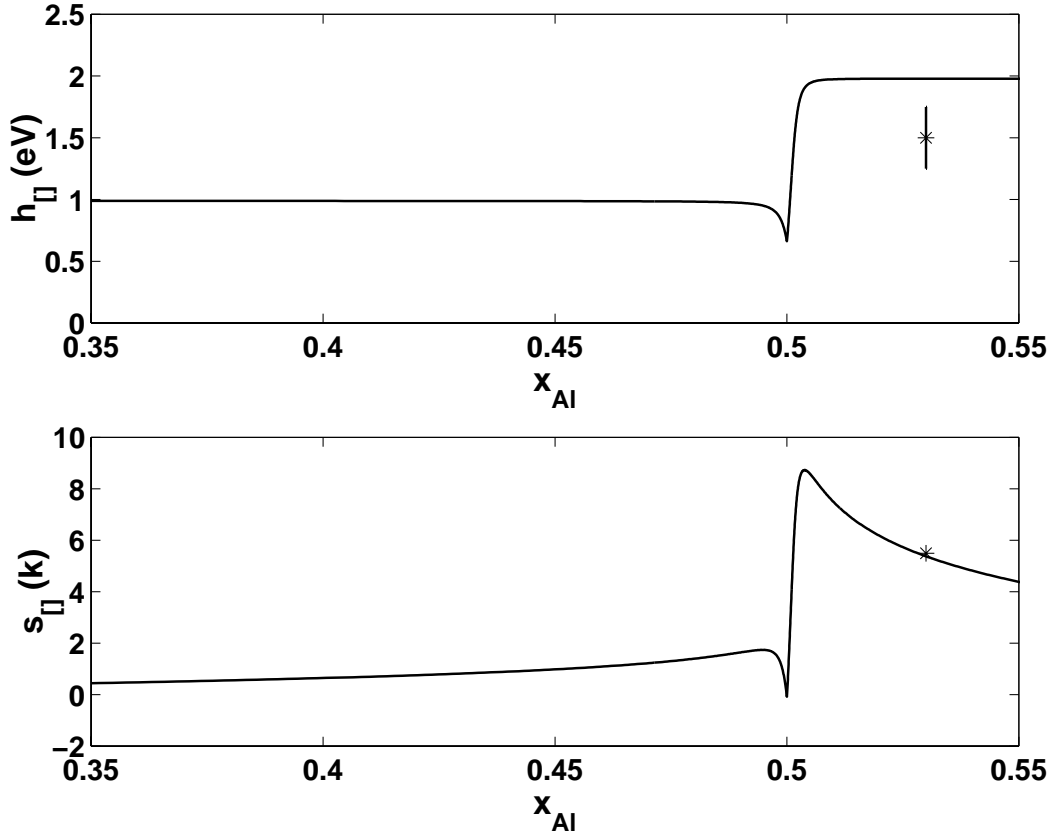


Figure 2.7: NiAl: (a) The calculated enthalpy of formation as function of atomic fraction Al (full line), \* experimental data from [33]; (b) The calculated effective entropy of formation of vacancies as function of atomic fraction Al (full line), \* experimental data from [33] (taking  $\Delta V/V = 1/2$ , see text); error bar as given in [33].

The experimental data for thermal vacancy formation, determined by time-differential length change measurements for  $\text{Ni}_{0.47}\text{Al}_{0.53}$  [33] and indicated in Figure 2.7, agree fairly well with the model predictions. The value for the effective enthalpy of formation of thermal vacancies calculated from the present model at  $x_{Al}=0.53$  (1.98 eV) is close to the one reported in [33]:  $1.5 \pm 0.25$  eV, see Figure 2.7a. A similar conclusion holds for the entropy of formation of vacancies at  $x_{Al}=0.53$ : 5.2 k from the present model compared to  $4.8 \text{ k} - k \ln \frac{\Delta V}{V}$  (where  $\Delta V$  denotes the vacancy formation volume and  $V$  the atomic volume) from [33] (for the data point from [33] shown in Fig-

ure 2.7b the vacancy formation volume was assumed to be half of the atomic volume, i.e.  $\Delta V=0.5 V$ ).

## 2.5 Conclusions

- A Bragg-Williams type model developed for B2 ordered compounds that is based on pair-interaction between both nearest and next nearest neighbour atoms, and that incorporates both the configurational and the vibrational entropy contributions, provides a good description of the thermodynamic properties of, in particular, binary NiAl and CoAl and ternary (Ni,Co)Al.
- Fitting of the model to, simultaneously, experimental data for the integral enthalpy of formation and the activity of one of the species, both as a function of composition, allows a straightforward determination of the enthalpy and entropy parameters in the model.
- The binary systems NiAl and CoAl can be described on the basis of nearest neighbour interaction only. The vibrational entropy contribution cannot be ignored for both NiAl and CoAl.
- The ternary system (Ni,Co)Al, as compared to the base binary systems, NiAl and CoAl, requires incorporation of next nearest neighbour interaction between Ni and Co and an additional, corresponding vibrational entropy contribution.
- The enthalpy and the entropy of formation of triple defects can be predicted by the model. The correspondingly calculated effective enthalpies and entropies of formation of thermal vacancies in NiAl, CoAl and (Ni,Co)Al agree well with experimental results and results from ab initio calculations.
- The vacancy concentrations as predicted by the model agree fairly well with the experimental data for NiAl and CoAl.



# *Thermodynamics of constitutional and thermal point defects in B2-Ni<sub>1-x</sub>Al<sub>x</sub>*

*J. Breuer, F. Sommer and E. J. Mittemeijer*

**Abstract:** In view of the discussion on the whether or not occurrence of constitutional vacancies in B2 intermetallic compounds, a recently proposed model for point defect formation in such compounds has been elaborated. In contrast to the results obtained by REN AND OTSUKA (2000, Philosophical Magazine A, 80, 2, pp. 467-491), it is shown that the statistical thermodynamic model applied to the available experimental data for B2-Ni<sub>1-x</sub>Al<sub>x</sub> (vacancy concentrations as functions of composition and temperature, activity data and enthalpy of formation data, both as functions of composition) does not lead to the conclusion that constitutional vacancies do not exist. In fact, all available data, except for the vacancy concentrations experimentally determined by KOGACHI ET AL., are found to be fully consistent with the triple defect model.





### 3.1 Introduction

The thermodynamics of point defects is much more complicated for ordered compounds than for monoatomic crystals (see e.g. [38]). One reason for this intricacy originates from the interdependence of the numbers and occupations of sites of the different sublattices. For example, in a  $B_2-A_{1-x}B_x$  compound, perfect order, i.e. all  $\alpha$  sublattice sites are occupied by A atoms and all  $\beta$  sublattice sites are occupied by B atoms, can only be achieved at the stoichiometric composition (i.e.  $x = 1/2$ ) and at absolute zero. For nonstoichiometric compositions and/or at temperatures above 0 K, defects have to be created in order to maintain the B2 structure, that comprises equally large (i.e. number of sites)  $\alpha$ - (ideally occupied by A atoms only) and  $\beta$ - (ideally occupied by B atoms only) sublattices. A deviation in composition at 0 K leads to so called constitutional defects, whereas an increase in temperature from 0 K generates so-called thermal defects. In the literature (see e.g. [9]) two limiting cases of defect structures have been distinguished for B2 structures that involve *two* types of defects respectively: the triple defect type and the antistructure defect type.

In so-called *triple defect* compounds the governing thermal defects are antistructure atoms on the one sublattice (say, A atoms on the  $\beta$  sublattice) and vacancies on the other sublattice (say, vacancies on the  $\alpha$  sublattice). In this case, B atoms may not occur as antistructure atoms, in correspondance with their size being larger than that of the A atoms. Thus at 0 K an excess of A atoms involves the presence of antistructure A atoms on the  $\beta$  sublattice, and an excess of B atoms involves the presence of vacancies on the  $\alpha$  sublattice. At  $T > 0$  K three defects, 'the triple defect', i.e. two vacancies on the  $\alpha$  sublattice and one antistructure atom on the  $\beta$  sublattice, have to be generated simultaneously [2].

In *antistructure defect* compounds the governing constitutional and thermal defects are antistructure atoms, i.e. A atoms on the  $\beta$  sublattice and/or B atoms on the  $\alpha$  sublattice.

The B2 phases NiAl and CoAl are usually considered as triple defect compounds whereas B2-AuCd would be an antistructure defect compound [9]. 'Hybrid' behaviour has been claimed for B2-FeAl [39].

Very recently a model was proposed [28] that allows for the presence of *three* types of defects in the B2 structure: antistructure atoms on both sublattices and vacancies only on the  $\alpha$  sublattice. From the application of this 'three defect types model' to experimentally determined vacancy concentrations as a function of composition (data taken only from experiments performed by [28] themselves) it was concluded [28] that the only defects existing in B2 compounds at absolute zero would be antistructure atoms on both sublattices. Hence, there would be no constitutional vacancies, implying that all vacancies in B2 intermetallic compounds would be caused by thermal activation.

Both, the triple defect model [29] and the three defect types model [28] are statistical thermodynamic models, and hence these models provide descriptions of the

thermodynamic properties as function of composition and temperature (at constant pressure). It was shown in [29] that the triple defect model successfully describes the available enthalpy of formation and activity data. In this work it will be investigated if the three defect types model [28] provides an even better description of the available experimental data of thermodynamic properties than the triple defect model, that accounts for only two types of defects. By extrapolation of the thereby obtained data and of data obtained by repeating the fitting work shown by [28, 40], the conclusion of the study of [28, 40] that constitutional vacancies do not occur, is tested. The focus will be on B2-NiAl because this intermetallic compound has an extended homogeneity range towards Al-rich compositions, which, according to the view until now, would imply abundant presence of constitutional vacancies (on the Ni sublattice).

Following a short comparative discussion of basic principles of the triple defect model and the three defect types model, equations for calculating the composition dependence of thermodynamic properties (enthalpies of formation and activity) within the three defect types model are developed (see Section 3.2). Application of the triple defect model for describing thermodynamic properties of B2-NiAl revealed that for the description of B2- $\text{Ni}_{1-x}\text{Al}_x$  incorporation of nearest neighbour pair interaction terms (considering vacancies also as 'atoms') was sufficient [29]. Therefore, the same basis has been adopted here. Equations for calculating the temperature dependence of the defect (especially vacancy) concentrations from the three defect types model (see above discussion) are developed in Section 3.3. The fitting procedures applied in this work are discussed in detail in the Appendix 3.A.

## 3.2 Models for point defect formation in B2 intermetallic compounds

### 3.2.1 Triple defect model vs. three defect types model

Both the triple defect model (see, e.g. [29]) and the three defect types model [28] utilize the Bragg-Williams approach [5] for expressing the enthalpy in terms of a sum of interaction enthalpies of one atom and a neighbouring atom or a neighbouring vacancy. In the triple defect model vacancies occur on only the  $\alpha$  sublattice and antistructure atoms occur on only the  $\beta$  sublattice. In the three defect types model vacancies also occur on the  $\alpha$  sublattice only, but antistructure atoms occur on both sublattices. The distribution of the atoms and defects on the two sublattices are given in Table 1 in [29] for the triple defect model and in Table 1 in [28] for the three defect types model. In the triple defect model there is only one independent variable: the vacancy concentration  $z$ . Knowing this quantity the other defect concentration, i.e. the concentration of antistructure atoms on the  $\beta$  sublattice, can be calculated. In the three defect types model there are two independent variables: the vacancy concentration  $z$  and the concentration of antistructure atoms on, say, the  $\alpha$  sublattice,  $y_B$ , and hence the concentration

of antistructure atoms on the  $\beta$  sublattice can be calculated from these two variables. Detailed discussion of further common assumptions in the models can be found in [29] and [28].

### 3.2.2 Composition dependence of thermodynamic properties according to the three defect types model

From the distribution of atoms and defects given in Table 1 of [28], one can straightforwardly calculate the enthalpy  $H$  of the  $B_2-A_{1-x}B_x$  compound according to the Bragg-Williams approach (see also [29]):

$$H = 4N[(1 - 2\chi)h_{AB} + 2\chi h_{BB}] - 2(z + 2y_B - 2\chi)\Delta H_{AB} + 2z\Delta H_{BV}, \quad (3.1)$$

where

$$\Delta H_{AB} = 4N[h_{AB} - (h_{AA} + h_{BB})/2] \quad (3.2)$$

$$\Delta H_{BV} = 4N[h_{BV} - h_{BB}/2]. \quad (3.3)$$

$N$  is Avogadro's number and the composition variable is  $\chi = x - 1/2$ . The terms  $\Delta H_{ij}$  have the same meaning as in [28], with  $Nh_{ij}$  as the enthalpy value per mole connected with the 'bond'  $ij$ . The enthalpy of formation  $\Delta H$  is given by

$$\Delta H = H - \left(\frac{1}{2} - \chi\right)H_A - \left(\chi + \frac{1}{2}\right)H_B, \quad (3.4)$$

where  $H_i$  ( $i=A,B$ ) are the enthalpies per mole of the pure elements at the same temperature and pressure as pertaining to the enthalpy  $H$ . Analogous to the enthalpy (see above) the vibrational entropy  $S^{vib}$  is written as

$$S^{vib} = 4N[(1 - 2\chi)s_{AB} + 2\chi s_{BB}] - 2(z + 2y_B - 2\chi)\Delta S_{AB} + 2z\Delta S_{BV}, \quad (3.5)$$

where

$$\Delta S_{AB} = 4N[s_{AB} - (s_{AA} + s_{BB})/2] \quad (3.6)$$

$$\Delta S_{BV} = 4N[s_{BV} - s_{BB}/2], \quad (3.7)$$

and the entropy parameters are denoted by  $s_{ij}$ . The formulation of the vibrational entropy as a linear function of the number of pairs found in the structure (Eq. (3.5)) is lacking a strong physical foundation. In the following not the individual parameters  $s_{ij}$  are dealt with but rather the total amount of the vibrational entropy is important. The given definition may be compared to the approach by Wagner who writes the vibrational entropy in terms of a linear function of the number of atoms [8].

The configurational entropy  $S^{conf}$  is determined by Boltzmann's relationship yielding

$$S^{conf} = \frac{R}{2}[2(1+z)\ln(1+z) - (1-2y_B-z)\ln(1-2y_B-z) - 2y_B\ln(2y_B) + -2z\ln(2z) - (z+2y_B-2\chi)\ln(z+2y_B-2\chi) - (1-2y_B+2\chi)\ln(1-2y_B+2\chi)]. \quad (3.8)$$

Inserting Eqs. (3.4), (3.5) and (3.8) into the expression for the Gibbs energy ( $G = H - T(S^{vib} + S^{conf})$ ), execution of the minimization conditions  $\partial G/\partial z = 0$  and  $\partial G/\partial y_B = 0$  (equilibrium at constant temperature and pressure) leads to

$$4(\Delta H_{AB} - T\Delta S_{AB}) = RT \ln[2y_B(z + 2y_B - 2\chi)] \quad (3.9)$$

$$4(\Delta H_{BV} - T\Delta S_{BV}) = RT \ln(y_B/2z^2). \quad (3.10)$$

The composition dependence of the activity of component B,  $a_B$ , is given by (see also [29])

$$RT \ln a_B = G + \left(\frac{1}{2} - \chi\right) \frac{dG}{d\chi} - G_B^0, \quad (3.11)$$

where  $G_B^0$  is the Gibbs energy of pure B in its reference state (cf. Eq. (22) in [29]).

### 3.2.3 Composition and temperature dependence of the defect concentrations according to the three defect types model

The procedure for deriving the temperature dependence of the defect concentrations according to the triple defect model was given by [29]. A similar treatment can be applied to the three defect types model considered here: the conditions for thermodynamic equilibrium (Eqs. (3.9) and (3.10)) provide an implicit expression for the vacancy concentration,  $z$ , and one of the two other defect concentrations,  $y_B$ . Solving Eq. (3.10) for  $y_B$  and inserting into Eq. (3.9) yields:

$$\exp\left(\frac{4(\Delta H_{BV} - T\Delta S_{BV})}{RT}\right) z^4 + \frac{1}{4} z^3 - \frac{\chi}{2} z^2 - \frac{\exp\left(\frac{4(\Delta H_{AB} - T\Delta S_{AB})}{RT}\right)}{16 \exp\left(\frac{4(\Delta H_{BV} - T\Delta S_{BV})}{RT}\right)} = 0. \quad (3.12)$$

According to Eq. (3.12) the vacancy concentration  $z$  is an implicit function of the composition variable  $\chi$  and the temperature  $T$  for known parameters  $\Delta H_{AB}$ ,  $\Delta H_{BV}$ ,  $\Delta S_{AB}$  and  $\Delta S_{BV}$ . Considering Eq. (3.12) it is noted that in general the vacancy concentration as function of temperature cannot be described by an Arrhenius-type equation  $z(T)|_{\chi=const.} = (\exp S/k)(\exp -H/kT)$ , where  $k$  denotes Boltzmann's constant and  $S$  and  $H$  are the entropy and enthalpy of formation of one vacancy, respectively. This is also true for the other two defects allowed in the three defect types model: the concentration of B antistructure atoms on the  $\alpha$  sublattice that is given by Eq. (3.10) as

$$y_B = 2z^2 \exp\left(\frac{4(\Delta H_{BV} - T\Delta S_{BV})}{RT}\right) \quad (3.13)$$

and the concentration of A antistructure atoms on the  $\beta$  sublattice that is given by (see eEq. (1') in [40])

$$y_A = \frac{z}{2} + y_B - \chi. \quad (3.14)$$

### 3.3 Results

The relation between  $z$ ,  $\chi$  and  $T$  is prescribed implicitly by Eq. (3.12). The task now is to determine  $z(\chi)$  by fitting Eq. (3.12) to experimentally determined vacancy concentrations as a function of composition at a constant temperature (see Section 3.3.1) or by simultaneous fitting of the enthalpy of formation and thermodynamic activity data, both as a function of composition at constant temperature (see Section 3.3.2). Having obtained the model parameters (note that these are  $\Delta H_{ij}$  and  $\Delta S_{ij}$  for the fitting of the vacancy concentration and  $h_{ij}$  and  $s_{ij}$  for the fitting of the thermodynamic properties, respectively), the temperature dependence of the vacancy concentration can also be determined using Eq. (3.12). One may also use experimental  $z(T)$  data measured for constant compositions  $\chi$  as input for the fitting, or a combination of all of these data sets ( $z(\chi)$ ,  $z(T)$ ,  $\Delta H(\chi)$  and  $a_B(\chi)$ ) as input for the fitting procedure (see Section 3.3.3).

Details about the two fitting procedures applied in this work, the 'numerical/ indirect' procedure and the 'analytical/ direct' procedure, are given in Appendix 3.A.

#### 3.3.1 Results using $z(\chi)$ at constant temperature as experimental input data

##### 3.3.1.1 Results of the fitting procedure

In the work of [28, 40] the three defect types model was applied to the experimentally determined vacancy concentrations [32] as function of composition at constant temperature  $T$  ( $T \sim 800 - 1000$  K). The fitting of Eq. (3.12) to the data was performed considering only the  $\Delta H_{AB}$ - and  $\Delta H_{BV}$ -parameters as fit parameters;  $\Delta S_{AB}$  and  $\Delta S_{BV}$  were set at zero. Since it was not stated by [28, 40] how the fitting to the experimental data of [32] was performed, both procedures proposed in this work, the 'numerical/ indirect' procedure and the 'analytical/ direct' procedure (see Appendix 3.A) have been applied here for fitting to the experimental data of [32]. The experimental results of [32] were obtained from slowly cooled (from a temperature of 1273 K with a cooling rate of 2 K/min) samples. Therefore in [32] a definite temperature for the vacancy-concentration data was not indicated. However, for the fitting of Eq. (3.12) to experimental  $z(\chi)$  data, it is necessary to assign a definite temperature to the vacancy-concentration data. In the present work for the fitting of the composition dependence of the vacancy concentration temperatures of 800, 1000 and 1273 K were used. The thereby obtained values for the fit parameters did not differ significantly. For the enthalpy of formation data and the activity data also regarded in this work (see Section 3.3.2) a temperature of 1273 K holds. Therefore, for the following presentation of the fitting of composition dependencies of experimental data (vacancy concentration data and enthalpy of formation and activity data), a uniform temperature of 1273 K was used.

The results of the fitting of Eq. (3.12) to the  $z(\chi)$  data of [32] are shown in Figure 3.1 and the values for the corresponding parameters have been given in Table 3.1. The results as obtained by [28, 40] have been given too for comparison.

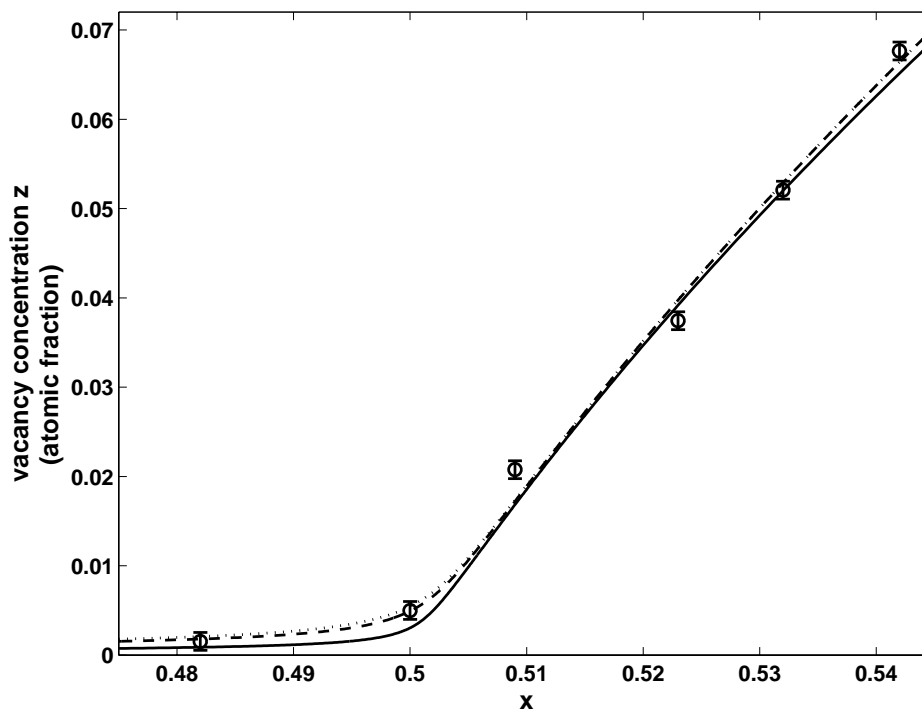


Figure 3.1:  $Ni_{1-x}Al_x$  ( $T=1273$  K): 'Atomic fraction' of vacancies as function of the atomic fraction of aluminium,  $x$ . Experimental data ( $\circ$ ) of [32] with error bars as given by the authors. Curves calculated with the three defect types model using the parameters from Table 3.1: solid: using the parameters given by [28, 40] (column 2 of Table 3.1); dashed: using the numerical/indirect method (parameters given in column 3 of Table 3.1); dotted: using the analytical/direct method (parameters given in column 4 of Table 3.1). The dashed and dotted curves almost coincide.

As can be seen, the numerical method and the analytical method yield somewhat lower absolute values for  $\Delta H_{AB}$  than the one given by [28, 40], whereas the  $\Delta H_{BV}$  values obtained from the two fitting procedures in this work differ considerably from the one given by [28, 40] (even the sign is different). Results from ab initio calculations for the parameters can be found in [41].

A comparison of the resulting  $(x-z)$  pairs as obtained by the two methods of fitting is provided by Table 3.2.

Table 3.1:  $\text{Ni}_{1-x}\text{Al}_x$  ( $T=1273\text{ K}$ ): Parameters (in  $\text{kJ/mol}$ ) obtained from fitting of the experimentally determined vacancy concentrations as function of composition from [32]; for details concerning the two methods see Appendix 3.A. The parameters  $\Delta S_{AB}$  and  $\Delta S_{BV}$  were taken as zero.

	from [28, 40]	numerical method, this work	analytical method this work
$\Delta H_{AB}$	-42	-38.44	-37.65
$\Delta H_{BV}$	0.28	-0.000245	-0.001364

Table 3.2:  $\text{Ni}_{1-x}\text{Al}_x$  ( $T=1273\text{ K}$ ): Comparison of the experimental data of the vacancy concentration as function of composition reported by [32] with calculated composition values  $\mathbf{x}$  and calculated corresponding vacancy concentrations  $\mathbf{z}$  as obtained from fitting of the same data with the three defect types model. See also Fig. 3.1.

	exp. from [32]	calc. with para- meters from [28] and [40]	calc. with parameters (numerical m.) from Table 3.1, column 3	calc. with parameters (analytical m.) from Table 3.1, column 4
$\mathbf{x}$	0.482	0.4821	0.4824	0.4823*
	0.500	0.5000	0.5000	0.5001*
	0.509	0.5090	0.5090	0.5090*
	0.523	0.5232	0.5231	0.5230*
	0.532	0.5323	0.5324	0.5320*
	0.542	0.5421	0.5421	0.5420*
$\mathbf{z}$	$1.5 \cdot 10^{-3}$	$9 \cdot 10^{-4}$	$1.8 \cdot 10^{-3}$	$2.1 \cdot 10^{-3}(+7 \cdot 10^{-18}i)$
	$5.0 \cdot 10^{-3\dagger}$	$3.1 \cdot 10^{-3}$	$4.9 \cdot 10^{-3}$	$5.5 \cdot 10^{-3}$
	$2.08 \cdot 10^{-2}$	$1.69 \cdot 10^{-2}$	$1.72 \cdot 10^{-2}$	$1.73 \cdot 10^{-2}(+1 \cdot 10^{-17}i)$
	$3.75 \cdot 10^{-2}$	$3.96 \cdot 10^{-2}$	$4.00 \cdot 10^{-2}$	$3.98 \cdot 10^{-2}(-4 \cdot 10^{-18}i)$
	$5.21 \cdot 10^{-2}$	$5.23 \cdot 10^{-2}$	$5.34 \cdot 10^{-2}$	$5.29 \cdot 10^{-2}$
	$6.76 \cdot 10^{-2}$	$6.52 \cdot 10^{-2}$	$6.65 \cdot 10^{-2}$	$6.64 \cdot 10^{-2}(-3 \cdot 10^{-18}i)$

The initial  $z$  array used in the application of the numerical method is sufficiently dense (see discussion in Appendix 3.A) as can be seen comparing the calculated values of the composition (columns 2 and 3 of the upper part of Table 3.2) with the experimental values (column 1): the maximum deviation found between calculated and experimental values is less than 0.1 at% which is far below the uncertainty limit of the composition.

The vacancy concentrations calculated with the parameter set for  $\Delta H_{AB}$  and  $\Delta H_{BV}$  given by [28, 40] show on average a larger deviation from the experimental values than the vacancy concentrations obtained in this work by the numerical and analytical procedures (see lower part of Table 3.2, columns 2-4).

When applying the analytical method for fitting to the vacancy concentrations, one uses the experimental values of the composition as mathematically exact numbers (see Appendix 3.A). In this case, for some of the experimental compositions,  $z$  values with very small imaginary parts (absolute value  $\leq 10^{-17}$ ) appear (see lower part of column 5 of Table 3.2). These physically unrealistic imaginary parts are due to nonexactness of the experimental values for the composition. The very small imaginary parts for the calculated  $z$  values can be neglected since they are many orders of magnitude smaller than the corresponding real parts (cf. Table 2). Indeed, inserting only the real part of the calculated  $z$  values into Eq. (3.12) and then calculating the corresponding composition values  $x$  it follows that the maximum deviation between the calculated and experimental data is below 0.1 at% (see upper part of column 5 in Table 3.2), which is about the experimental inaccuracy.

### 3.3.1.2 Results for the temperature dependence of the vacancy concentration

Within the three defect types model the variation with temperature of the vacancy concentration  $z$  for a compound with fixed composition  $\chi$  is given by Eq. (3.12) as well. Inserting the parameters of Table 3.1 the curves shown in Figure 3.2 are obtained for the Al-rich compounds  $Ni_{0.466}Al_{0.534}$  and  $Ni_{0.477}Al_{0.523}$ .

These are the alloys with the highest Al-contents for which the authors of [28, 40] determined vacancy concentrations as a function of temperature [32, 42]. These experimental values are also shown in Figure 3.2. The temperature dependencies obtained from the parameter sets calculated in this work by the numerical method and the analytical method (dashed and dotted curves, respectively, in Figure 3.2; columns 2 and 3 in Table 3.1) almost coincide. However, a strongly deviating behaviour is obtained for the  $z - T$  curves obtained with the parameter set of [28, 40] (full curves; column 1 in Table 3.1).

The experimentally determined vacancy concentrations at room temperature agree very well with the curves obtained using the fit parameters obtained in this work, and not with the curves obtained using the fit parameters of [28, 40]. By [40] it was argued

\* from reinsertion of the real part of the calculated  $z$  values into Eq. (3.12)

† mean value from two experiments, see Ref. [32]



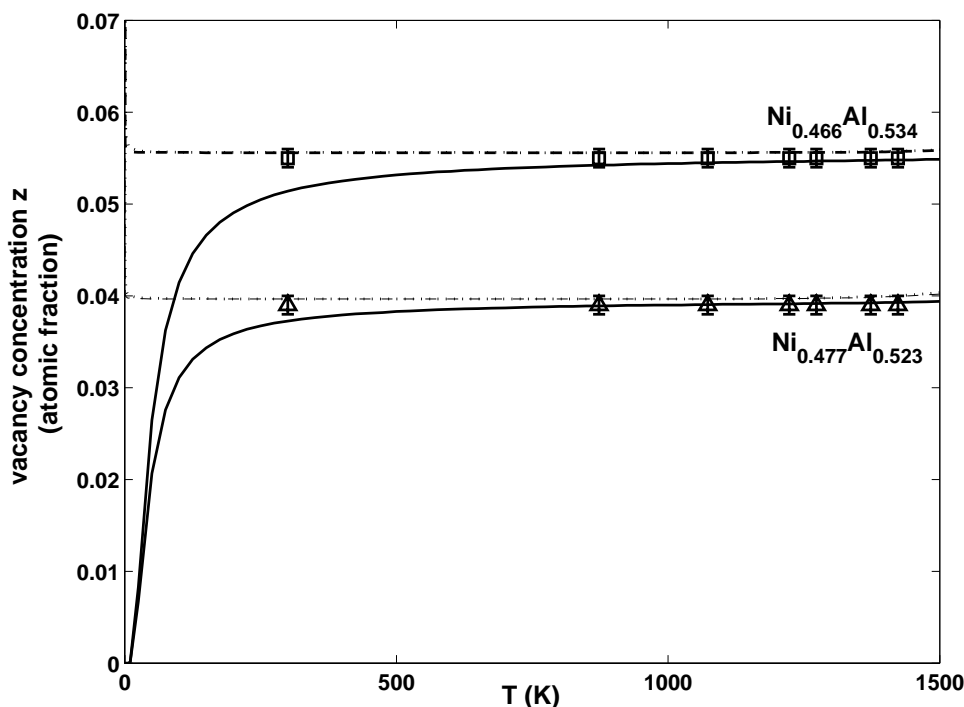


Figure 3.2: 'Atomic fraction' of vacancies as function of the temperature for the compounds  $\text{Ni}_{0.466}\text{Al}_{0.534}$  and  $\text{Ni}_{0.477}\text{Al}_{0.523}$ : Experimental data ( $\circ$ ,  $\triangle$ ) of [32, 42] with error bars as given by the authors. Curves calculated with the three defect types model using the parameters from Table 3.1: solid: using the parameter set given by [28, 40] (column 2 of Table 3.1); dashed: using the numerical/indirect method (parameters given in column 3 of Table 3.1); dotted: using the analytical/direct method (parameters given in column 4 of Table 3.1). The dashed and dotted curves almost coincide. For details concerning the two methods of fitting see Appendix 3.A.

that the data points at room temperature are affected by 'freezing in' of vacancies, implying that thermodynamic equilibrium would not have been reached. Apparently this reasoning is incorrect.

The present results clearly demonstrate that using only the vacancy concentrations as a function of composition at constant temperature as reported by [32], as the experimental input data for the fitting of the three defect types model, even then the vacancy concentration does not decrease to zero when the temperature approaches zero. This invalidates the argument used by [28] to claim that there would be no constitutional vacancies, which was based on the extrapolation of  $z$  at constant composition to 0 K (see Figure 3.2).

### 3.3.2 Results using $\Delta H(\chi)$ and $a_B(\chi)$ at constant temperature as experimental input data

#### 3.3.2.1 Results of the fitting procedure

The results of the fitting of the three defect types model to, simultaneously, data for the activity of aluminium [12] and the enthalpy of formation [11] of  $Ni_{1-x}Al_x$ , as obtained by applying the numerical/indirect method and the analytical/direct method, are shown in Figure 3.3.

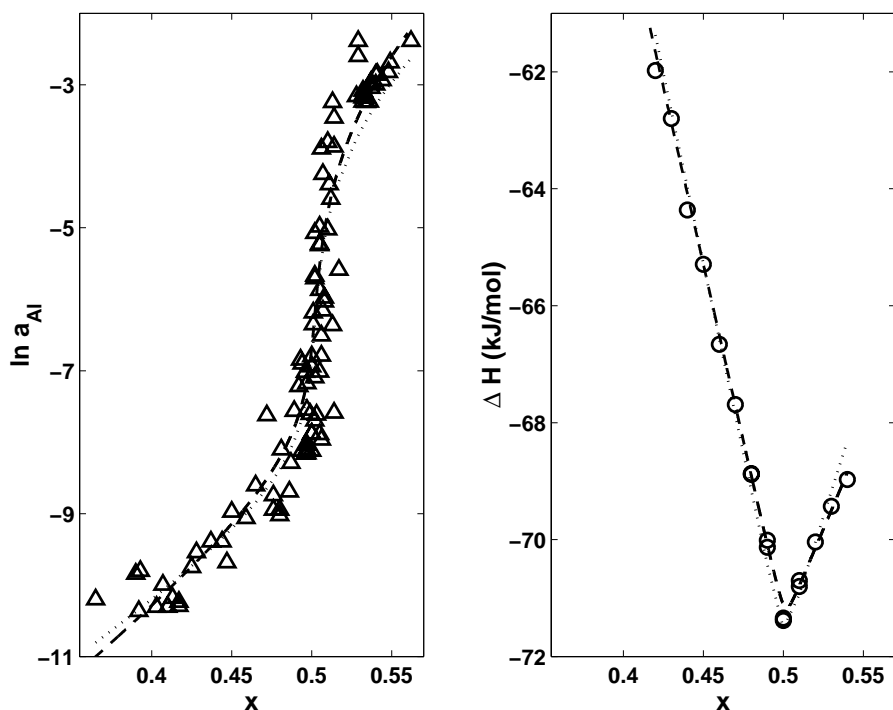


Figure 3.3: (a) Natural logarithm of Al-activity as function of the atomic fraction Al,  $x$ ,  $\Delta$  rectified data from [12] (see [29]), (b) Enthalpy of formation as function of the atomic fraction Al,  $x$ ,  $\circ$  corrected data (see [29]) from [11]; dashed curves calculated with the parameters from Table 3.3 according to the numerical/indirect method; dotted curves calculated with the parameters from Table 3.3 according to the analytical/direct method. For details concerning the two methods of fitting see Appendix 3.A.

The values for the reference quantities  $H_A$ ,  $H_B$  and  $G_B^0$  (see Eqs. (3.4) and (3.11)) were taken from [22]. Similar to the results obtained by the application of the triple defect model [29], it was found that the aluminium activity and enthalpy of formation

can be described adequately taking into account enthalpy and entropy contributions of already only nearest neighbour pairs of species. The corresponding values for the enthalpy and entropy parameters,  $h_{ij}$  and  $s_{ij}$  have been given in Table 3.3.

Table 3.3:  $\text{Ni}_{1-x}\text{Al}_x$  ( $T=1273\text{ K}$ ): Enthalpy parameters  $Nh_{ij}$  (in  $\text{kJ/mol}$ ) and entropy parameters  $s_{ij}$  (in  $\text{J/K}$ ) obtained from the simultaneous fitting of the thermodynamic activity data and the enthalpy of formation data, both as function of composition; for details concerning the two methods see Appendix 3.A.

	$Nh_{AA}$	$Nh_{BB}$	$Nh_{AB}$	$Nh_{BV}$	$s_{AA}$	$s_{BB}$	$s_{AB}$	$s_{BV}$
numerical/ indirect	3.37	0	-9.90	0.06	-4.7	0	4.7	8.1
analytical/ direct	4.38	0.03	-10.01	1.93	24.2	2.7	8.0	7.3

Note that for the fitting to the thermodynamic properties using Eqs. (3.4) and (3.11) one has to determine values for the model parameters  $h_{ij}$  and  $s_{ij}$  separately, whereas for the fitting to the vacancy concentration as function of composition (see Section 3.3.1.1) values have to be determined for a combination of these, yielding  $\Delta H_{AB}$  and  $\Delta H_{BV}$  according to Eqs. (3.2) and (3.3) and  $\Delta S_{AB}$  and  $\Delta S_{BV}$  according to Eqs. (3.6) and (3.7).

The parameters obtained from the fitting using the numerical and the analytical method yield good descriptions of the thermodynamic activity and enthalpy of formation data of practically identical quality (i.e. the residual error values of the two fitting procedures (see Figures 3.6 and 3.7) are practically the same). This means, that one cannot prefer one of the two parameter sets given in Table 3.3.

### 3.3.2.2 Results for the composition dependence of the vacancy concentration

Using the thus determined values for the fit parameters, the vacancy concentration as a function of composition can be calculated applying Eq. (3.12). The results obtained for the composition dependence of the vacancy concentration at 1273 K for the two sets of parameters given in Table 3 are shown in Figure 3.4.

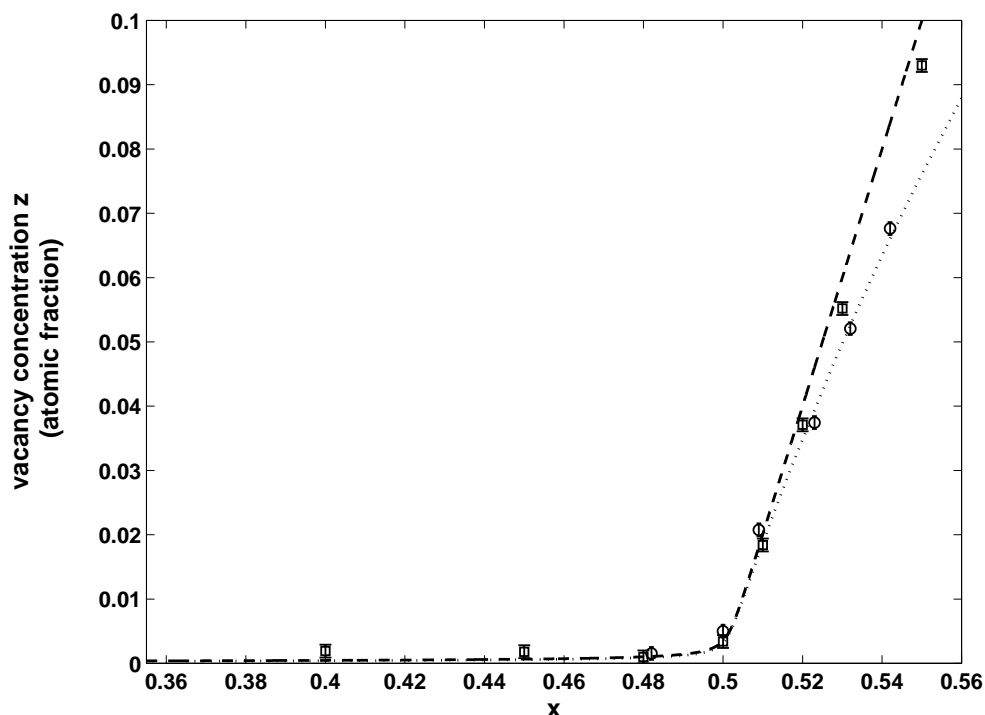


Figure 3.4:  $Ni_{1-x}Al_x$  ( $T=1273$  K): 'Atomic fraction' of vacancies as function of the atomic fraction of aluminium,  $x$ . Experimental data with error bars as given by the authors:  $\circ$  from [32],  $\square$  from [30]. Curves calculated with the three defect types model using the parameters from Table 3.3 obtained from the simultaneous fitting of the thermodynamic activity and the enthalpy of formation, both as function of composition; dashed curve calculated with the parameters from Table 3.3 according to the numerical/indirect method and dotted curve calculated with the parameters from Table 3.3 according to the analytical/direct method. For details concerning the two methods of fitting see Appendix 3.A.

Experimental data for the vacancy concentration as reported by [32] (which have been used for the fitting presented in Section 3.3.1.1;  $\circ$ ), and those reported by [30] ( $\square$ ) have been given in the figure as well. The vacancy concentration vs. composition curve calculated using the parameter set obtained by application of the numerical/indirect procedure practically reproduces the curve typical for triple defect behaviour (i.e.  $z \geq 2\chi$  for  $\chi > 0$ ; see [29]) and agrees well with the experimental data of [30]. The vacancy concentration vs. composition curve calculated using the parameter set obtained by application of the analytical/direct procedure yields somewhat lower vacancy-concentration values for the Al-rich compounds and agrees well with the experimental data of [32].

The results concerning experimentally determined vacancy concentrations obtained by different authors do not agree (i.e. the authors of [32] find the lower values marked by  $\circ$  in Figure 3.4, whereas other authors (see, e.g. [7] and references therein) find values similar or even higher ones than the ones obtained by [30] (which would mean triple defect behaviour [29]) marked by  $\square$  in Figure 3.4).

### 3.3.2.3 Results for the temperature dependence of the vacancy concentration

Inserting the values determined for the fit parameters into Eq. (3.12) the vacancy concentration vs. temperature curves for constant composition can be calculated. The results obtained for the two sets of fit parameters (Table 3.3) for the two Al-rich compounds  $\text{Ni}_{0.466}\text{Al}_{0.534}$  and  $\text{Ni}_{0.477}\text{Al}_{0.523}$  are shown in Figure 3.5 (dashed curves using the numerical method, dotted curves using the analytical method).

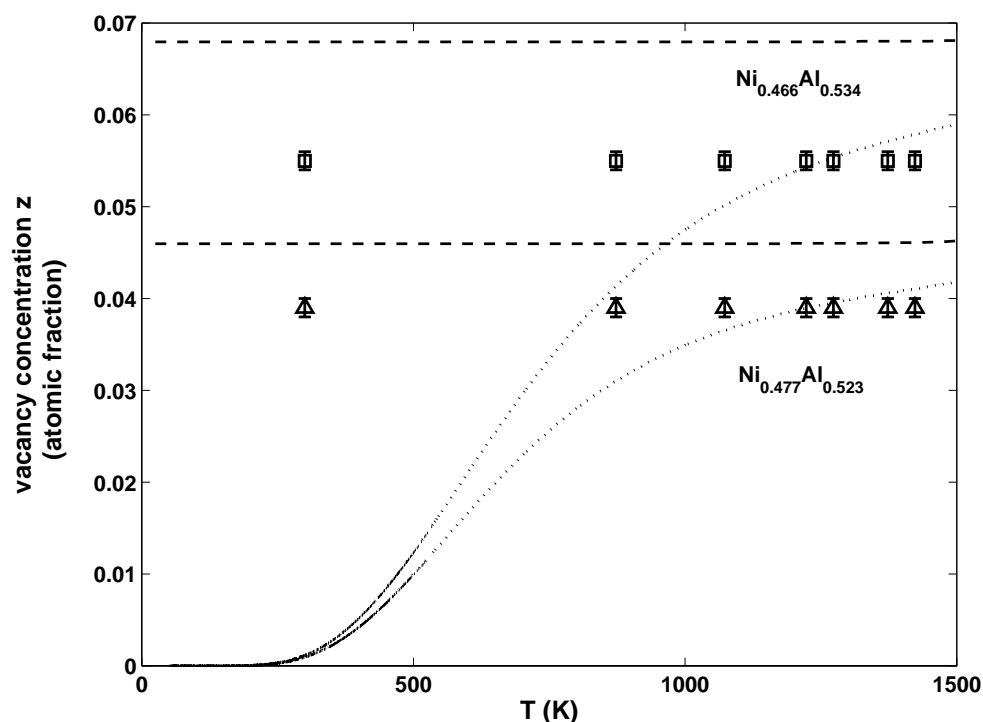


Figure 3.5: 'Atomic fraction' of vacancies as function of the temperature for the compounds  $\text{Ni}_{0.466}\text{Al}_{0.534}$  and  $\text{Ni}_{0.477}\text{Al}_{0.523}$ : Experimental data ( $\circ$ ,  $\triangle$ ) from [32, 42] with error bars as given by the authors. Curves calculated with the three defect types model using the parameters from Table 3.3: dashed: using the numerical/indirect method (parameters in Table 3.3); dotted: using the analytical/direct method (parameters given in Table 3.3). For details concerning the two methods of fitting see Appendix 3.A.

Experimental data for the vacancy concentration reported by [32] and [42] (see also Figure 3.2 of this work) have been included in the figure as well. Comparing the calculated horizontal lines/curves with the experimental data it follows that neither of the two sets of parameters gives agreement with the experimental results reported by [32, 42] but predicts a triple defect type behaviour (horizontal lines) or predicts a fast decrease of the vacancy concentration with temperature.

### 3.3.3 Results using $z(T)$ or a combination of the $z(\chi)$ -, $z(T)$ -, $\Delta H(\chi)$ - and $a_B(\chi)$ - data as experimental input data

Applying the three defect types model one may also use experimental vacancy-concentration data as function of temperature for constant compositions as input data for the fitting. Or- and this is allowed by the present approach and would naturally be the best choice- use *all* of the experimental results available so far (i.e.  $z(\chi)$ -,  $z(T)$ -,  $\Delta H(\chi)$ - and  $a_B(\chi)$ - data) as input data for a 'general' fit.

The vacancy-concentration data as function of temperature for constant composition of [32] may be described by the parameters  $\Delta H_{AB}$  and  $\Delta H_{BV}$  only- see e.g. the results presented in Section 3.3.1.2 of this work. This is also true for the  $z(\chi)$ - data. However, for the description of the thermodynamic data, the parameters  $h_{ij}$  and  $s_{ij}$  have been found to be necessary; see Section 3.3.2. This explains why it is impossible to arrive at a description of the thermodynamic data with parameters obtained from fitting  $z(T)$  (or  $z(\chi)$ ) data only.

In the present study, the fitting to, simultaneously, *all* experimental data ( $z(\chi)$ -,  $z(T)$ -,  $\Delta H(\chi)$ - and  $a_B(\chi)$ - data) for the three defect types model was performed many times using various fit criteria, i.e. the total residual error (i.e. the sum of the individual errors of the fitting result for each experimental data set) to be minimized was defined differently by weighing the individual errors in different ways. Such a 'general' fit did not lead to a consistent description of all available experimental data (see further Section 3.3.4). However, if the vacancy concentration-data of [32, 42] are ignored, while keeping the vacancy concentration data of the other authors ([30] and [7]), fitting of the three defect types model yields the same result as obtained by the less general triple defect model [29]. Using the experimental results on the activity and enthalpy of formation together with the vacancy concentration-data as function of composition and temperature of [32, 42] as input data for the fitting of the three defect types model, a parameter set yielding a consistent description was not obtained.

### 3.3.4 Final remark

Reviewing the results obtained in the present study, the vacancy-concentration data of [32, 42] ( $z$  as function of composition and temperature) appear to be the only  $z(\chi)$  and  $z(T)$  data that are not consistent with a description according to the triple defect model. Hence, one may wonder if these data are correct. The vacancy-concentration

data of [32] and [42] were obtained by the combination of measurements of lattice parameters with measurements of the density. Comparing the lattice-parameter data obtained in [32] with values reported elsewhere (see, e.g. [7] and references therein), the differences seem to be negligible. The deviations in the vacancy-concentration data reported by [32] and [42] are to a great extent caused by the differences in the density values obtained: [32] and [42] claim, that in former studies of the density of (especially Al-rich) B2-Ni<sub>1-x</sub>Al<sub>x</sub> (see [7]) too low density values (implying higher vacancy concentrations) were obtained, because of the use of bulk samples that may contain voids or cracks. [32] and [42] obtained their values using powder samples. A verification of the reported density values appears required.

### 3.4 Conclusions

An elaboration of the three defect types model for the thermodynamics of point defects in B2-type ordered compounds makes it possible to determine the parameters of the model not only by fitting to experimentally determined vacancy concentrations, but also to experimentally determined enthalpy of formation and thermodynamic activity data.

#### A. Fitting to experimentally determined vacancy concentrations

- Fitting of the three defect types model to (only) experimentally determined vacancy concentrations as function of composition at constant temperature and at constant pressure in B2-Ni<sub>1-x</sub>Al<sub>x</sub> shows that the fitting procedures presented in this paper lead to at least as good fits of the model to the experimental data than obtained by using the values for the fit parameters as given by [28, 40].
- Adopting the results for the fit parameters as obtained in this work leads to a dependence of the vacancy concentration on temperature that well agrees with the experimental data and that implies the occurrence of constitutional vacancies, in contrast with the results and the assertion given by [28] and [40].

#### B. Fitting to experimentally determined enthalpy of formation and thermodynamic activity data

- Fitting of the three defect types model to (only) experimentally determined enthalpies of formation and Al-activities in B2-Ni<sub>1-x</sub>Al<sub>x</sub> at constant temperature and at constant pressure provides good description of the experimental data. However, fitting the simpler triple defect model containing less fit parameters [29] yields fits of the same good quality.
- Adopting the results for the fit parameters as obtained in this work leads to a dependence of the vacancy concentration on alloy composition that

agrees within the experimental variation with the available experimental data. Using the same parameters, the calculated dependence of the vacancy concentration on temperature does not agree with the experimental results provided by [32] and [42] at all, but yields triple defect type behaviour or shows a continuous decrease with decreasing temperature.

- C. Fitting to all available experimental data, i.e. vacancy concentrations as function of composition and temperature, apart from the vacancy-concentration data of [32] and [42], and enthalpy of formation and thermodynamic activity data as function of composition, adopting the triple defect model, and therefore allowing the occurrence of constitutional vacancies, leads to a consistent description of all data. The experimental results given by [32, 42] are the only data that are not compatible with this description.



### 3.A Appendix: Algorithm for fitting the model equations

The  $z$ - $\chi$ - $T$ - relationship given by Eq. (3.12) is the equation to work with when starting any of the fitting procedures presented in this work. There are two different ways of solving the implicit relationship provided by this equation: a "numerical/indirect" procedure (see Appendix 3.A.1) and an "analytical/direct" procedure (see Appendix 3.A.2).

Because of their physical meaning, Eq. (3.12) is to be fulfilled by only real (i.e. not complex) values for the  $\Delta H_{ij}$ - and  $\Delta S_{ij}$ -parameters, by only positive real  $z$ -values and by only real  $\chi$ -values with absolute values less than 0.5. Applying Descartes' rule of signs (see, e.g. [43]) to the polynomial Eq. (3.12), it is seen that there can be only one positive root for  $z$  that can be real or complex for every eligible  $\chi$  value.

#### 3.A.1 The "numerical/indirect" procedure

For the *numerical/ indirect* method (see Figure 3.6),  $z$  as a function of  $\chi$  and  $T$  can be obtained from Eq. (3.12) numerically for given parameters  $\Delta H_{AB}$ ,  $\Delta H_{BV}$ ,  $\Delta S_{AB}$  and  $\Delta S_{BV}$ .

First an array of (real) values for the vacancy concentration  $z$  (i.e.  $0 \leq z < 1$ ) is chosen. Using Eq. (3.12) for a given  $T$ , this array of  $z$  values can be transferred into an array of  $\chi$  values. Then, the physically relevant  $\chi$  values, i.e. the  $\chi$  values pertaining to the alloys concerned, are selected. Thereby a "calculated" data set  $z(\chi)$  results. Clearly, this indirect procedure requires that the density of the initial  $z$  array is much larger than that of the array of experimental  $\chi$  values. When performing the numerical/indirect method, there are two options for the  $z$ - $\chi$  (triple defect model) or the  $z$ - $\chi$ - $y_B$  (three defect types model) set, that is taken for the actual fitting to the experimental data of the vacancy concentration and the thermodynamic properties: one may either take the  $\chi$  values that come out of the computation of Eq. (3.12) (and Eq. (3.10)) or replace the calculated  $\chi$ - values by the experimental ones (while keeping the  $z$  (and  $y_B$ ) values corresponding to the calculated  $\chi$ -values; the  $z$  values (and  $y_B$  values) then become approximate ones.). If the fitting is carried out with a sufficiently dense array of  $z$  values, the difference in the results obtained by both options is insignificant.

For the *fitting to the measured data for the vacancy concentration*  $z$  one now calculates the difference, i.e. the error between the "calculated"  $z(\chi)$  and the experimental  $z(\chi)$  values. For the *fitting to the thermodynamic properties* (enthalpy of formation and thermodynamic activity values) one inserts the calculated  $z - \chi - y_B$  set into Eq. (3.4) (using Eq. (3.1)) and (3.11) and compares the calculated and experimental values of the enthalpy of formation and the activity by determining the differences. For both fittings then the procedure starts again with a new set for the parameters  $\Delta H_{AB}$ ,  $\Delta H_{BV}$ ,  $\Delta S_{AB}$  and  $\Delta S_{BV}$  and it is continued until the calculated differences are minimal.

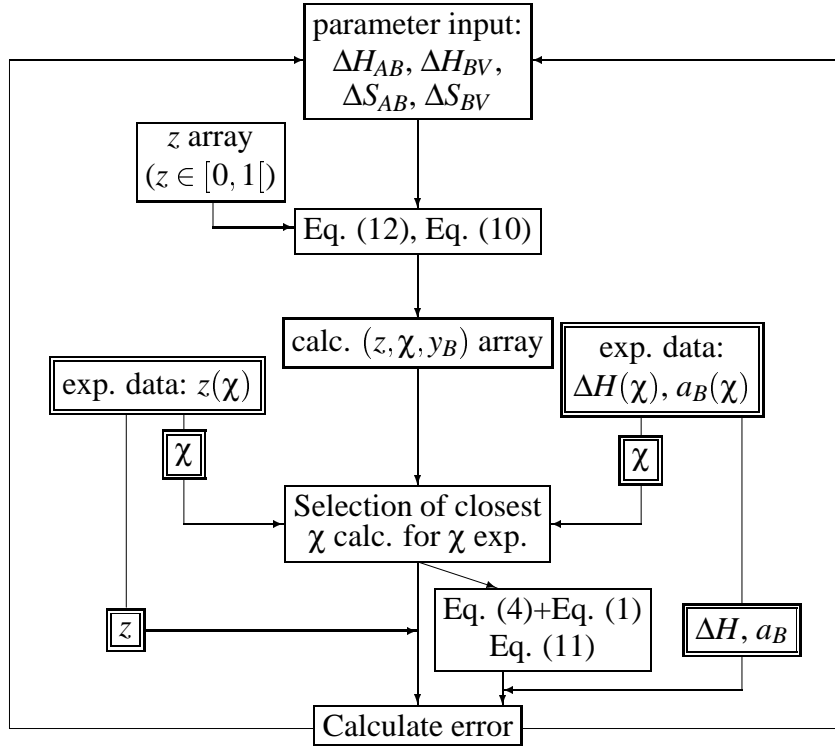


Figure 3.6: Scheme for the 'numerical/ indirect' procedure used in the fitting of the three defect types model; see text.

### 3.A.2 The "analytical/direct" procedure

For the "analytical/direct" procedure an appropriate mathematical software program is used that finds *directly* extensive analytical equations for the four roots of Eq. (3.12) for  $z$  (see Figure 3.7), for given parameters  $\Delta H_{AB}$ ,  $\Delta H_{BV}$ ,  $\Delta S_{AB}$  and  $\Delta S_{BV}$  and a given temperature  $T$ .

In the present work the symbolic math toolbox supplementing the MATLAB 5 [44] environment that combines MATLAB with the computational engine of MAPLE V Release 4 [45] was applied successfully. Inserting the experimental  $\chi$  values into the equations of the four roots of Eq. (3.12) for  $z$ , the four possible  $z$ - $y_B$ - $\chi$  arrays are computed. There can be only one positive root for  $z$  (see introduction of the Appendix) and this root (that can be real or complex) is selected. If the root is complex, it is accepted if the imaginary part can be neglected (see footnote of Table 2).

The fittings to the vacancy concentration or to the thermodynamic properties then proceed as described for the numerical/indirect method (see Section 3.A.1).

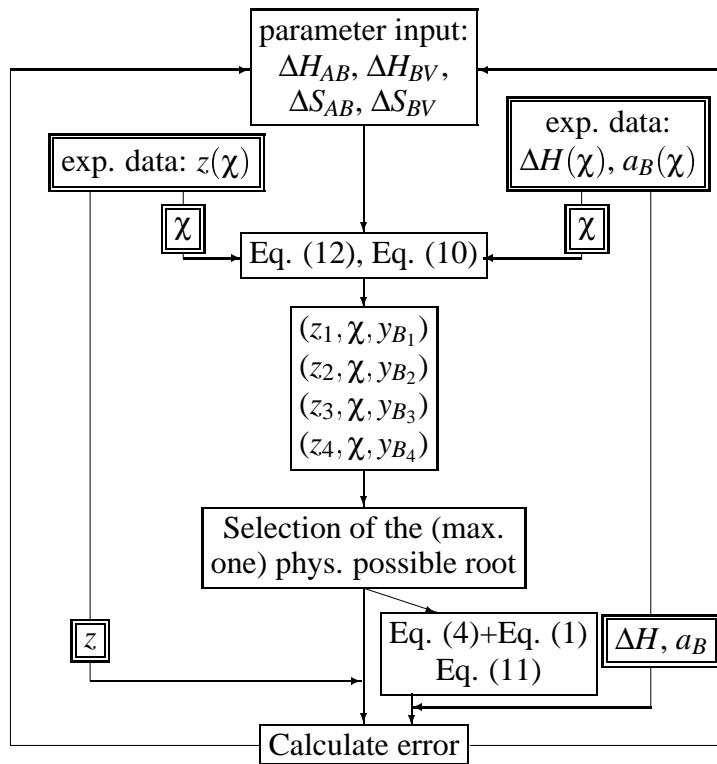


Figure 3.7: Scheme for the 'analytical/direct' procedure used in the fitting of the three defect types model; see text.



*Thermodynamics of ordering in  
intermetallics*  
*–A new life for pair interaction  
models?–*

*J. Breuer, F. Sommer and E. J. Mittemeijer*

**Abstract:** A pair interaction model applying the Bragg-Williams approach is presented. The formalism is given in a general form; ternary ordered compounds with different crystal structures and all possible point defect types are considered. Some applications are discussed. As compared with other statistical-thermodynamic methods (Wagner-Schottky approach, grand canonical thermodynamic formalism combined with *ab initio* calculations), the Bragg-Williams approach is an easily applicable formalism that leads- proper use supposed- to accurate predictions concerning thermodynamic data as well as defect concentrations.



## 4.1 Introduction

Ordered intermetallic compounds draw great interest at the present time because of both possible applications and fundamental scientific importance. The scientific interest is derived from the recognition that many intermetallics exhibit considerable ranges of nonstoichiometry which correspond to the presence of constitutional point defects which are temperature independent. Additional to these constitutional point defects thermally activated point defects can occur. The total defect structure (i.e. the types and the concentrations of the point defects) determines important properties of the intermetallic compounds (e.g. all diffusion dependent properties). Hence, for understanding and control of these properties a detailed knowledge of the defect structure in intermetallic compounds as function of composition and temperature within the homogeneity range of the compounds is a prerequisite [10].

In intermetallic compounds the most important point defects generally assumed are vacancies and antistructure atoms, i.e. atoms occupying a "wrong" site in the ordered crystal structure, occur. To our knowledge the existence of atoms located on interstitial sites has not been observed and discussed in literature so far.

The experimental analysis of the defect structure of intermetallic compounds is difficult: other than in elementary metals, where in many cases monovacancies dominate as point defects at least in some temperature range, in intermetallics more than one type of point defect can occur: different types of point defects are created simultaneously in order to maintain the ordered structure (see e.g. [29]). Different experimental techniques may be used for the determination of the various defect concentrations (for a survey, see e.g. [46]). The absolute concentration of vacancy type defects can be determined by comparison of thermal expansion data measured by X-ray diffraction and by dilatometry (unit cell size change vs volume/length change) [47, 48]. Positron annihilation experiments [49] provide a sensitive means for the study of vacancies too. Other possible experiments for the determination of point defects involve intensity methods using X-ray diffraction [27], field ion microscopy [50], magnetic susceptibility [35] and Mössbauer measurements [51]. Despite of the large number of available experimental methods, many of these methods provide only information on "effective" defect properties (i.e. they respond to the total defect structure) and often they can be applied only in a certain defect concentration window.

The theoretical analysis of the defect structure of intermetallic compounds may be subdivided into two groups: statistical methods associated with *ab initio* calculations and statistical methods associated with *experimentally* measured data (see [6]).

In the *ab initio* statistical methods (see e.g. [38]) an expression for the grand canonical potential is minimized with respect to the defect concentrations. The input parameters are defect energy parameters which are obtained by *ab initio* calculations. The defect formation entropies are neglected.

In the second group of statistical methods (for a survey, see [52]) an expression for the free energy as a function of the various defect concentrations is minimized with

respect to the defect concentrations. The input parameters appearing in the expression for the free energy are determined by fitting the theoretical expressions to experimental data. In approaches based on the Bragg-Williams concept [5] the input parameters are the energies of interaction of neighbouring atoms (and the corresponding entropy parameters, see [29]). In approaches based on the Wagner-Schottky concept [8] the input parameters are the concentrations of antisite atoms on each of the sublattices and the total vacancy concentration (combining the sublattices) at the stoichiometric composition and at the considered temperature (i.e. in this case the input parameters include information on both the energy and the entropy). Other possible input parameters in Wagner-Schottky approaches are the enthalpies of formation of the four types of point defects (neglecting defect formation entropies) [18].

In both types of statistical methods, i.e. using *ab initio* calculations or experimental data, it is assumed that the input parameters are independent of the defect concentrations and of the temperature.

Our group has recently carried out a study on statistical thermodynamics of intermetallic compounds on the basis of a Bragg-Williams approach. The proposed modelling was successfully applied to B2 compounds, namely B2-NiAl and B2-CoAl, using measured thermodynamic properties and defect concentrations [29]. On the same basis a successful model description of the ternary B2 phase (Ni,Co)Al was possible [29]. A drawback of the Bragg-Williams calculations performed until now is that it is assumed from the beginning what types of defects occur in the intermetallic compound. However, in principle the Bragg-Williams approach can be easily generalized avoiding such restriction [40]. The present paper reports such an extension of the model for a ternary  $(A,C)_mB_n$  compound that is composed of two sublattices. The treatment parallels to a certain extent the one given in [40], but here the role of the vibrational entropy is included and it is not limited to the B2 structure. With the new, general model the essential equations for three common ordered structures (B2, L1<sub>0</sub> and L1<sub>2</sub>) can be derived easily. Applications of the model to B2-NiAl, B2-(Ni,Co)Al and B2-FeAl are presented in Section 3. Section 4 provides an evaluation of the different statistical methods, i.e. employing either *ab initio* calculations or applying the Bragg-Williams or Wagner-Schottky approaches. The discussion about applicability and outcome of pair interaction models based on the Bragg-Williams approach emphasizes its role as an easily utilized and powerful tool in the determination of defect concentrations from thermodynamic properties.

## 4.2 Theory

### 4.2.1 The model

Consider a ternary compound whose chemical formula is  $(A,C)_mB_n$ . Then the following definitions and assumptions are used for describing its (defect) structure.

- A. The total numbers of A, B and C atoms in the crystal are  $N_A$ ,  $N_B$  and  $N_C$ , respec-



tively.  $N$  denotes the constant total number of atoms (here one mole of atoms is considered, so  $N = \text{Avogadro's number}$ ):  $N \equiv N_A + N_B + N_C$ .

- B. The overall composition of the ternary system is specified by two composition variables  $\chi \equiv \frac{N_B}{N} - \frac{n}{m+n} = -\frac{N_A+N_C}{N} + \frac{m}{m+n}$  and  $\psi \equiv N_A/(N_A + N_C)$ .
- C. The defects considered are A and C atoms on the  $\beta$  sublattice (numbers:  $N_A^\beta$ ,  $N_C^\beta$ ), B atoms on the  $\alpha$  sublattice (number:  $N_B^\alpha$ ) and vacancies on the  $\alpha$  sublattice (number:  $N_\square^\alpha$ ) and on the  $\beta$  sublattice (number:  $N_\square^\beta$ ).
- D. The crystal consists of  $m$   $\alpha$  sites and  $n$   $\beta$  sites. In the ideal crystal (i.e. the defect free crystal that can only exist at the stoichiometric composition at 0 K) all A and C atoms occupy all  $\alpha$  sublattice sites, while all B atoms occupy all  $\beta$  sublattice sites. The total number of sites  $N_S$ ,  $N_S = N + N_\square = N + N_\square^\alpha + N_\square^\beta$ , is variable.
- E. The concentration of A atoms plus C atoms on the  $\beta$  sublattice is defined as  $y_A \equiv \frac{N_A^\beta + N_C^\beta}{N}$  and the concentration of B atoms on the  $\alpha$  sublattice is defined as  $y_B \equiv \frac{N_B^\alpha}{N}$ , respectively. The vacancy concentration on the  $\alpha$  sublattice is defined as  $z_\alpha \equiv \frac{N_\square^\alpha}{N}$  and the vacancy concentration on the  $\beta$  sublattice is defined as  $z_\beta \equiv \frac{N_\square^\beta}{N}$ . The total concentration of vacancies,  $z$ , is given by  $z = z_\alpha + z_\beta$ .
- F. The probability of forming antistructure atoms is the same for A and C. The probability of forming vacancies on the  $\alpha$  sublattice does not depend on whether the site is occupied initially by an A or a C atom. Note that this restriction can be easily suspended by inserting a parameter that indicates the probability that an A atom rather than a C atom forms an antistructure atom. Here, this parameter is equal to one.
- G. For small deviations from the stoichiometric composition the concentration of defects is small. Then it can be supposed that the defects are randomly distributed and do not interact. Therefore, enthalpy and entropy contributions containing  $z$ ,  $z_\alpha$ ,  $z_\beta$ ,  $y_A$ ,  $y_B$  and/ or  $\chi$  in the second or higher power are neglected. The approximation  $1/(1+z) \approx 1-z$  is applied.

The numbers of atoms and vacancies on the  $\alpha$  and  $\beta$  sublattice can be expressed in terms of  $N$ ,  $y_A$ ,  $y_B$ ,  $z_\alpha$ ,  $z_\beta$ ,  $z$  and  $\chi$ ; see the expressions in Table 4.1.

Table 4.1: Numbers of atoms and vacancies on the  $\alpha$ - and  $\beta$ -sublattice.

	$\alpha$ -sites	$\beta$ -sites	total number of sites
A atoms	$N_A^\alpha = \Psi\left(\frac{m}{m+n}\right)N\left[1 - (\chi + y_A)\binom{m+n}{m}\right]$	$N_A^\beta = \Psi\left(\frac{n}{m+n}\right)Ny_A\binom{m+n}{n}$	$N_A = \Psi\left(\frac{m}{m+n} - \chi\right)N$
C atoms	$N_C^\alpha = (1 - \Psi)\left(\frac{m}{m+n}\right)N\left[1 - (\chi + y_A)\binom{m+n}{m}\right]$	$N_C^\beta = (1 - \Psi)\left(\frac{n}{m+n}\right)Ny_A\binom{m+n}{n}$	$N_C = (1 - \Psi)\left(\frac{m}{m+n} - \chi\right)N$
B atoms	$N_B^\alpha = \left(\frac{m}{m+n}\right)Ny_B\binom{m+n}{m}$	$N_B^\beta = \left(\frac{n}{m+n}\right)N\left[1 - (y_B - \chi)\binom{m+n}{n}\right]$	$N_B = (\chi + \frac{n}{m+n})N$
Vacancies	$N_\square^\alpha = \left(\frac{m}{m+n}\right)Nz\alpha\binom{m+n}{m}$	$N_\square^\beta = \left(\frac{n}{m+n}\right)Nz\beta\binom{m+n}{n}$	$N_\square = N(z\alpha + z\beta)$
Total sites	$N^\alpha = \left(\frac{m}{m+n}\right)N_S = \left(\frac{m}{m+n}\right)N(1+z)$	$N^\beta = \left(\frac{n}{m+n}\right)N_S = \left(\frac{n}{m+n}\right)N(1+z)$	$N_S = N(1+z)$

The site- number conditions (i.e.  $N^\alpha = (\frac{m}{m+n})N_S$  and  $N^\beta = (\frac{n}{m+n})N_S$ ) lead to the following relationships between the defect concentrations:

$$z_\alpha = \left(\frac{m}{m+n}\right)z + \chi + y_A - y_B \quad (4.1a)$$

$$z_\beta = \left(\frac{n}{m+n}\right)z - \chi - y_A + y_B. \quad (4.1b)$$

In view of Eqs. (4.1a) and (4.1b), it follows that only three of the five unknown concentrations,  $z_\alpha$ ,  $z_\beta$ ,  $z$ ,  $y_A$  and  $y_B$ , can be considered as independent variables. Since the total vacancy concentration  $z$  and the concentration of antistructure atoms on both sublattices,  $y_A$  and  $y_B$ , seem to be the quantities that can most easily be obtained experimentally, one can choose these concentrations as independent variables.

According to the Bragg-Williams approach, the interaction of (only) pairs of atoms is considered (a vacancy is considered as an "atom"). The interaction enthalpy and the vibrational or phonical entropy of each type of bond between pairs of atoms is assumed to be independent of composition and temperature.

For the enthalpy of the intermetallic compound, nearest and next-nearest-neighbour interactions are considered. The general expression for the enthalpy then is

$$H = \sum_{ij} n_{ij} h_{ij} + \sum_{ij} n'_{ij} h'_{ij} \quad (4.2)$$

where  $n_{ij}$  is the number of nearest-neighbour pairs  $i - j$  and  $h_{ij}$  is the corresponding interaction enthalpy ( $i$  and  $j$  can be A, B or C atoms, or vacancies  $\square$ ), and the analogous terms for the next-nearest-neighbour interaction are represented by  $n'_{ij}$  and  $h'_{ij}$ .

On the basis of the relations given in Table 4.1 for the numbers of atoms and vacancies on the  $\alpha$  and  $\beta$  sublattices and taking into consideration the coordination number  $Z$  for nearest-neighbour pairs and  $Z'$  for next-nearest-neighbour pairs, the following expression is obtained for the enthalpy  $H$ :

$$\begin{aligned} H = & \frac{NZ}{2} \left[ \psi^2 y_A \left(\frac{m}{n} + 1\right) h_{AA} + (1 - \psi)^2 y_A \left(\frac{m}{n} + 1\right) h_{CC} + \psi(1 - \psi) y_A \left(\frac{m}{n} + 1\right) h_{AC} + \right. \\ & + \psi \left(1 - y_A \left(\frac{n}{m} + 1\right) - y_B \left(\frac{m}{n} + 1\right) - \chi \left(\frac{n}{m} - \frac{m}{n}\right) - z\right) h_{AB} + \\ & + (1 - \psi) \left(1 - y_A \left(\frac{n}{m} + 1\right) - y_B \left(\frac{m}{n} + 1\right) - \chi \left(\frac{n}{m} - \frac{m}{n}\right) - z\right) h_{BC} + \\ & + \psi z_\beta \left(\frac{m}{n} + 1\right) h_{A\square} + (1 - \psi) z_\beta \left(\frac{m}{n} + 1\right) h_{C\square} + z_\alpha \left(\frac{n}{m} + 1\right) h_{B\square} + \\ & \left. + y_B \left(\frac{n}{m} + 1\right) h_{BB} \right] + \dots \end{aligned}$$

$$\begin{aligned}
& \dots + \frac{NZ'}{2} [\psi^2 (1 - 2(\chi + y_A) (\frac{m+n}{m}) - z) h'_{AA} + (1 - \psi)^2 \cdot \\
& \cdot (1 - 2(\chi + y_A) (\frac{m+n}{m}) - z) h'_{CC} + \\
& + \psi(1 - \psi) (1 - 2(\chi + y_A) (\frac{m+n}{m}) - z) h'_{AC} + \\
& + \psi ((\frac{m+n}{m}) y_B + (\frac{m+n}{n}) y_A) h'_{AB} + (1 - \psi) ((\frac{m+n}{m}) y_B + (\frac{m+n}{n}) y_A) h'_{BC} + \\
& + \psi (\frac{m+n}{m}) z_\alpha h'_{A\Box} + (1 - \psi) (\frac{m+n}{m}) z_\alpha h'_{C\Box} + (\frac{m+n}{n}) z_\beta h'_{B\Box} + \\
& + (1 - 2(y_B - \chi) (\frac{m+n}{n}) - z) h'_{BB}] \tag{4.3}
\end{aligned}$$

The entropy consists of the configurational entropy  $S^c$  and the vibrational (phonon) entropy  $S^v$ :

$$S = S^c + S^v \tag{4.4}$$

For the configurational entropy,  $S^c$ , a random distribution of each species on the two sublattices is assumed. On the basis of the relations given in Table 4.1 for the numbers of atoms and vacancies on the  $\alpha$  and  $\beta$  sublattices, and applying Stirling's approximation to the Boltzmann equation for the entropy, it is obtained:

$$\begin{aligned}
S^c = & R \left\{ \left( \frac{m}{m+n} \right) \left[ z + (\chi + y_A) \left( \frac{m+n}{m} \right) \right] \ln \left( \frac{m}{m+n} \right) + \right. \\
& + \left( \frac{n}{m+n} \right) \left[ z + (y_B - \chi) \left( \frac{m+n}{n} \right) \right] \ln \left( \frac{n}{m+n} \right) + \\
& + (1+z) \ln(1+z) - [y_A \ln y_A + y_B \ln y_B + z_\alpha \ln z_\alpha + z_\beta \ln z_\beta] + \\
& - \left( \frac{m}{m+n} \right) \left[ 1 - (\chi + y_A) \left( \frac{m+n}{m} \right) \right] \ln \left( 1 - (\chi + y_A) \left( \frac{m+n}{m} \right) \right) + \\
& - \left( \frac{n}{m+n} \right) \left[ 1 - (y_B - \chi) \left( \frac{m+n}{n} \right) \right] \ln \left( 1 - (y_B - \chi) \left( \frac{m+n}{n} \right) \right) + \\
& - \psi \left[ \left( \frac{m}{m+n} \right) \left[ 1 - (\chi + y_A) \left( \frac{m+n}{m} \right) \right] + y_A \right] \ln(\psi) + \\
& \left. - (1 - \psi) \left[ \left( \frac{m}{m+n} \right) \left[ 1 - (\chi + y_A) \left( \frac{m+n}{m} \right) \right] + y_A \right] \ln(1 - \psi) \right\}, \tag{4.5}
\end{aligned}$$

where  $R = Nk$ , with  $k$  as Boltzmann's constant. Analogous to the enthalpy (see above), the total vibrational entropy is written as

$$S^v = \sum_{ij} n_{ij} s_{ij} + \sum_{ij} n'_{ij} s'_{ij}, \tag{4.6}$$

where the entropy parameters for the nearest and next-nearest-neighbour interaction are denoted by  $s_{ij}$  and  $s'_{ij}$ , respectively. Accordingly, an expression analogous to Eq. (4.3) holds for  $S^v$ . The given formulation of the vibrational entropy as a linear function

of the number of pairs found in the crystal structure (Eq. (4.6)) lacks a strong physical foundation. However, since in the following not the individual parameters  $s_{ij}$  and  $s'_{ij}$  are dealt with, but rather certain combinations of  $s_{ij}$  and  $s'_{ij}$  that have a well-defined physical meaning (see the discussion in Section 4), the given definition may serve as a valid approach.

Thermodynamic equilibrium at constant temperature and pressure requires the Gibbs energy  $G$  to be minimal. Thus the equilibrium defect concentrations at a specific temperature, pressure and overall composition can be obtained by minimizing  $G$  with respect to the three independent defect concentrations  $z$ ,  $y_A$  and  $y_B$ . After substitution of the above derived expressions for  $H$  (Eq. (4.3)) and  $S$  (Eqs. (4.4)-(4.6)) in the Gibbs-Helmholtz relationship  $G = H - TS$  and applying the minimization conditions ( $\partial G/\partial z = 0$ ,  $\partial G/\partial y_A = 0$  and  $\partial G/\partial y_B = 0$ ) one obtains:

$$\begin{aligned}
& \frac{1}{2}NZ[-\psi h_{AB} - (1 - \psi)h_{BC} + \\
& \quad + \psi\left(\frac{n}{m+n}\right)\left(\frac{m}{n} + 1\right)h_{A\Box} + (1 - \psi)\left(\frac{n}{m+n}\right)\left(\frac{m}{n} + 1\right)h_{C\Box} + \left(\frac{m}{m+n}\right)\left(\frac{n}{m} + 1\right)h_{B\Box}] + \\
& + \frac{1}{2}NZ[-\psi^2 h'_{AA} - (1 - \psi)^2 h'_{CC} - \psi(1 - \psi)h'_{AC} + \psi h'_{A\Box} + (1 - \psi)h'_{C\Box} + h'_{B\Box} - h'_{BB}] + \\
& - \frac{1}{2}NZT[-\psi s_{AB} - (1 - \psi)s_{BC} + \\
& \quad + \psi\left(\frac{n}{m+n}\right)\left(\frac{m}{n} + 1\right)s_{A\Box} + (1 - \psi)\left(\frac{n}{m+n}\right)\left(\frac{m}{n} + 1\right)s_{C\Box} + \left(\frac{m}{m+n}\right)\left(\frac{n}{m} + 1\right)s_{B\Box}] + \\
& - \frac{1}{2}NZ'T[-\psi^2 s'_{AA} - (1 - \psi)^2 s'_{CC} - \psi(1 - \psi)s'_{AC} + \psi s'_{A\Box} + (1 - \psi)s'_{C\Box} + s'_{B\Box} - s'_{BB}] \\
& = RT\left[\left(\frac{m}{m+n}\right)\ln\left(\frac{m}{m+n}\right) + \left(\frac{n}{m+n}\right)\ln\left(\frac{n}{m+n}\right) + \ln(1+z) + \right. \\
& \quad \left. - \left(\frac{m}{m+n}\right)\ln\left(\frac{mz}{m+n} + \chi + y_A - y_B\right) - \left(\frac{n}{m+n}\right)\ln\left(\frac{nz}{m+n} - \chi - y_A + y_B\right)\right] \quad (4.7a)
\end{aligned}$$

$$\begin{aligned}
& \frac{1}{2}NZ\left[\psi^2\left(\frac{m}{n} + 1\right)h_{AA} + (1 - \psi)^2\left(\frac{m}{n} + 1\right)h_{CC} + \psi(1 - \psi)\left(\frac{m}{n} + 1\right)h_{AC} + \right. \\
& \quad + \psi\left(-\frac{n}{m} - 1\right)h_{AB} + (1 - \psi)\left(-\frac{n}{m} - 1\right)h_{BC} + \\
& \quad \left. - \psi\left(\frac{m}{n} + 1\right)h_{A\Box} - (1 - \psi)\left(\frac{m}{n} + 1\right)h_{C\Box} + \left(\frac{n}{m} + 1\right)h_{B\Box}\right] + \\
& + \frac{1}{2}NZ\left[-2\psi^2\left(\frac{m+n}{m}\right)h'_{AA} - 2(1 - \psi)^2\left(\frac{m+n}{m}\right)h'_{CC} - 2\psi(1 - \psi)\left(\frac{m+n}{m}\right)h'_{AC} + \right. \\
& \quad + \psi\left(\frac{m+n}{n}\right)h'_{AB} + (1 - \psi)\left(\frac{m+n}{n}\right)h'_{BC} + \\
& \quad \left. + \psi\left(\frac{m+n}{m}\right)h'_{A\Box} + (1 - \psi)\left(\frac{m+n}{m}\right)h'_{C\Box} - \left(\frac{m+n}{n}\right)h'_{B\Box}\right] + \dots
\end{aligned}$$

$$\begin{aligned}
& \dots - \frac{1}{2}NZT \left[ \psi^2 \left( \frac{m}{n} + 1 \right) s_{AA} + (1 - \psi)^2 \left( \frac{m}{n} + 1 \right) s_{CC} + \psi(1 - \psi) \left( \frac{m}{n} + 1 \right) s_{AC} + \right. \\
& \quad \left. + \psi \left( -\frac{n}{m} - 1 \right) s_{AB} + (1 - \psi) \left( -\frac{n}{m} - 1 \right) s_{BC} + \right. \\
& \quad \left. - \psi \left( \frac{m}{n} + 1 \right) s_{A\Box} - (1 - \psi) \left( \frac{m}{n} + 1 \right) s_{C\Box} + \left( \frac{n}{m} + 1 \right) s_{B\Box} \right] + \\
& - \frac{1}{2}NZ'T \left[ -2\psi^2 \left( \frac{m+n}{m} \right) s'_{AA} - 2(1 - \psi)^2 \left( \frac{m+n}{m} \right) s'_{CC} - 2\psi(1 - \psi) \left( \frac{m+n}{m} \right) s'_{AC} + \right. \\
& \quad \left. + \psi \left( \frac{m+n}{n} \right) s'_{AB} + (1 - \psi) \left( \frac{m+n}{n} \right) s'_{BC} + \right. \\
& \quad \left. + \psi \left( \frac{m+n}{m} \right) s'_{A\Box} + (1 - \psi) \left( \frac{m+n}{m} \right) s'_{C\Box} - \left( \frac{m+n}{n} \right) s'_{B\Box} \right] \\
& = RT \left[ \ln \left( \frac{m}{m+n} \right) - \ln(y_A) - \ln \left( \frac{mz}{m+n} + \chi + y_A - y_B \right) + \right. \\
& \quad \left. + \ln \left( \frac{nz}{m+n} - \chi - y_A + y_B \right) + \ln \left( 1 - \frac{(\chi + y_A)(m+n)}{m} \right) \right] \tag{4.7b}
\end{aligned}$$

$$\begin{aligned}
& \frac{1}{2}NZ \left[ \psi \left( -\frac{m}{n} - 1 \right) h_{AB} + (1 - \psi) \left( -\frac{m}{n} - 1 \right) h_{BC} + \right. \\
& \quad \left. + \psi \left( \frac{m}{n} + 1 \right) h_{A\Box} + (1 - \psi) \left( \frac{m}{n} + 1 \right) h_{C\Box} - \left( \frac{n}{m} + 1 \right) h_{B\Box} + \left( \frac{n}{m} + 1 \right) h_{BB} \right] + \\
& + \frac{1}{2}NZ' \left[ \psi \left( \frac{m+n}{m} \right) h'_{AB} + (1 - \psi) \left( \frac{m+n}{m} \right) h'_{BC} + \right. \\
& \quad \left. - \psi \left( \frac{m+n}{m} \right) h'_{A\Box} - (1 - \psi) \left( \frac{m+n}{m} \right) h'_{C\Box} + \left( \frac{m+n}{n} \right) h'_{B\Box} - 2 \left( \frac{m+n}{n} \right) h'_{BB} \right] + \\
& - \frac{1}{2}NZT \left[ \psi \left( -\frac{m}{n} - 1 \right) s_{AB} + (1 - \psi) \left( -\frac{m}{n} - 1 \right) s_{BC} + \right. \\
& \quad \left. + \psi \left( \frac{m}{n} + 1 \right) s_{A\Box} + (1 - \psi) \left( \frac{m}{n} + 1 \right) s_{C\Box} - \left( \frac{n}{m} + 1 \right) s_{B\Box} + \left( \frac{n}{m} + 1 \right) s_{BB} \right] + \\
& - \frac{1}{2}NZ'T \left[ \psi \left( \frac{m+n}{m} \right) s'_{AB} + (1 - \psi) \left( \frac{m+n}{m} \right) s'_{BC} + \right. \\
& \quad \left. - \psi \left( \frac{m+n}{m} \right) s'_{A\Box} - (1 - \psi) \left( \frac{m+n}{m} \right) s'_{C\Box} + \left( \frac{m+n}{n} \right) s'_{B\Box} - 2 \left( \frac{m+n}{n} \right) s'_{BB} \right] \\
& = RT \left[ \ln \left( \frac{n}{m+n} \right) - \ln(y_B) + \ln \left( \frac{mz}{m+n} + \chi + y_A - y_B \right) + \right. \\
& \quad \left. - \ln \left( \frac{nz}{m+n} - \chi - y_A + y_B \right) + \ln \left( 1 - \frac{(y_B - \chi)(m+n)}{n} \right) \right]. \tag{4.7c}
\end{aligned}$$

The value of the Gibbs energy of component  $i$  ( $i = A, C$  or  $B$ ),  $G_i$ , is related to the thermodynamic activity,  $a_i$ , by

$$G_i = G_i^0 + RT \ln a_i, \tag{4.8}$$

where  $G_i^0$  is the partial Gibbs energy of component  $i$  in a standard state. On the other hand, the partial Gibbs energy of component  $i$ ,  $G_i$ , in a ternary system is derived from

the free enthalpy,  $G$ , as

$$G_A = G + \left(1 - \frac{N_A}{N}\right)N \frac{\partial G}{\partial N_A} - \frac{N_B}{N}N \frac{\partial G}{\partial N_B} \quad (4.9a)$$

$$G_B = G - \frac{N_A}{N}N \frac{\partial G}{\partial N_A} + \left(1 - \frac{N_B}{N}\right)N \frac{\partial G}{\partial N_B} \quad (4.9b)$$

$$G_C = G - \frac{N_A}{N}N \frac{\partial G}{\partial N_A} - \frac{N_B}{N}N \frac{\partial G}{\partial N_B}, \quad (4.9c)$$

where the independent variables are  $N_A$  and  $N_B$ . By changing the concentration variables to those used here, i.e.  $\chi$  and  $\psi$ , the equations (4.9a-c) take the following form:

$$G_A = G - \psi \left[ -\frac{1}{\psi \left(\frac{m}{m+n} - \chi\right)} + 1 + \frac{\chi + \frac{n}{m+n}}{\frac{m}{m+n} - \chi} \right] \frac{\partial G}{\partial \psi} - \left(\chi + \frac{n}{m+n}\right) \frac{\partial G}{\partial \chi} \quad (4.10a)$$

$$G_B = G + \left(\frac{m}{m+n} - \chi\right) \frac{\partial G}{\partial \chi} \quad (4.10b)$$

$$G_C = G - \psi \left[ 1 + \frac{\chi + \frac{n}{m+n}}{\frac{m}{m+n} - \chi} \right] \frac{\partial G}{\partial \psi} - \left(\chi + \frac{n}{m+n}\right) \frac{\partial G}{\partial \chi}. \quad (4.10c)$$

Inserting the above derived expression for  $G$  (Eqs. (4.2-4.6)) into Eqs. (4.10a-c), the thermodynamic activity of component  $i$  can readily be calculated.

The experimentally accessible (e.g. by solution calorimetry) enthalpy of formation  $\Delta H$  is given by

$$\Delta H = H - \left[ \psi \left(\frac{m}{m+n} - \chi\right) H_A + \left(\chi + \frac{n}{m+n}\right) H_B + (1 - \psi) \left(\frac{m}{m+n} - \chi\right) H_C \right], \quad (4.11)$$

where  $H_i$  ( $i = A, B, C$ ) are the enthalpies per mole of the pure elements at the same temperature and pressure as pertaining to  $H$  and  $\Delta H$ .

The model presented here is written in its most general form, i.e. occurrence of all *four* possible defect types (vacancies on the  $\alpha$  sublattice and on the  $\beta$  sublattice, A/C antistructure atoms on the  $\beta$  sublattice and B antistructure atoms on the  $\alpha$  sublattice) has been incorporated. If one or the other defect type does not occur (e.g. vacancies on the  $\beta$  sublattice can be neglected or B atoms do not occupy sites on the  $\alpha$  sublattice (e.g. because of their relatively large size)), the less general three defect types model (see Ref. [40, 53] for binary phases) or the triple defect model [29] follow directly from the equations derived here.

The treatment given here is restricted to the case of ternary alloys with *two* sublattices. Analogous results can be derived straightforwardly for the case of ordered alloys with more than two sublattices: e.g. a ternary  $A_2BC$  alloy that is constituted of *four* fcc sublattices with their origins at  $(000)$ ,  $(\frac{1}{2}\frac{1}{2}\frac{1}{2})$ ,  $(111)$  and  $(\frac{3}{2}\frac{3}{2}\frac{3}{2})$  in the overall fcc unit cell. The Heusler structure is then obtained by placing A atoms on the first and third sublattices, and B and C atoms on the second and fourth sublattices, respectively. If, further, B is identified with A, the  $DO_3$  structure, that is composed of *three* sublattices,

is obtained. If B is identified with C the B2 structure is obtained [54].

For the case that only antisite atoms occur as point defect and considering configurational entropy as the only entropy contribution, a generalized multi-component multi-sublattice model for intermetallic compounds has been given by [55].

For three common ordered structures constituted of two sublattices (B2, L1<sub>0</sub> and L1<sub>2</sub>) the model equations for the enthalpy of formation (Eqs. (4.3) and (4.11)), the thermodynamic activity (Eqs. (4.8) and (10)) and the three minimization conditions which govern the point defect concentrations (Eqs. (4.7a-c)) can be obtained easily by inserting the  $m$ ,  $n$ ,  $Z$  and  $Z'$  data given in Table 4.2.

Table 4.2:  $m$  and  $n$  numbers and coordination numbers for nearest ( $Z$ ) and next nearest neighbours ( $Z'$ ) of three ordered crystal structures.

Structure	Prototype	$m$	$n$	$Z$	$Z'$
B2	CsCl	1	1	8	6
L1 <sub>0</sub>	CuAu	1	1	12	6
L1 <sub>2</sub>	Cu <sub>3</sub> Au	3	1	12	6

## 4.3 Applications of the Bragg-Williams method

### 4.3.1 B2-NiAl

The B2 phase Ni<sub>1-x</sub>Al<sub>x</sub> exists on both sides of the stoichiometric composition Ni<sub>0.50</sub>Al<sub>0.50</sub>. The lattice parameter and density measurements given in Ref. [56] showed that the constitutional defects of B2-NiAl are likely as follows: on the Al-rich part of the stoichiometric composition vacancies occur at the Ni sublattice, whereas on the Ni-rich side Ni atoms substitute for Al atoms, i.e. Ni antistructure atoms are formed in the Al sublattice. Since in the B2 structure equal numbers of sites are required for the  $\alpha$  and  $\beta$  sublattices, the occurrence of one A (Ni) antistructure atom on an additional  $\beta$  (Al) sublattice site as compared to the stoichiometric composition has to be balanced by the introduction of two A (Ni) vacancies (one on the  $\alpha$  (Ni) sublattice site left by the A (Ni) atom now on the  $\beta$  (Al) sublattice and one generated for compensation of the additional A (Ni) sublattice site): such a combination of defects is called triple defect [2], which is a thermal defect.

The proposed general model given in Section 4.2 can be reduced to the triple defect model by setting  $y_A \equiv 0$  and  $z_\beta \equiv 0$ . Using very accurate enthalpy of formation data and activity data the model parameters  $h_{ij}$ ,  $h'_{ij}$ ,  $s_{ij}$  and  $s'_{ij}$  (i.e. including up to next-nearest-neighbour interactions) can be determined and the defect concentrations can be calculated. This was successfully undertaken by [29], who showed that taking



only nearest-neighbour interaction into account, *simultaneous* fitting of the enthalpy of formation data [11] and the thermodynamic activity data [12], both as a function of composition, leads to very good descriptions of the experimental input data: the difference between experimental and calculated (according to the triple defect model) data; referring to the absolute values of the thermodynamic activity data and the enthalpy of formation data; is shown in Fig. 4.1. Inserting the thereby obtained model parameters

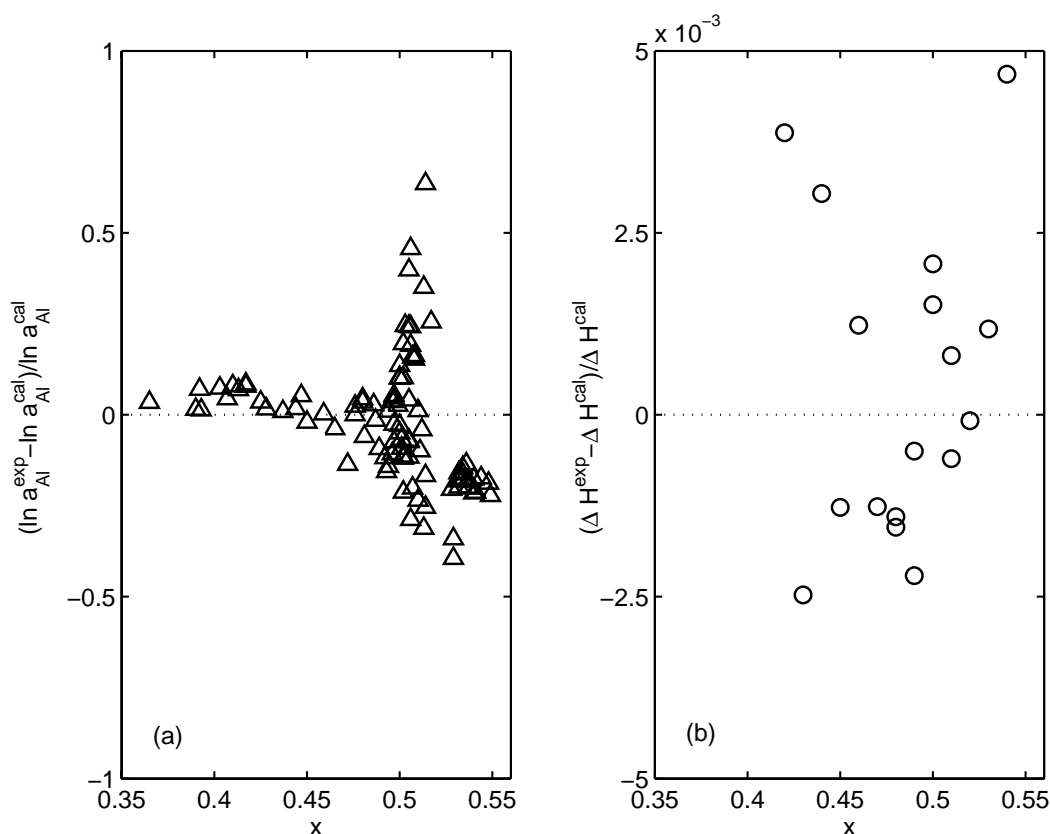


Figure 4.1:  $\text{Ni}_{1-x}\text{Al}_x$  ( $T=1273$  K), Triple defect model, parameters from [29]: (a) Difference in the experimentally determined natural logarithm of Al-activity and the calculated values, referring to the total value, as function of the atomic fraction Al,  $\Delta$  rectified (see [29]) data from [12], (b) Difference in the experimentally determined enthalpy of formation and the calculated values, referring to the total values, as function of the atomic fraction Al,  $\circ$  experimental data corrected (see [29]) from [11]

(three enthalpy parameters and three entropy parameters, see Ref. [29]) into the model equations, the defect concentrations were calculated as a function of composition (Fig. 4.2). The calculated defect concentration curves are fully consistent with almost all (see what follows) experimental data.

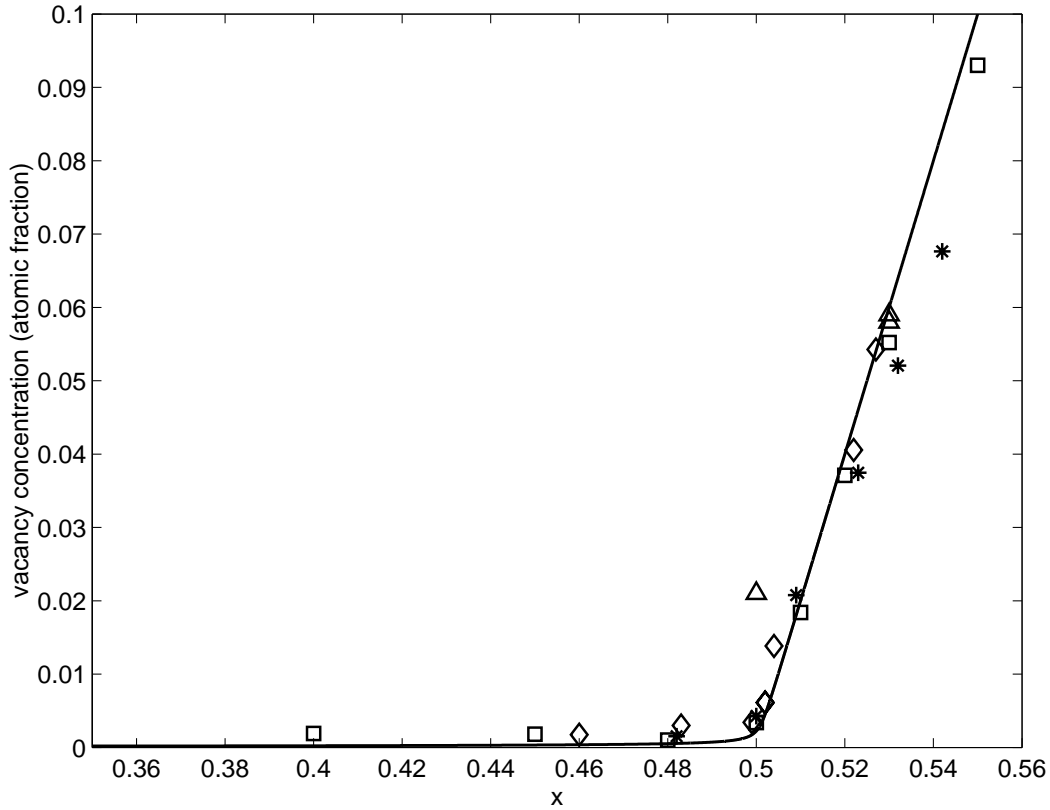


Figure 4.2:  $\text{Ni}_{1-x}\text{Al}_x$  ( $T=1273$  K), Triple defect model, parameters from [29]: Atomic fraction of vacancies, — as calculated, experimental data from X-ray/density/dilatometric measurements from different authors (\* Ref. [57],  $\square$  Ref. [30],  $\triangle$  Ref. [31],  $\diamond$  Ref. [56]).

Using the model with the obtained parameters, also calculations for temperatures other than the one pertaining to the thermodynamic input data can be performed. The thus obtained values for the effective enthalpy,  $h_{\square}^{eff}(\chi)$ , and entropy of formation of vacancies,  $s_{\square}^{eff}(\chi)$ , according to the Arrhenius relation  $z(\chi, T) = \exp(s_{\square}^{eff}(\chi)/k) \exp(-h_{\square}^{eff}(\chi)/kT)$ , agree very well with the results of ab initio calculations [58].

Recently, new experiments for the determination of the vacancy content from lattice parameter and density measurements for Al-rich B2-NiAl compounds (using powder samples) by [42, 57] resulted in vacancy concentration values lower than compatible with the triple defect model for the constitutional vacancies. This discrepancy was ascribed [28, 40] to the occurrence of Al antistructure atoms on the Ni sublattice. Then, to describe the experimentally determined vacancy concentration curve as a function of composition and temperature, the model described in Section 2 can be applied using  $z_{\beta} \equiv 0$ . The experimental data obtained at elevated temperatures could very well be described [28, 40]. However, inserting the model parameters obtained by fitting to the

vacancy concentration data as a function of composition at higher temperatures, the temperature dependence of the vacancy concentration as calculated by the model is unusual: at absolute zero temperature no vacancies would exist and all defects would be antistructure atoms. Raising the temperature by only a few degrees, the vacancy concentration shoots up to its almost temperature independent high level (see, e.g. Figure 2a in Ref. [40]). From a reanalysis [53] of the data set of [42, 57] and also incorporating data for the thermodynamic properties (enthalpy of formation data and thermodynamic activity data, see above) it was concluded that *all* available experimental data (i.e. enthalpy of formation data, thermodynamic activity data and vacancy concentration data of different authors (for references, see [53]), with the only exception of the data of [42, 57], can be described consistently with the (less general) triple defect model.

### 4.3.2 B2 phase (Ni,Co)Al

The binary B2 phase  $\text{Co}_{1-x}\text{Al}_x$  can be treated with the proposed Bragg-Williams model setting  $y_A \equiv 0$  and  $z_\beta \equiv 0$ , i.e. assuming triple defect behaviour and incorporating only nearest-neighbour interaction [29]. Adopting the nearest-neighbour interaction parameters as obtained for the binary phases B2-Ni $_{1-x}$ Al $_x$  and B2-Co $_{1-x}$ Al $_x$ , the enthalpy of formation curve for the ternary B2-phase (Ni,Co) $_{1-x}$ Al $_x$  [16] could be consistently described by allowing for two additional ternary enthalpy parameters: the interaction parameters for Ni and Co as nearest- and next-nearest neighbour pairs. This is a reasonable result because only nearest neighbour interaction between Ni and Co involves the formation of antistructure defects, since regularly Ni and Co atoms are located on the same sublattice.

### 4.3.3 B2 phase FeAl

The homogeneity range of the B2 phase Fe $_{1-x}$ Al $_x$  extends from about 25 to about 50 at.% Al at 1073 K [59]. In FeAl large numbers of vacancies were detected experimentally (see, e.g. [60] and references therein) even at the stoichiometric composition and for the Fe-rich compounds. It has accordingly been suggested that the defect structure of this compound may be considered as "hybrid" [9, 52], i.e. all four possible types of point defects would occur.

Recently, very accurate measurements of the enthalpy of formation as function of composition of Fe $_{1-x}$ Al $_x$  were conducted by our group [61]. An unusual discontinuity was found in the enthalpy of formation vs. composition curve at about 38 at.% Al, that seems to hint at a "phase transformation" occurring in the homogeneity range of the B2 phase. The model proposed in the present work departs from the stoichiometric composition; therefore in the present work only thermodynamic data (i.e. enthalpy of formation data and thermodynamic activity data) for B2-Fe $_{1-x}$ Al $_x$  phases with  $0.38 \leq x \leq 0.50$  at.% Al were used for the fitting.

The fitting of the model presented here in its most general form, i.e. considering all four possible point defect types, to, *simultaneously*, the enthalpy data and data for

the thermodynamic activity [52] (after measurements conducted by [62]) did not lead to satisfactory results. Although the number of data points was sufficiently large (this was ensured by adding hypothetical data that were obtained by linear interpolation of the measured data points, thus creating a continuous "experimental" data set), the final parameter set was not unique, also not if the fitting was performed to, simultaneously, all available data (i.e. not only to enthalpy of formation data and thermodynamic activity data but also including data for the vacancy concentration): the resulting values for the interaction parameters depended on the start values as well as on the numerical route followed.

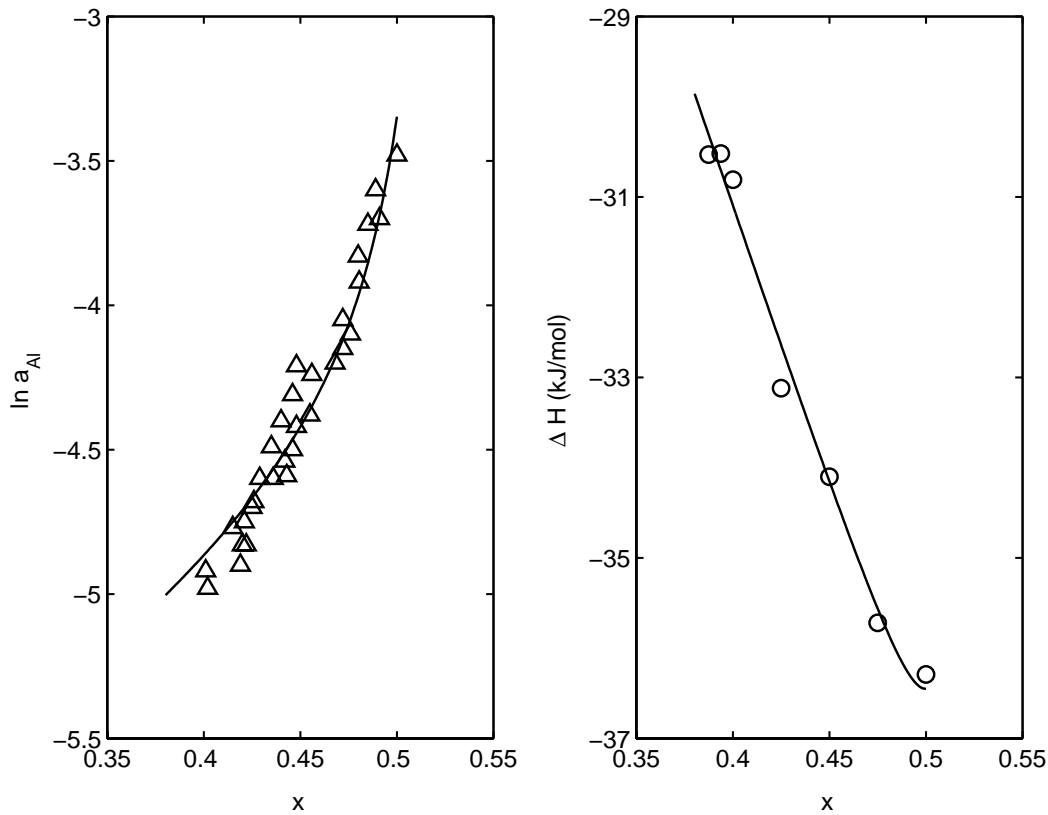


Figure 4.3:  $\text{Fe}_{1-x}\text{Al}_x$  ( $T=1073$  K), example of a fit considering all four possible types of point defects: (a) Natural logarithm of Al- activity as function of the atomic fraction Al,  $\triangle$  data from [52] (after measurements conducted by [62]), – fitted, (b) Enthalpy of formation as function of the atomic fraction Al,  $\circ$  data from [61], – fitted.

Details concerning the possible numerical routes considering *three* defect types (antistructure atoms on both sublattices, vacancies on the  $\alpha$  sublattice) can be found in the appendix of [53] and can easily be adapted for the application of the model incorporating *four* defect types (since the number of independent variables increases by one (two when considering three defect types, three when considering four defect types), so does

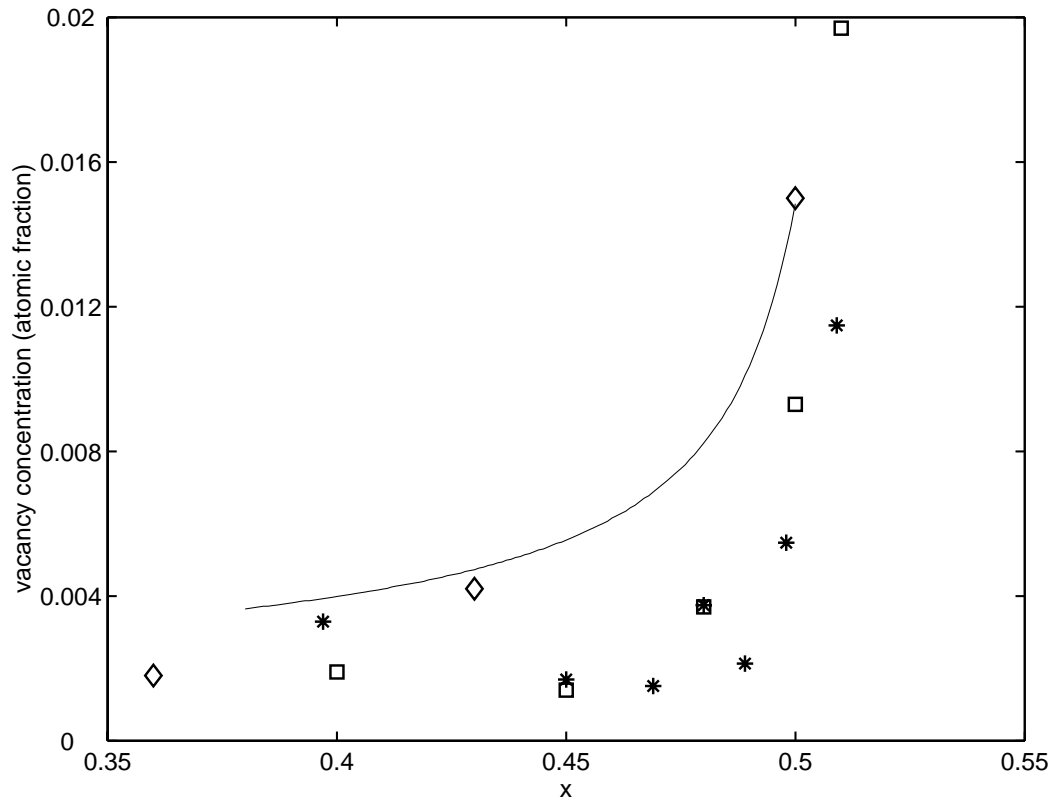


Figure 4.4:  $\text{Fe}_{1-x}\text{Al}_x$  ( $T=1073$  K): Calculated vacancy concentration as a function of composition corresponding to the simultaneous fit of thermodynamic activity and enthalpy of formation data shown in Fig. 4.3 (full line); experimental data from Refs. [48] ( $\diamond$ ), [60] ( $\square$ ) and [63] (\*).

the number of minimization conditions (see Eqs. (4.7a)-(4.7c)); therefore the number of the possible starting variable of the fitting procedure increases by one, yielding altogether three possible ways of starting the numerical routine.). As an example of the results of the fitting procedure considering all four possible point defects, the simultaneous fit of the model to the thermodynamic activity data and the enthalpy of formation data, both as a function of the composition, are shown in Fig. 4.3. The corresponding, calculated vacancy concentration as a function of the composition at the constant temperature pertaining to the data in Fig. 4.3, is shown in Fig. 4.4 and found to be in quite good agreement with the experimental data. However, the parameter set obtained by the fitting is not unique (see above). The inconclusiveness of the result appears to be due to the lack of experimental data on the Al-rich side of the homogeneity range of the phase concerned. To test this hypothesis hypothetical experimental data for the Al-rich alloys were used. Then the fitting was found to be unique, indeed. In any case it could be shown that the more simple three defect types model [53] (by setting  $z_\beta \equiv 0$ ) or the even more simple triple defect model (by setting  $y_A \equiv 0$  and  $z_\beta \equiv 0$ ) or the likewise

simple antistructure defect model (by setting  $z_\alpha \equiv 0$  and  $z_\beta \equiv 0$ ) cannot describe the data (enthalpy of formation, activity, vacancy concentration) in a consistent manner.

#### 4.3.4 Ordered compounds with other crystal structures

The model presented in the present paper can be applied to ordered compounds other than B2 ordered compounds (as considered in Sections 4.3.1-4.3.3) as well: e.g. TiAl (L1<sub>0</sub> crystal structure) or Ni<sub>3</sub>Al (L1<sub>2</sub>). From the results obtained for the B2-phases (see above) it is clear that successful application of the model requires availability of (very) accurate thermodynamic data at *both* sides of the stoichiometric composition. Further, it is noted here that the enthalpy of formation data largely determine the values obtained for the enthalpy parameters  $h_{ij}$  and  $h'_{ij}$ . A similar statement cannot be made for the entropy parameters  $s_{ij}$  and  $s'_{ij}$  that are significantly determined by both kinds of experimental thermodynamic data, i.e. the enthalpy of formation data and the thermodynamic activity data. At the moment, to our knowledge sufficiently accurate data are not available for any intermetallic compound other than B2 ordered compounds (see the examples discussed above). Our literature review shows that in most cases the enthalpy of formation data have been measured either in composition intervals too large to allow reliable interpolation or essentially lack the necessary accuracy.

### 4.4 Comparison: Wagner-Schottky, Bragg-Williams and ab-initio methods

When defects are introduced in a defect free crystalline solid, existing "ideal" interactions are replaced by other "imperfect" interactions. Thus the origin of the Bragg-Williams approach, that is based on the assumption that the total enthalpy (internal energy) of the crystal can be represented as a sum of the interaction energies of (nearest, next-nearest, next-next-nearest, ... etc.) neighbouring pairs of atoms may be understood. However, the restriction to nearest and next-nearest interactions only (i.e. incorporating  $h_{ij}$ ,  $h'_{ij}$ ,  $s_{ij}$ ,  $s'_{ij}$ , see above) affects a (direct) physical interpretation of the values obtained (by fitting) for the interaction parameters: the parameters in fact stand for some average response for all interactions occurring with all atoms in the lattice. Because the parameters do not have a direct physical meaning in the above sense, the Bragg-Williams approach may even be applicable when the defect concentrations in the ordered compound may be too large to be treated ab initio (see [3]).

Considering the enthalpy only, the ab-initio method may be physically more reasonable: here, the model parameters are defined as the difference in energy between the perfect crystal (without any defect) and the crystal with one of the four types of point defects (vacancy or one antistructure atom on one sublattice) built in. Using this approach, one faces the problem of arbitrariness of the zero-level of internal energy as pointed out by [6], i.e. the energy level for the perfect crystal cannot be calculated

directly.

In principle, the same difficulty is encountered using the Wagner-Schottky approach, that -as the formalism combined with ab-initio methods- departs from the approach that (at constant pressure) the internal energy of the crystal is a linear function of the numbers of atoms and vacancies. To circumvent the zero-level energy problem, Wagner-Schottky methods were formulated such that they describe thermodynamic data, particularly activity data and partial enthalpy of formation data, normalized with respect to their value at the stoichiometric composition. The thereby used parameters are the defect concentrations of the stoichiometric compounds, termed disorder parameters (see, e.g. [7]) or effective enthalpy of formation values of the point defects [18].

From the given discussion it is clear, that the fit parameters used in the present Bragg-Williams approach ( $h_{ij}$ ,  $h'_{ij}$ ,  $s_{ij}$ ,  $s'_{ij}$ ) cannot directly be related to the ab-initio defect energy parameters (see e.g. [6]). However, a comparison of parameters is possible if one turns to higher level parameters: the effective defect formation energies, describing the exponential temperature dependence of the defect concentration (i.e. Arrhenius-type equations), can be calculated according to the different approaches. This has been performed for the ternary triple defect model by [29] and explicit equations for the most general binary statistical point defect model have been derived by [41]. For the calculation of the effective enthalpy and entropy of formation of vacancies in the framework of the given model one may use the following recipe can be used: solve Eq. (2.7b) for  $y_B$ , insert into Eqs. (4.7a) and (4.7c), solve Eq. (4.7c) for  $y_A$  and insert into Eq. (4.7a), solve for  $z$ . (The (elaborate) analytical solution may be obtained using an appropriate mathematical software program, e.g. Maple V [45].) Then, from comparison of the obtained equation with the usual Arrhenius-type relation, one can identify the effective enthalpy and entropy of the vacancy formation.

Provided with sufficient experimental data for thermodynamic properties (i.e. enthalpy of formation data and data for the thermodynamic activity), that allow reliable assessment of the interaction parameters, the statistical method based on the Bragg-Williams approach provides a powerful instrument for the determination of types and concentrations of point defects. As follows from the discussion in this paper, the available experimental data are either of insufficient quality, or, in case high quality data are available, they can be well described on the basis of the pair-interaction approach described. The revisited statistical-thermodynamic method applying pair interactions is a viable approximation of nature that leads to satisfactory predictions on atomic level from knowledge of properties on macroscopic level.

## 4.5 Conclusions

A pair interaction model of the Bragg-Williams type for ternary intermetallic compounds  $(A,C)_mB_n$  composed of two sublattices and exhibiting various crystal structures is presented. The model incorporates the contribution of the vibrational entropy. It is

capable of describing intermetallic compounds that incorporate all four possible point defects: vacancies and antistructure atoms on both sublattices. The general model as presented can be adjusted (i.e. simplified) easily to more special cases, e.g. when certain defect types can be ignored.

Using accurate experimental data for the enthalpy of formation and the thermodynamic activity, both as a function of the composition (and, if available, of the temperature) in the homogeneity range of the  $(A,C)_{1-x}B_x$  compound, the model parameters for the enthalpy and the entropy interaction terms of pairs of atoms can be determined. This is demonstrated by the examples  $B2-Ni_{1-x}Al_x$  and  $B2-(Ni,Co)_{1-x}Al_x$ . If, however, experimental input data are not available to a sufficient degree (as is the case for  $B2-Fe_{1-x}Al_x$ , that exist predominantly only on the Fe-rich side of the stoichiometric composition), the model may not lead to satisfactory results: no unique parameter set can be determined.

A comparison of the Bragg-Williams statistical thermodynamical method with methods that apply the Wagner-Schottky approximation for fitting of experimental data or methods that calculate the model parameters by ab initio approaches, shows that the model parameters of the individual methods cannot be transferred into each other directly. Yet, the methods can be compared considering "higher level parameters" as the effective enthalpy of formation of the point defects, that can be calculated assuming the usual Arrhenius-type temperature dependence of the defect concentrations.

On the basis of the current evaluation of literature data, it follows that the revisited statistical method based on pair interactions provides a consistent description of important properties of intermetallic compounds.



## *Enthalpy of formation of B2-Fe<sub>1-x</sub>Al<sub>x</sub> and B2-(Ni,Fe)<sub>1-x</sub>Al<sub>x</sub>*

*J. Breuer, A. Grün, F. Sommer and E. J. Mittemeijer*

**Abstract:** The enthalpy of formation of the ordered B2-phases in the systems Fe-Al and Fe-Ni-Al was measured with very good accuracy using a special, laboratory built differential solution calorimeter. The measurements were performed at 1073 K as a function of composition with an accuracy of about 1%. The enthalpy of formation of B2-FeAl is most negative for the composition Fe<sub>0.50</sub>Al<sub>0.50</sub> ( $-36.29$  kJ/mol). Compounds with Al contents less than about 40 at.% show a deviation from a linear dependence of the enthalpy of formation with composition that prevails for Al contents larger than 40 at. Upon replacing Fe by Ni while maintaining a constant Al content, the enthalpy of formation of B2- (Fe,Ni)Al compounds becomes more negative. With decreasing Al content and for a constant Fe/Ni ratio the enthalpy of formation of the ternary phase becomes less negative.



## 5.1 Introduction

Some intermetallic compounds with CsCl- structure (B2-type) are stable over a relatively wide range of composition at normal temperatures and pressures, e.g. CoAl, NiAl, FeAl, CoGa, NiGa, PdAl (see e.g. [7]). A wide range of homogeneity for ordered compounds always entails the existence of constitutional defects (in addition to defects that are due to thermal disorder), since the surplus of one or the other component has to be balanced in order to maintain the overall ordered structure (i.e. to preserve the number of sites on all sublattices).

The defect equilibrium as function of composition and temperature at constant pressure may be described by statistical thermodynamic models (see, e.g. [7, 18, 29]). The validity of a model for a particular phase can be tested comparing measured and calculated data for the Gibbs free energies of formation as function of composition. Then the experimental values for the Gibbs free energy of formation have to be known with sufficient accuracy.

Calorimetric measurements of the enthalpy of formation of several B2-compounds (see, e.g. [11] for B2-NiAl and [13] for B2-CoAl) were conducted in the past. It was shown [11, 13, 29] that applying a Wagner-Schottky or Bragg-Williams approach for the description of the interaction between pairs of species in the compounds (atoms/atoms and atoms/defects), the enthalpy of formation, the Gibbs free energy as well as the defect structure of these compounds can be described very well (see, in particular [29]).

To our knowledge the enthalpy of formation as function of composition of the B2-phase  $\text{Fe}_{1-x}\text{Al}_x$  has not been measured over a distinct composition range with, for the modeling, necessary accuracy. The present study is devoted to such experiments to enable a subsequent model description. To this end a special, laboratory built differential calorimeter was used that allows heat of dissolution measurements with high accuracy.

Recently, enthalpy of formation values were reported for the ternary B2-phase  $(\text{Ni,Co})_{1-x}\text{Al}_x$  [16]. It was shown [29] that, with some modifications of the binary model used to describe the data of the binary phases B2- $\text{Ni}_{1-x}\text{Al}_x$  and B2- $\text{Co}_{1-x}\text{Al}_x$ , it is possible to provide a satisfactory model description for the thermodynamic properties and the defect structure of the ternary phase as well. Against this background and in addition to the enthalpy of formation measurements of the binary B2-compound  $\text{Fe}_{1-x}\text{Al}_x$ , in this work measurements of the enthalpy of formation of the ternary B2-phase  $(\text{Fe,Ni})_{1-x}\text{Al}_x$  were performed too.

## 5.2 Experimental

### 5.2.1 Calorimeter

An isoperibolic heat-flow differential solution calorimeter has been employed for the measurements of the enthalpy of solution reported in the present study. The apparatus

has been described in detail elsewhere [11, 16]; therefore, here only a short description will be given. The calorimeter is made up of four compartments that are arranged in a large cylindrical nickel block. Each calorimeter compartment contains an alumina crucible with liquid Al as the metallic solvent (mass of Al in the order of 20 – 30 g). The four samples (mass about 0.5 g) are mounted on small alumina stirrers above the four baths. Between each two of the compartments a differential thermopile (see [11]) is located that measures the temperature difference between the two adjacent calorimeters. This is why each temperature effect as a function of time, that is induced when a stirrer is moved down into the liquid Al and the sample dissolves in the Al solvent, is recorded by two adjacent thermopiles. During one measurement run, four samples are dissolved consecutively and eight temperature-time areas are recorded. These areas are "translated" in amounts of energy on the basis of a calibration for each calorimeter compartment performed by electrical resistance heating. The arithmetic mean of the two measurements for each heat effect in each calorimeter compartment provides the experimental result presented here.

For the accuracy of the measurement the constancy of the calorimeter block temperature is most important. To ensure this temperature stability, the apparatus is equipped with an elaborate heating and temperature control system. It is designed with six individual units which allow the regulation of the constant temperature of the calorimeter block.

The measurements reported in this study are performed under dynamic vacuum conditions ( $< 10^{-2} Pa$ ) at a constant temperature of 1073 K. The stability of the block temperature for the time of the experiments was found to be better than  $\pm 10^{-3} K/day$  yielding a resolution of the heat effects (enthalpy of solution) in the order of 1 J and a very good accuracy of the measurements in the order of 1 % for the enthalpy of formation. The reproducibility of the results (see Section III) of individual measurements is excellent.

### 5.2.2 Sample preparation

Iron (99.98 wt.%), aluminium (99.999 wt.%) and nickel (99.98 wt.%), were used for the preparation of the samples (alloys and pure iron) and the solvent (Al). The intermetallic compounds (weight of each sample about 20-25 g) were prepared by melting the constituents under an argon atmosphere in an induction furnace and casting into copper molds. The alloys thus prepared were sealed in silica glass tubes under a protective atmosphere ( $5 \cdot 10^4 Pa$  argon) and annealed for 10 days at 1323 K. To avoid contamination with Si from the tubes during annealing, alumina underlays were used. A spark erosion device was used for cutting the alloys into cylindrical discs (diameter 6 – 7 mm, thickness 1.5 – 2 mm) and providing them with a hole for the ceramic stirrer. The discs surfaces were ground and cleaned with acetone. The homogeneity of the samples was verified metallographically and by X-ray diffraction analysis. The compositions of the compounds were checked by chemical analysis of a randomly selected specimen of each alloy prepared.

## 5.3 Results and Discussion

In the following the enthalpy of formation of solid B2 (Fe,Ni)<sub>1-x</sub>Al<sub>x</sub> phase is defined such that solid B2 (Fe,Ni)<sub>1-x</sub>Al<sub>x</sub> is formed from solid Fe, solid Ni and liquid Al.

From the thermal effects of dissolution at infinite dilution, the enthalpies of formation of the solid B2 compounds,  $\Delta H_{B2}$ , at the temperature of the bath ( $T = 1073$  K) were calculated using the following equation, utilizing Hess' law of constant heat summation (i.e. the enthalpy is a state variable):

$$\Delta H_{B2} = x_{Fe}\Delta H_{L,Fe}^0 + x_{Ni}\Delta H_{L,Ni}^0 - \Delta H_{L,B2}^0, \quad (5.1)$$

where  $\Delta H_{L,i}^0$  ( $i = Fe, Ni, B2$ ) denotes the enthalpy of solution at infinite dissolution of the pure solid elements Fe and Ni and the solid B2 compound, respectively. The molar fractions of Fe and Ni are given by  $x_{Fe}$  and  $x_{Ni}$ , respectively. An "infinitely large" reservoir of liquid aluminium is used in the present study as the solvent. At infinite dilution the enthalpies of solution of Fe and Ni, separately, are equal to the enthalpy of solution both Fe and Ni simultaneously, and this leads to Eq. (5.1).

### 5.3.1 Enthalpy of solution of solid Fe in liquid Al and partial enthalpy of mixing liquid Fe in liquid Al

The measured heat effect and the enthalpy of solution of pure solid Fe in liquid Al have been given in Table 5.1. Each heat effect value  $\Delta h_{L,Fe}$  given in the table represents the mean value of two measured heat effects (Section 5.2.1). A dependence on the amount of the dissolved Fe was not observed, so  $\Delta H_{L,Fe}^0$  is obtained as the arithmetic mean of the results of all experiments (Table 5.1). Note that this statement is valid for the relatively narrow compositional range considered.

Table 5.1: Heat effect of dissolution of solid Fe in liquid Al and the corresponding enthalpy of solution, at 1073 K.

Solvent $n_{Al}$ (mol)	Sample $n_{Fe}$ (mol)	Fe content of bath $x_{Fe}$	Heat effect $\Delta h_{L,Fe}$ (kJ)	Enthalpy of solution $\Delta H_{L,Fe}$ (kJ/mol)
1.06684	0.00683	0.0064	-0.7615	-111.5
0.99965	0.00672	0.0067	-0.7504	-111.7
0.99626	0.00734	0.0073	-0.8440	-115.0
0.98892	0.00711	0.0071	-0.8129	-114.3
1.05918	0.00424	0.0040	-0.4713	-111.2
1.05911	0.00451	0.0042	-0.5032	-111.7
1.05804	0.00398	0.0038	-0.4510	-113.3
1.05150	0.00870	0.0082	-0.9775	-112.3

$$\Delta H_{L,Fe}^0 = -112.6 \pm 1.3$$

The partial enthalpy of mixing at infinite dilution for liquid iron in liquid aluminium,  $\Delta\bar{H}_{Fe}$ , is given by

$$\Delta\bar{H}_{Fe} = \Delta H_{L,Fe}^0 - \Delta H_{Fe}^m. \quad (5.2)$$

For the enthalpy of melting of Fe extrapolated to the measurement temperature,  $\Delta H_{Fe}^m$ , a value of 12.08 kJ/mol [22] was used. The result obtained in this study for the partial enthalpy of mixing at infinite dilution is compared with literature data in Table 5.2. It follows that the present result is in good agreement with the value reported in Ref. [64] for about the same temperature. The values reported in Ref. [65] for Fe, Ni and Co are systematically less negative than the ones obtained in this study for Fe and in the earlier study [16] for Ni and Co. The data given in Table 5.2 show that with increasing temperature the partial enthalpy of mixing at infinite dilution becomes less negative.

Table 5.2: Partial enthalpy of mixing at infinite dilution for liquid Fe in liquid Al. Error limits as given by the corresponding authors.

$\Delta\bar{H}_{Fe}$ (kJ/mol)	Measurement temperature (K)	Reference
-128.5	971	[66]
-114.7 ± 1.2	994	[67]
-123.4 ( $x_{Fe} = 0.0082$ )	1023	[64]
-124.7 ± 1.3	1073	this work
-106.7 ± 1.8	1073	[65]
-110.8 ± 3	1212	[68]
-95.2	1873	[69]

The values for the enthalpy of solution of solid Ni in liquid Al (used in this work; cf. Eq. (5.1)) and for the partial enthalpy of mixing liquid Ni in liquid Al have been reported in [16].

### 5.3.2 Enthalpy of formation of B2-Fe<sub>1-x</sub>Al<sub>x</sub>

The heat effects measured and the corresponding calculated enthalpy of formation values for the solid binary B2-compounds Fe<sub>1-x</sub>Al<sub>x</sub> (Eq. (5.1) with  $x_{Ni} \equiv 0$ ) have been summarized in Table 5.3. Each indicated heat effect  $\Delta h_{L,B2}$  is the mean of two measured heat effects (see Section 5.2.1). The last value in each row of Table 5.3 is the arithmetic mean obtained from the experiments.

Table 5.3: Heat effect of dissolution of solid B2-Fe<sub>1-x</sub>Al<sub>x</sub> compounds in liquid Al and the enthalpy of formation of solid B2-Fe<sub>1-x</sub>Al<sub>x</sub> at 1073 K- as calculated applying Eq. (5.1). The error ranges indicated represent the standard deviation of the measurements.

Composition	Solvent $n_{Al}$ (mol)	Sample $n_{B2}$ (mol)	Heat effect $\Delta h_{L,B2}$ (kJ)	Enthalpy of formation $\Delta H_{B2}$ (kJ/mol)	
Fe <sub>0.70</sub> Al <sub>0.30</sub>	1.02548	0.01512	-0.7831	-27.05	
	1.02660	0.01287	-0.6599	-27.57	
	1.02248	0.01158	-0.5994	-27.04	-27.15 ± 0.21
	1.02344	0.01327	-0.6866	-27.06	
	0.72390	0.01426	-0.7386	-27.01	
Fe <sub>0.675</sub> Al <sub>0.325</sub>	0.73321	0.01021	-0.4990	-27.15	
	0.72668	0.01024	-0.5000	-27.18	
	0.72078	0.01023	-0.4981	-27.30	
	0.70314	0.01015	-0.4943	-27.30	
Fe <sub>0.65</sub> Al <sub>0.35</sub>	0.73275	0.01457	-0.6619	-27.75	
	0.74408	0.01494	-0.6827	-27.48	-27.83 ± 0.29
	0.73275	0.01514	-0.6815	-28.17	
	0.72747	0.01485	-0.6717	-27.95	
Fe <sub>0.6375</sub> Al <sub>0.3625</sub>	0.73291	0.01015	-0.4367	-28.75	
	0.74128	0.01022	-0.4484	-27.92	-28.35 ± 0.29
	0.73291	0.01025	-0.4450	-28.35	
	0.74128	0.01024	-0.4442	-28.39	
Fe <sub>0.63125</sub> Al <sub>0.36875</sub>	0.64504	0.00531	-0.2271	-28.30	
	0.67953	0.00508	-0.2154	-28.68	-28.61 ± 0.33
	0.61190	0.00520	-0.2186	-29.06	
	0.64504	0.00518	-0.2210	-28.44	
Fe <sub>0.625</sub> Al <sub>0.375</sub>	1.07694	0.01007	-0.3911	-31.65	
	1.05869	0.01004	-0.3955	-30.99	-31.19 ± 0.32
	1.07694	0.01005	-0.3926	-31.30	
	0.84425	0.01005	-0.3977	-30.82	
	0.70676	0.00917	-0.3516	-30.63	
	0.74246	0.00914	-0.3459	-31.14	

Table 5.3: (continued)

Fe <sub>0.6125</sub> Al <sub>0.3875</sub>	0.70671	0.00906	-0.3500	-30.34	-30.53 ± 0.33
	0.74246	0.00919	-0.3553	-30.31	
	0.74128	0.00918	-0.3556	-30.25	
Fe <sub>0.60625</sub> Al <sub>0.39375</sub>	0.64403	0.00501	-0.1910	-30.12	-30.52 ± 0.36
	0.64900	0.00502	-0.1905	-30.32	
	0.70503	0.00499	-0.1873	-30.73	
	0.64874	0.00499	-0.1862	-30.91	
Fe <sub>0.60</sub> Al <sub>0.40</sub>	1.02277	0.01464	-0.5375	-30.73	-30.81 ± 0.11
	1.02465	0.01459	-0.5375	-30.73	
	1.02519	0.01408	-0.5153	-30.97	
	1.01698	0.01113	-0.4090	-30.81	
Fe <sub>0.575</sub> Al <sub>0.425</sub>	0.98874	0.00997	-0.3130	-33.35	-33.12 ± 0.22
	0.72302	0.00990	-0.3114	-33.30	
	0.74418	0.00991	-0.3144	-33.02	
	0.74418	0.00988	-0.3155	-32.80	
Fe <sub>0.55</sub> Al <sub>0.45</sub>	0.70676	0.00888	-0.2482	-33.98	-34.10 ± 0.39
	0.74246	0.00824	-0.2326	-33.70	
	0.73291	0.00881	-0.2404	-34.63	
	0.70676	0.00837	-0.2331	-34.08	
Fe <sub>0.525</sub> Al <sub>0.475</sub>	0.84425	0.00999	-0.2353	-35.57	-35.72 ± 0.15
	0.98874	0.00989	-0.2308	-35.77	
	0.75578	0.00994	-0.2304	-35.94	
	0.74117	0.01001	-0.2356	-35.58	
Fe <sub>0.50</sub> Al <sub>0.50</sub>	0.82358	0.01378	-0.2783	-36.11	-36.29 ± 0.32
	0.84980	0.01435	-0.2967	-35.74	
	0.71805	0.01251	-0.2484	-36.44	
	0.74408	0.01424	-0.2807	-36.59	
	0.74117	0.01003	-0.1980	-36.56	

The results obtained for the enthalpy of formation are shown in Figure 5.1 as a function of the atomic fraction of Al in B2-Fe<sub>1-x</sub>Al<sub>x</sub>. For comparison the data reported in



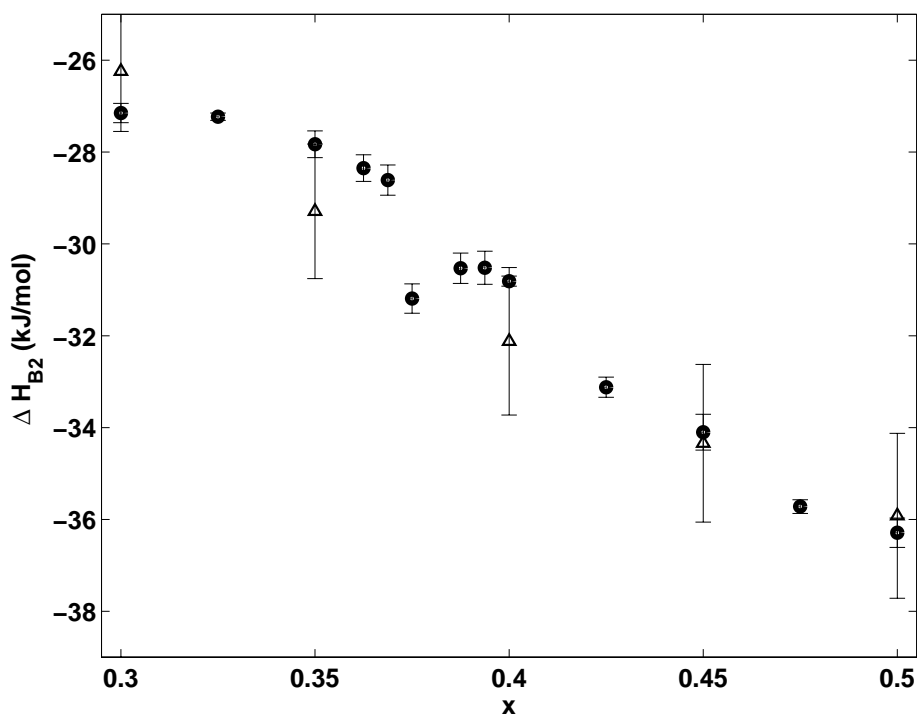


Figure 5.1: Enthalpy of formation of solid B2-Fe<sub>1-x</sub>Al<sub>x</sub> compounds as function of the atomic fraction of Al,  $x$ : ● represents results of the present study ( $T = 1073\text{ K}$ ), error bars as determined in this work (see text); △ represents data reported in [62] ( $T = 1173\text{ K}$ ), error bars estimated to be 5%.

[62], that were obtained from the measured temperature and composition dependencies of the thermodynamic activity, have been included in the figure as well. The data obtained in the present study (marked by ● in Figure 5.1) are the data with the smallest error margin. The data in Figure 5.1 derived from activity measurements [62] (marked by △), are in good agreement with the present data but are afflicted with relatively large errors of about 5%. (Note that enthalpy of formation data do not depend strongly on temperature.)

The enthalpy of formation of the stoichiometric composition Fe<sub>0.50</sub>Al<sub>0.50</sub> is found to be the most negative one for the composition range investigated (see Figure 5.1). The number of data points, i.e. the number of alloys of different compositions and the accuracy were much larger in this study than in the previous one. This may be the reason that interesting features are exhibited by the present data, which were not noted earlier (see [62]). In general the enthalpy of formation becomes less negative with decreasing Al content. Additionally, the present results show a discontinuity at about 38 *at.*% Al (see arrow in Figure 5.1): the enthalpy curve for compounds with Al

contents lower than about 38 *at. %* Al cannot simply be conceived as a continuation of the enthalpy curve for Al contents between about 38 and 50 *at. %*.

As compared to B2-Ni<sub>1-x</sub>Al<sub>x</sub> and B2-Co<sub>1-x</sub>Al<sub>x</sub> the enthalpy of formation values obtained of B2-Fe<sub>1-x</sub>Al<sub>x</sub> are the least negative ones (see Figure 5.2). In contrast with (the present results for) B2-Fe<sub>1-x</sub>Al<sub>x</sub>, B2-Ni<sub>1-x</sub>Al<sub>x</sub> and B2-Co<sub>1-x</sub>Al<sub>x</sub> show linear dependencies for the enthalpy of formation on composition for  $x < 0.5$  (and  $x > 0.5$ ).

The unusual shape of the enthalpy vs. composition curve of B2-Fe<sub>1-x</sub>Al<sub>x</sub> seems to bear a relationship to the phase diagram of the Fe-Al system as reported in [70]. According to [70] the composition range of the B2 phase is subdivided into three parts: the  $\alpha_2(h)$ - phase, the  $\alpha_2(l)$ - phase and the  $\alpha'$ - phase. Following in this phase diagram the isothermal line of 1073 K from the stoichiometric composition (50 *at. %* Al) to lower Al contents, at about 38 *at. %* Al the boundary between the  $\alpha_2(h)$ - phase and the  $\alpha'$ - phase is crossed, which parallels the occurrence of the discussed discontinuity in the enthalpy of formation vs. composition curve (Figure 5.1). The transformation of  $\alpha_2(h)$  into  $\alpha'$  was suggested by thermal analysis and dilatometry, but X-ray diffraction did not provide evidence [71]. However, the subdivision of the B2 phase region of the Fe-Al system is controversial (see also, e.g. the phase diagram given in [59]). To arrive at a better understanding of this phenomenon, at present systematic measurements of the heat capacity,  $c_P$ , in the questioned composition and temperature range are carried out currently by our group.

### 5.3.3 Enthalpy of formation of B2-(Fe,Ni)<sub>1-x</sub>Al<sub>x</sub>

The heat effects measured and the corresponding, calculated (using Eq. (5.1)) enthalpy of formation for the solid ternary B2-compounds (Fe,Ni)<sub>1-x</sub>Al<sub>x</sub> have been given in Table 5.4. The indicated heat effects again are the mean of two recorded values.

Table 5.4: Heat effect of dissolution of solid B2-(Fe,Ni)<sub>1-x</sub>Al<sub>x</sub> compounds in liquid Al and the enthalpy of formation of solid B2-(Fe,Ni)<sub>1-x</sub>Al<sub>x</sub> at 1073 K- as calculated applying Eq. (5.1). The error ranges indicated represent the standard deviation of the measurements.

Composition	Solvent $n_{Al}$ (mol)	Sample $n_{B2}$ (mol)	Heat effect $\Delta h_{L,B2}$ (kJ)	Enthalpy of formation $\Delta H_{B2}$ (kJ/mol)
Fe <sub>0.42</sub> Ni <sub>0.08</sub> Al <sub>0.50</sub>	0.84506	0.01139	-0.1784	-42.58
	0.72112	0.01174	-0.1831	-42.64 -42.78 ± 0.28
	1.08981	0.01350	-0.2043	-43.11
Fe <sub>0.34</sub> Ni <sub>0.16</sub> Al <sub>0.50</sub>	1.05933	0.00658	-0.0739	-48.95
	1.07099	0.00683	-0.0802	-48.44
	1.06498	0.00671	-0.0764	-48.81 -48.73 ± 0.22

Table 5.4: (continued)

	1.07926	0.00658	-0.0754	-48.73	
$\text{Fe}_{0.25}\text{Ni}_{0.25}\text{Al}_{0.50}$	1.06498	0.00641	-0.0519	-54.28	$-54.42 \pm 0.24$
	1.05933	0.00650	-0.0495	-54.76	
	1.07114	0.00637	-0.0519	-54.23	
	1.02618	0.00813	-0.0648	-54.41	
$\text{Fe}_{0.16}\text{Ni}_{0.34}\text{Al}_{0.50}$	1.06933	0.00671	-0.0253	-60.78	$-60.86 \pm 0.23$
	1.06990	0.00628	-0.0234	-60.84	
	1.07926	0.00629	-0.0212	-61.20	
	1.08423	0.00649	-0.0237	-60.91	
	1.07095	0.00618	-0.0246	-60.58	
$\text{Fe}_{0.08}\text{Ni}_{0.42}\text{Al}_{0.50}$	1.07562	0.00619	-0.0057	-65.58	$-65.74 \pm 0.27$
	1.02370	0.00702	-0.0070	-65.51	
	1.02665	0.00702	-0.0028	-66.11	
	1.02549	0.00702	-0.0052	-65.77	
$\text{Fe}_{0.46}\text{Ni}_{0.09}\text{Al}_{0.45}$	1.07305	0.00905	-0.2170	-40.13	$-39.87 \pm 0.23$
	1.06663	0.00898	-0.2203	-39.58	
	1.06030	0.00898	+0.2174	-39.90	
$\text{Fe}_{0.37}\text{Ni}_{0.18}\text{Al}_{0.45}$	1.06665	0.00857	-0.1767	-45.68	$-45.74 \pm 0.05$
	1.06680	0.00863	-0.1779	-45.70	
	1.07006	0.00884	-0.1816	-45.76	
	1.07177	0.00893	-0.1830	-45.81	
$\text{Fe}_{0.275}\text{Ni}_{0.275}\text{Al}_{0.45}$	1.07248	0.00887	-0.1482	-51.91	$-51.92 \pm 0.14$
	1.06237	0.00872	-0.1448	-52.00	
	1.05004	0.00859	-0.1452	-51.70	
	1.05789	0.00863	-0.1427	-52.08	
$\text{Fe}_{0.18}\text{Ni}_{0.37}\text{Al}_{0.45}$	1.06618	0.00891	-0.1138	-58.16	$-58.07 \pm 0.11$
	1.06922	0.00944	-0.1216	-58.04	
	1.06818	0.00914	-0.1191	-57.90	
	1.06225	0.00867	-0.1105	-58.18	
	1.06793	0.00916	-0.0910	-63.16	
	1.06732	0.00869	-0.0876	-63.03	

Table 5.4: (continued)

Fe <sub>0.09</sub> Ni <sub>0.46</sub> Al <sub>0.45</sub>	1.06849	0.00925	-0.0929	-63.07	$-63.11 \pm 0.06$
	1.06762	0.00905	-0.0899	-63.17	
Ni <sub>0.55</sub> Al <sub>0.45</sub>	1.05526	0.00893	-0.0873	-65.51	$-65.38 \pm 0.10$
	1.07083	0.00897	-0.0898	-65.28	
	1.05733	0.00901	-0.0889	-65.43	
	1.06487	0.00910	-0.0910	-65.30	
Fe <sub>0.59</sub> Ni <sub>0.06</sub> Al <sub>0.35</sub>	0.64504	0.00961	-0.4228	-30.67	$-30.92 \pm 0.24$
	0.64290	0.00949	-0.4129	-31.14	
	0.68224	0.00941	-0.4114	-30.94	
Fe <sub>0.53</sub> Ni <sub>0.12</sub> Al <sub>0.35</sub>	0.72283	0.00962	-0.3953	-35.03	$-35.46 \pm 0.31$
	0.67912	0.00963	-0.3928	-35.34	
	0.68224	0.00963	-0.3897	-35.62	
	0.72283	0.00958	-0.3857	-35.86	
Fe <sub>0.145</sub> Ni <sub>0.505</sub> Al <sub>0.35</sub>	0.67953	0.01000	-0.3384	-51.62	$-51.52 \pm 0.29$
	0.61190	0.01006	-0.3425	-51.40	
	0.64874	0.01008	-0.3375	-51.97	
	0.61190	0.01045	-0.3479	-52.16	

The results obtained for the enthalpy of formation are shown as a function of nickel content (relative to the sum of the iron and nickel contents) for various aluminium contents in Figure 5.3.

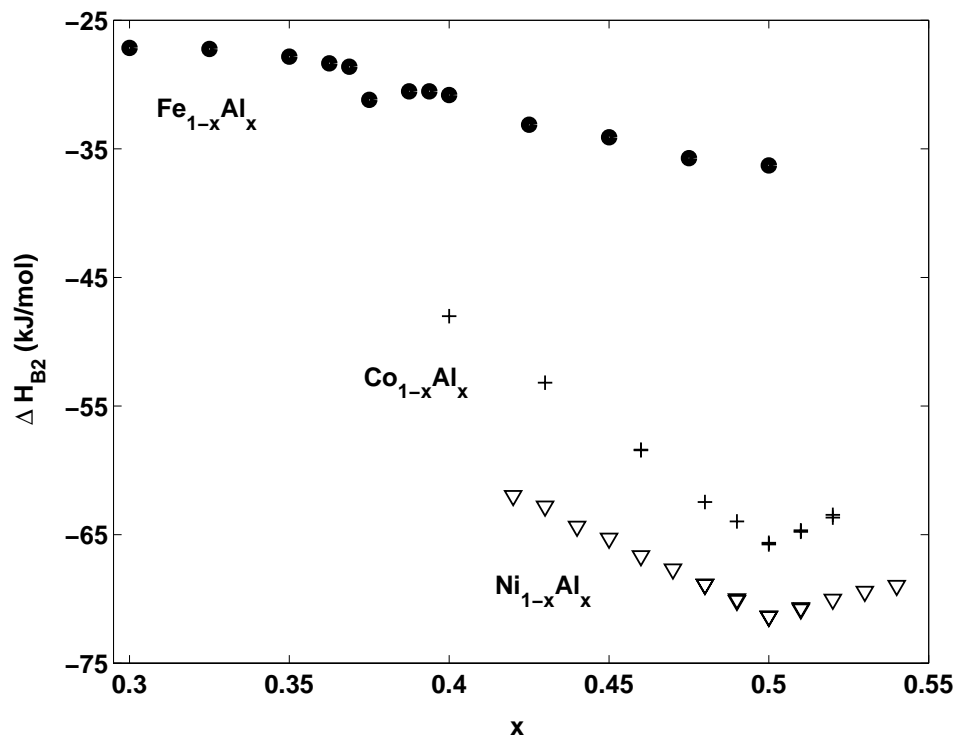


Figure 5.2: Enthalpy of formation of binary aluminides, for the particular homogeneity range of the indicated B2 phases, as function of the atomic fraction of Al: ● represents results of the present study for B2-Fe<sub>1-x</sub>Al<sub>x</sub> ( $T = 1073\text{ K}$ ), + represents data from [13] for B2-Co<sub>1-x</sub>Al<sub>x</sub> ( $T = 1100\text{ K}$ ), ▽ represents data from [11] for B2-Ni<sub>1-x</sub>Al<sub>x</sub> ( $T = 1100\text{ K}$ ).

The present data show that starting with binary B2-Fe<sub>1-x</sub>Al<sub>x</sub> and replacing Fe with Ni, while keeping the Al content at a constant value, the enthalpy of formation becomes more negative. Keeping the (Fe,Ni) content in (Fe,Ni)<sub>1-x</sub>Al<sub>x</sub> at a constant value, the enthalpy of formation becomes less negative with decreasing Al content. The curves in Figure 5.3 represent mechanical mixing of the binary intermetallic phases at constant Al content. It follows that the deviation from mechanical mixing for the enthalpy of formation is negative at the three Al contents investigated. This deviation increases distinctly with decreasing Al content. Note that for an Al content of 35 at.% the ternary B2 phase is only stable at compositions near the binary phases B2-Fe<sub>1-x</sub>Al<sub>x</sub> and B2-Ni<sub>1-x</sub>Al<sub>x</sub> [72] and therefore the investigation of the enthalpy of the ternary B2 phase with this Al content could not be performed over the whole range of variable Ni/Fe atomic ratio.

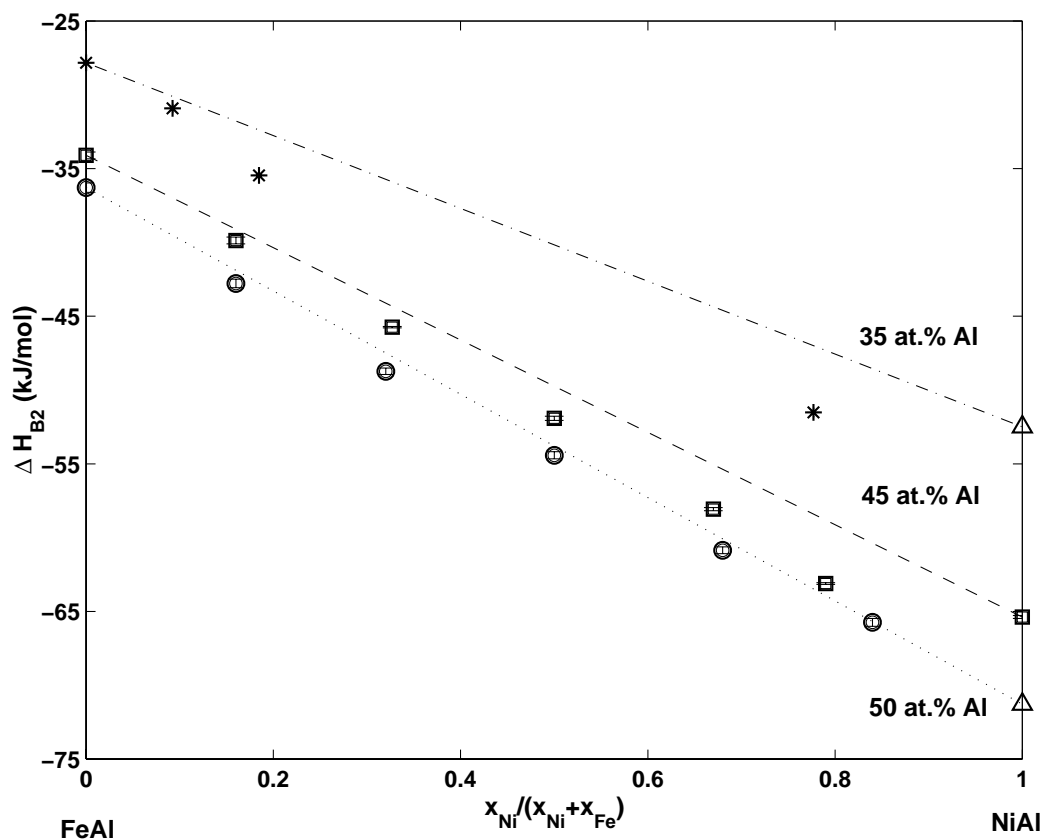


Figure 5.3: Enthalpy of formation of solid  $B2\text{-(Fe,Ni)}_{1-x}\text{Al}_x$  compounds as function of the relative amount of Ni ( $x_{Ni}$  and  $x_{Fe}$  denote the atomic fractions of Ni and Fe, respectively), for various atomic fractions of Al;  $x = 0.50$ :  $\circ$ , ...;  $x = 0.45$ :  $\square$ , ---;  $x = 0.35$ :  $*$ , -.-.-;  $\triangle$  represents data from [16] ( $x = 0.50$ ) and data extrapolated from the data of [11] ( $x = 0.35$ ). The error bars are of the size of the symbols. The curves represent the lines for the case of mechanical (ideal) mixing.

## 5.4 Conclusions

- Application of a special, laboratory built isoperibolic heat-flow differential solution calorimeter allowed determination of the enthalpy of formation of the B2 phases of the systems Fe-Al and Fe-Ni-Al with very good accuracy.
- The enthalpy of formation of  $B2\text{-Fe}_{1-x}\text{Al}_x$  is most negative for the stoichiometric composition  $\text{Fe}_{0.50}\text{Al}_{0.50}$ . An unusual discontinuity was found in the enthalpy of formation vs. composition curve at about 38 at.% Al. This result parallels

the observation of a "phase transition" at this temperature and composition as reported in the literature cited.

- Upon replacing Fe by Ni atoms, while keeping the Al content constant, the enthalpy of formation of  $B2-(Fe,Ni)_{1-x}Al_x$  becomes increasingly more negative. Keeping the Ni/Fe atomic ratio constant, for decreasing Al content (starting with 50 at.% Al), the enthalpy of formation becomes less negative and shows an increasing deviation from the values predicted for the case of mechanical mixing of the two binary intermetallic phases  $B2-Fe_{1-x}Al_x$  and  $B2-Ni_{1-x}Al_x$ .





## *Kurzfassung der Dissertation*

Beziehungen zwischen Punktdefekteigenschaften von geordneten intermetallischen Phasen und thermodynamischen Daten können mit statistisch-thermodynamischen Modellen vom Bragg-Williams Typ quantifiziert werden. Aus der Kenntnis von thermodynamischen Eigenschaften als Funktion der Zusammensetzung und, falls vorhanden der Temperatur, können durch Anpassung Enthalpie- und Entropieparameter bestimmt werden, die die Wechselwirkungen zwischen zwei nächsten bzw. übernächsten Nachbaratomen charakterisieren. In der vorliegenden Arbeit wird gezeigt, daß die B2-Phasen NiAl, CoAl und (Ni,Co)Al mit dem Tripel-Defekt-Modell beschrieben werden können.

Im Vergleich mit anderen statistisch-thermodynamischen Methoden (Wagner-Schottky Ansatz und auf ab initio elektronentheoretischen Berechnungen basierender Ansatz) stellt sich der Bragg-Williams Formalismus als einfach anwendbare Methode dar, die, sachgerechte Anwendung vorausgesetzt, zu genauen Vorhersagen bzgl. thermodynamischer Daten als auch der Defektkonzentrationen führt.

Die Bildungsenthalpiewerte der binären Phase B2-Fe<sub>1-x</sub>Al<sub>x</sub> und der ternären B2-Phase (Ni,Fe)<sub>1-x</sub>Al<sub>x</sub> wurden mit einem isoperibol arbeitenden Differential-Lösungskalorimeter experimentell ermittelt. Die größte exotherme Bildungsenthalpie von B2-FeAl weist die Zusammensetzung Fe<sub>0,50</sub>Al<sub>0,50</sub> ( $-36.29 \text{ kJ/mol}$ ) auf. Legierungen mit Al-Gehalten von unter 40 At.-% zeigen eine Abweichung von der sonst linearen Abhängigkeit der Bildungsenthalpie von der Zusammensetzung. Ersetzt man Fe durch Ni bei konstantem Al-Gehalt, wird die Bildungsenthalpie von (Ni,Fe)Al exothermer. Mit sinkendem Al-Gehalt bei konstantem Ni/Fe-Verhältnis werden die Bildungsenthalpiewerte weniger exotherm.



## Einleitung

Wichtige Eigenschaften von Legierungen, u.a. Informationen über die thermische Stabilität, sind in thermodynamischen Daten enthalten. Da sich thermodynamische Daten und Kenntnisse über die atomare Struktur von Werkstoffen gegenseitig bedingen, ergibt sich über die „Brücke“ thermodynamisch-statistischer Modelle einerseits die Möglichkeit, aus der genauen Kenntnis der atomaren Strukturen auf thermodynamische Daten zu schließen und andererseits eröffnet sich der gegenläufige Weg: aus der Kenntnis von thermodynamischen Daten können Rückschlüsse auf die atomaren Strukturen von Materialien gezogen werden. Die vorliegende Arbeit verfolgt das Hauptziel, einen Beitrag zum Studium der wechselseitigen Beziehungen zwischen thermodynamischen Daten und atomaren Strukturen von Legierungen zu leisten.

Intermetallische Phasen mit B2-Struktur eignen sich als Modellsysteme für ein solches Vorhaben. Sie liegen einerseits in einer relativ einfachen geordneten Kristallstruktur (CsCl) vor und erleichtern somit jede Modellbeschreibung. Gleichzeitig stoßen geordnete B2-Phasen aber auch auf nicht nur wissenschaftliches Interesse. Aufgrund meist geringer Dichte und vorteilhaften Korrosionseigenschaften sind industrielle Anwendungen für diese Werkstoffe mittlerweile schon Realität [10].

Binäre B2-Phasen AB kann man sich als aus zwei, jeweils mit einer Atomsorte belegten, gleich großen kubisch primitiven Untergittern bestehend vorstellen. Diese ergeben ineinandergestellt ein kubisch raumzentriertes Gitter. Perfekte Ordnung, d.h. das eine Untergitter ( $\alpha$ -Untergitter) ist nur mit A Atomen belegt und alle B Atome befinden sich auf dem anderen Untergitter ( $\beta$ -Untergitter), kann es nur unter gleichzeitiger Erfüllung von zwei Bedingungen geben: die Temperatur beträgt null Kelvin und die Phasenzusammensetzung ist exakt stöchiometrisch  $A_{\frac{1}{2}}B_{\frac{1}{2}}$ . Bei Abweichung von der Temperaturbedingung, d.h. bei jeder endlichen Temperatur, ist die perfekte Ordnung durch sogenannte thermische Defekte aufgehoben. Abweichungen von der Zusammensetzungsbedingung, d.h. Abweichungen vom exakten Verhältnis von 1:1 für A und B Atome werden in der Natur ebenfalls angetroffen. Viele geordnete B2-Phasen zeigen einen nicht auf die exakt stöchiometrische Zusammensetzung beschränkten Homogenitätsbereich, sondern kristallisieren auch noch etwa bei einer Abweichung von einigen Atom-% zu einer oder beiden Seiten der stöchiometrischen Zusammensetzung in der geordneten Struktur. Um die grundlegende Ordnung bei nicht-stöchiometrischen Phasen aufrecht erhalten zu können, müssen sogenannte konstitutionelle Defekte eingebaut werden. Die Defekte sind in beiden Fällen (thermisch wie konstitutionell) atomarer Art, d.h. es werden Punktdefekte auf dem geordneten Gitter der B2-Struktur gebildet. Die Gesamtanzahl der Defekte ist die Summe aus den thermischen und den konstitutionellen Defekten. Dabei ist die Art der Defekte für beide Abweichungen von der perfekten Ordnung dieselbe.

Da man bisher keine Zwischengitteratome in intermetallischen B2-Phasen beobachtet hat, gibt es vier mögliche Mechanismen der Defektbildung: Substitution eines A Atoms auf dem  $\alpha$ -Untergitter durch ein B Atom (Bildung eines sogenannten B Anti-

strukturatoms), Substitution eines B Atoms auf dem  $\beta$ -Untergitter durch ein A Atom (Bildung eines sogenannten A Antistrukturatoms), Bildung einer Leerstelle auf dem  $\alpha$ -Untergitter und Bildung einer Leerstelle auf dem  $\beta$ -Untergitter. Verglichen mit der Defektbildung in reinen Metallen ist die Defektbildung in intermetallischen Phasen komplexer. Da die insgesamt geordnete Struktur, d.h. die Homogenität der Phasen bis zu hohen Temperaturen hin und bei relativ großen Abweichungen von der stöchiometrischen Zusammensetzung aufrecht erhalten wird, werden Kombinationen von Defekten der beschriebenen vier Einzeldefektbildungsmechanismen eingebaut (siehe z.B. [2, 3]).

## Modelle

In der vorliegenden Arbeit werden statistisch-thermodynamische Modelle vom Bragg-Williams Typ [5] entwickelt und verwendet, um die Beziehungen zwischen thermodynamischen Daten (Bildungsenthalpie und thermodynamischen Aktivität) und Defekteigenschaften von intermetallischen Phasen (z.B. den Verlauf der Leerstellenkonzentration als Funktion der Zusammensetzung und der Temperatur) quantitativ zu beschreiben. Dabei werden die Wechselwirkungen zwischen zwei Nachbaratomen (wobei auch Leerstellen als eine Atomsorte betrachtet werden) als Ausgangspunkt der Beschreibung verwendet. Die Wechselwirkungsenthalpie und -entropie einer „Bindung“ zwischen zwei Atomen wird als unabhängig von der Zusammensetzung der Phase und der Temperatur angenommen. In den verwendeten Modellen werden Wechselwirkungen zwischen Atomen in nächster Nachbarschaft (auf verschiedenen Untergittern) und Atomen in übernächster Nachbarschaft (auf demselben Untergitter) berücksichtigt. Damit läßt sich die Gesamtenthalpie  $H$  der zu beschreibenden Phase als

$$H = \sum_{ij} n_{ij} h_{ij} + \sum_{ij} n'_{ij} h'_{ij} \quad (6.1)$$

ausdrücken. In Gleichung (6.1) bedeuten  $n_{ij}$  die Anzahl der Atompaare in nächster Nachbarschaft  $i - j$  und  $h_{ij}$  bezeichnet den zugehörigen Enthalpiebeitrag. Analoge Ausdrücke für die Anzahl der Atompaare in übernächster Nachbarschaft werden durch  $n'_{ij}$  und  $h'_{ij}$  repräsentiert. Die Anzahlen  $n_{ij}$  und  $n'_{ij}$  können für den Fall einer binären Phase durch eine Zusammensetzungsvariable (für ternäre Phasen durch zwei Zusammensetzungsvariablen) und Defektkonzentrationsvariable beschrieben werden. Die Defektkonzentrationsvariablen sind wegen des Auftretens von kombinierten, die Homogenität der Phasen aufrechterhaltenden Defekten nicht unabhängig voneinander, so daß im allgemeinsten Fall der Berücksichtigung aller vier möglichen Defektbildungsmechanismen (Kapitel 4 dieser Arbeit) nur drei unabhängige Defektkonzentrationsvariable auftreten (siehe Gleichung (4.3)). Bei Berücksichtigung von weniger Defektbildungsmechanismen ergeben sich gegenüber dem allgemeinsten Modell Vereinfachungen. In Kapitel 2 dieser Arbeit wird das sogenannte Triple-Defekt-Modell behandelt,

bei dem nur Leerstellen im  $\alpha$ -Untergitter und Antistrukturatome im  $\beta$ -Untergitter zugelassen werden (eine unabhängige Defektkonzentrationsvariable, siehe Gleichung (2.2)) und in Kapitel 3 ein sogenanntes Dreidefekttyp-Modell, bei dem Leerstellen auf dem  $\alpha$ -Untergitter und Antistrukturatome auf beiden Untergittern zugelassen werden (zwei unabhängige Defektkonzentrationsvariable, siehe Gleichung (3.1)). Die Entropie setzt sich in den Modellen als Summe aus einem konfigurationellen Beitrag, der mit der Boltzmann-Formel aus der als zufällig angenommenen Verteilung der einzelnen Defekte auf den jeweiligen Untergittern berechnet wird, und einem Schwingungsbeitrag zusammen, der in Analogie zum Enthalpieansatz (siehe Gleichung (6.1)) formuliert wird. Im thermodynamischen Gleichgewicht bei konstanter Temperatur und konstantem Druck ist die Gibbs'sche Energie  $G$ , die sich aus der Enthalpie  $H$  und der Entropie  $S$  gemäß  $G = H - TS$  zusammensetzt, wobei  $T$  die absolute Temperatur bezeichnet, minimal. Deshalb lassen sich die Gleichgewichtsbedingungen für die einzelnen in dieser Arbeit betrachteten Modelle aus der Minimalisierung von  $G$  erhalten (siehe Gleichungen (2.7a), (3.9, 3.10) und (4.7a-c)).

In dieser Arbeit werden als Eingangsgrößen der Modellbeschreibung, d.h. als Daten an die die Modelle angepaßt und die Modellparameter bestimmt werden, meist thermodynamische Daten verwendet. Dies sind Daten der thermodynamischen Aktivität der Komponente  $i$  der intermetallischen Phase ( $i = A$  oder  $B$ ),  $a_i$ , und die Bildungsenthalpie,  $\Delta H$ , der Phase  $A_{1-x_B}B_{x_B}$ . Die beschriebene Modellentwicklung umfaßt diese experimentell zugänglichen Größen durch die Gleichungen

$$G_i = G_i^0 + RT \ln a_i \quad (6.2)$$

$$\Delta H = H - ((1 - x_B)H_A + x_B H_B), \quad (6.3)$$

wobei  $G_i$  die partielle freie Enthalpie der Komponente  $i$ ,  $G_i^0$  die partielle freie Enthalpie der Komponente  $i$  in einem Standardzustand,  $R$  die Gaskonstante und  $H_A$  und  $H_B$  die Enthalpien der reinen Elemente, bezogen auf dieselbe Temperatur und denselben Druck wie  $H$ , bedeuten.

## Modellanpassungen und Ergebnisse

Ausgehend von einer Beschreibung mit dem Triple-Defekt-Modell wurden simultan Daten der thermodynamischen Aktivität und der Bildungsenthalpie als Funktion der Zusammensetzung bei konstanter Temperatur von B2-NiAl und B2-CoAl angepaßt (siehe Kapitel 2 dieser Arbeit). Dabei zeigte sich, daß die Berücksichtigung von Wechselwirkungen zwischen zwei Atomen in nächster Nachbarschaft bereits ausreichend ist. Abbildung 6.1 zeigt beispielhaft die Anpassung für die B2-Phase NiAl.

Mit den durch die Anpassung erhaltenen Parametern (je drei Enthalpieparameter und drei Entropieparameter für NiAl und CoAl) konnten die Verläufe der Leerstellenkonzentration sowohl in Abhängigkeit von der Zusammensetzung bei der konstanten

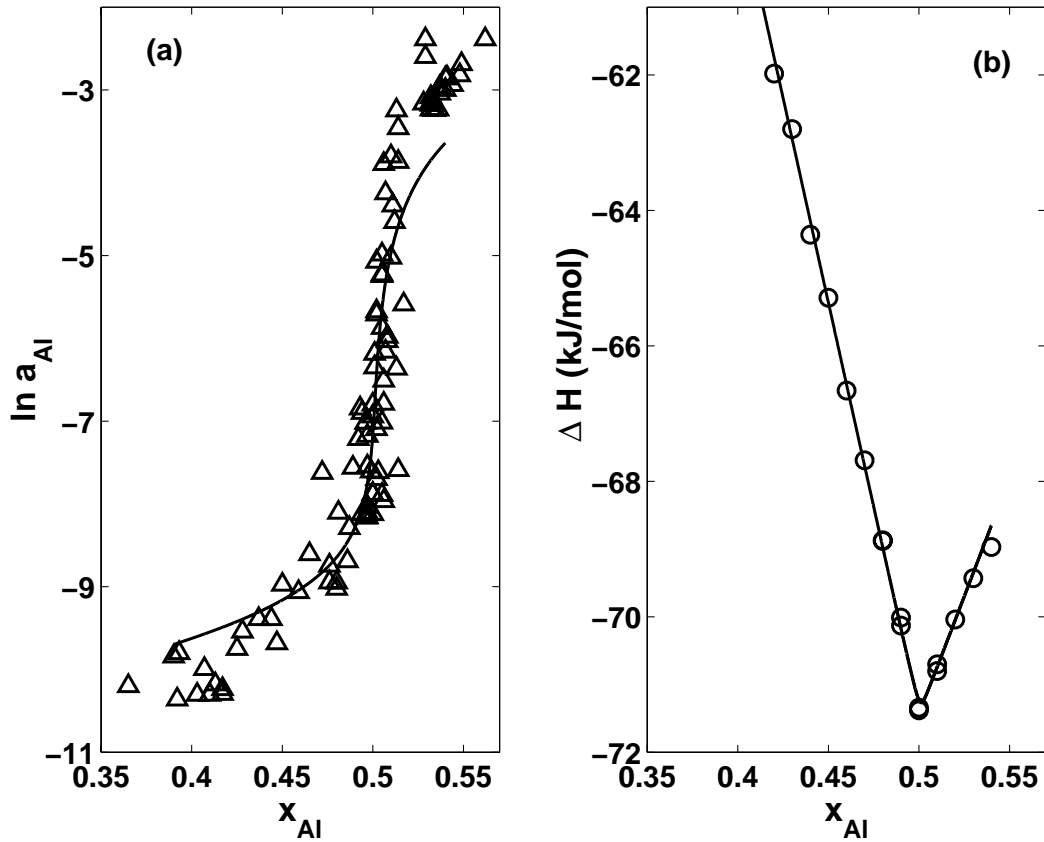


Abbildung 6.1:  $Ni_{1-x_{Al}}Al_{x_{Al}}$  ( $T=1273$  K), Tripel-Defekt-Modell: (a) Natürlicher Logarithmus der thermodynamischen Aktivität des Aluminiums in Abhängigkeit vom Molenbruch,  $\Delta$  berichtige Daten nach [12], – berechnet mit Modellparametern (siehe Tabellen 2.2 und 2.3), (b) Bildungsenthalpie in Abhängigkeit vom Molenbruch,  $\circ$  berichtige Daten nach [11], – berechnet mit Modellparametern (siehe Tabellen 2.2 und 2.3).

Temperatur der vorgenommenen Anpassung als auch in Abhängigkeit von der Temperatur für konstante Zusammensetzung mit den Modellgleichungen berechnet werden. Es ergaben sich hier gute Übereinstimmungen mit z.B. durch die Kombination von Röntgen- und Dichtemessungen bzw. Röntgen- und Dilatometermessungen experimentell bestimmten Leerstellenkonzentrationen (siehe Abbildungen 4.2 und 2.6). Die berechneten Leerstellenkonzentrationen als Funktion der Zusammensetzung der Phase und der Temperatur,  $c_V(x_{Al}, T)$ , erlauben es, unter der Annahme eines Arrhenius-Verhaltens

$$c_V(x_{Al}, T) = \exp\left(\frac{s^{eff}(x_{Al})}{R}\right) \exp\left(\frac{-h^{eff}(x_{Al})}{RT}\right) \quad (6.4)$$

die effektive Leerstellenbildungsentropie als Funktion der Zusammensetzung,

$s^{eff}(x_{Al})$ , und die effektive Leerstellenbildungsenthalpie als Funktion der Zusammensetzung,  $h^{eff}(x_{Al})$ , zu berechnen. Die hierbei erhaltenen Werte können mit Ergebnissen von ab-initio Berechnungen verglichen werden. Es ergaben sich sowohl für B2-NiAl (effektive Leerstellenbildungsenthalpie nach dem in dieser Arbeit verwendeten Triple-Defekt-Modell: 0.66 eV, ab-initio-Berechnungen [36]: 0.74 eV) als auch für B2-CoAl (0.83 eV, [37]: 1.29 eV) gute Übereinstimmungen.

Das in der Anwendung auf B2-NiAl und B2-CoAl erfolgreiche Triple-Defekt-Modell kann auf ternäre B2-Phasen übertragen werden. Dies wird in Kapitel 2 am Beispiel von B2-(Ni,Co)<sub>1-x<sub>Al</sub></sub>Al<sub>x<sub>Al</sub></sub> gezeigt. Für diese ternäre Phase konnten die gemessenen Bildungsenthalpiendaten [16] bei Beibehaltung der zuvor durch die Anpassung an thermodynamische Daten der binären Randphasen B2-NiAl und B2-CoAl gewonnenen Parameter durch die Anpassung von zwei zusätzlichen Enthalpieparametern sehr gut beschrieben werden (siehe Abb. 2.3). Die zusätzlichen Parameter quantifizieren die in der ternären Phase auftretenden Wechselwirkungen von Nickel- und Kobalt-Atomen auf nächsten- und übernächsten-Nachbar-Plätzen. Dieses Ergebnis erscheint sinnvoll: Nickel und Kobalt besetzen in der vollständig geordneten Struktur dasselbe Untergitter; deshalb sollte zur Beschreibung der Wechselwirkung auch ein übernächster-Nachbar-Parameter (Wechselwirkung auf demselben Untergitter innerhalb der B2-Struktur) notwendig sein. Mit den bestimmten Modellparametern ist es möglich, sowohl Vorhersagen über den Verlauf der Defektkonzentrationen (insbesondere der Leerstellenkonzentration) als Funktion der Zusammensetzung und der Temperatur als auch über Aktivitätsverlauf in der ternären B2-Phase (Ni,Co)Al zu treffen (siehe Abbildungen 2.5 und 2.4). Die Vorhersagen können z.Zt. wegen fehlender entsprechender experimenteller Daten noch nicht überprüft werden.

Eine Gruppe japanischer Experimentatoren führte in jüngster Vergangenheit Messungen des Gitterparameters und der Dichte von intermetallischen B2-Phasen an Einkristallen durch (siehe z.B. [32]). Die bzgl. der Leerstellenkonzentration ausgewerteten Daten ( $c_V = (\rho_X - \rho_M)/\rho_X$ , wobei  $\rho_X$  und  $\rho_M$  die Röntgen- bzw. makroskopische Dichte sind) sind besonders für die Al-reiche Phasen der B2-Strukturen NiAl und CoAl interessant: es ergeben sich Werte, die deutlich unterhalb der Konzentration von 2 mal der Abweichung von der stöchiometrischen Zusammensetzung liegen. Dies ist der Wert, den die konstitutionellen Leerstellen einnehmen, wenn man von einem dem Tripel-Defekt-Modell entsprechenden Verhalten ausgeht. Wenn gezeigt werden kann, daß die Leerstellenkonzentration unterhalb der angegebenen Grenze der konstitutionellen Leerstellen liegt, ist das Tripel-Defekt-Modell als Erklärungsmodell eindeutig auszuschließen. Die experimentellen Ergebnisse [57] stehen im Widerspruch zu sonstigen in der Literatur bekannten Arbeiten (siehe z.B. [30]): diese finden stets Leerstellenkonzentrationen für Al-reiche B2-NiAl und B2-CoAl Phasen, die oberhalb des konstitutionellen Grenzwertes liegen. Um genauer zu analysieren, welches Defektverhalten die untersuchten B2-Phasen zeigen, wurde von REN UND OTSUKA [40] ein Dreidefekttyp-Modell vorgeschlagen. Dieses Modell ist als direkte Erweiterung des Tripel-Defekt-Modells zu sehen, da zu den bereits im Tripel-Defekt-Modell berücksichtigten Leerstellen im Übergangsmetall-Untergitter und den Antistrukturato-

men im Al-Untergitter zusätzlich Antistrukturatome im Übergangsmetall-Untergitter berücksichtigt werden. Durch den Einbau dieser Defekte kann ein Absinken der Leerstellenkonzentration unter den für konstitutionelle Leerstellen erforderlichen Grenzwert erklärt werden. Die Anwendung des Modells auf die von der japanischen Gruppe gemessenen Leerstellenkonzentrationen erbrachte das Resultat, daß sämtliche gemessenen Leerstellenkonzentrationen als Funktion der Zusammensetzung mit dem Dreidefekttyp-Modell erklärt werden können. Die Extrapolation der Leerstellenverläufe als Funktion der Temperatur ergibt mit den aus den Anpassungen erhaltenen Modellparametern ein überraschendes Ergebnis. Sämtliche untersuchten intermetallischen B2-Phasen enthalten bei niedrigen (absoluten) Temperaturen keine Leerstellen, sondern nur Antistrukturdefekte. Die Existenz von konstitutionellen Leerstellen wurde somit in Frage gestellt.

Die Beschreibung von thermodynamischen Daten der B2-Phasen NiAl und B2-CoAl war mit dem Tripel-Defekt-Modell möglich. Es stellte sich daher die Frage, ob die für die Anpassung und die Bestimmung der Modellparameter benutzten experimentellen Daten zu ungenau sind, um den genauen Defekttyp einer intermetallischen Phase mit einem Bragg-Williams-Modell zu beschreiben, oder ob die experimentellen Daten der japanischen Gruppe möglicherweise in Widerspruch zu den thermodynamischen Daten stehen. Als Beispiel wurde die Phase B2-NiAl gewählt, da diese einen ausgedehnteren Homogenitätsbereich zu beiden Seiten der stöchiometrischen Zusammensetzung zeigt als B2-CoAl. Zunächst wurde der von REN UND OTSUKA begangene Weg jedoch wiederholt: die vom Tripel-Defekt-Modell abweichenden experimentellen Daten der Leerstellenkonzentration wurden mit dem Dreidefekttyp-Modell angepaßt (siehe Abbildung 3.1). Dabei zeigte sich, daß das Ergebnis der Fitprozedur von der Art der numerischen Berechnung innerhalb der Routine abhängt (genaue Angaben hierzu finden sich im Anhang von Kapitel 3). Es konnten Parametersätze gefunden werden, die einerseits die Leerstellenkonzentrationsdaten als Funktion der Zusammensetzung ebenso gut beschreiben wie die in [40] angegebenen. Andererseits steht der mit diesen Parametern berechnete Temperaturverlauf der Leerstellenkonzentration im Gegensatz zu dem von REN UND OTSUKA gefundenen Verlauf. Sind die in dieser Arbeit gefundenen Parameter (und das verwendete Dreidefekttyp-Modell) als richtig anzusehen, gibt es in der B2-Phase konstitutionelle Leerstellen, die in geringer Anzahl ebenfalls vorhandenen konstitutionellen Antistrukturatome überwiegen.

Es stellte sich heraus, daß die aus der Anpassung an Leerstellenkonzentrationen erhaltenen Parameter aus zwei Gründen nicht direkt für die Beschreibung von thermodynamischen Daten (Aktivitäten und Bildungsenthalpien) verwendet werden können: erstens werden für die Beschreibung der Leerstellenkonzentrationen nur Kombinationen der für die Beschreibung der thermodynamischen Daten notwendigen Enthalpieparameter verwendet und zweitens sind für die Beschreibung der thermodynamischen Aktivitäten unbedingt Entropieparameter erforderlich, die im Modell von REN UND OTSUKA nicht enthalten sind.

Die simultane Anpassung der thermodynamischen Aktivität und der Bildungsenthalpie mit dem Dreidefekttyp-Modell erbrachte eine gute Beschreibung. Die Beschreibung



derselben Daten mit dem einfacheren Tripeldefekt-Modell ist jedoch von gleich guter Qualität. Benutzt man die nach dem Dreidefekttyp-Modell erhaltenen Parameter für die Berechnung der Leerstellenkonzentration, ergibt sich, daß der Leerstellenkonzentrationsverlauf als Funktion der Zusammensetzung sehr gut zu allen experimentellen Daten (sowohl denen nach [32] als auch denen anderer Experimentatoren) paßt (siehe Abb. 3.4), der Leerstellenkonzentrationsverlauf als Funktion der Temperatur jedoch nicht zu dem Ergebnis von [40] führt, sondern entweder Tripel-Defekt-Verhalten oder einen kontinuierlichen Abfall mit sinkender Temperatur zeigt, in Abhängigkeit von der für die Anpassung und die Berechnung gewählte numerische Routine (siehe Abb. 3.5). Benutzt man für eine simultane Anpassung sämtliche vorhandenen Daten (Leerstellenkonzentration als Funktion der Zusammensetzung und der Temperatur, thermodynamische Aktivitätsdaten und Bildungsenthalpien) - mit Ausnahme der Daten aus [57] - ergibt sich eine konsistente Beschreibung mit dem Tripel-Defekt-Modell. Die Daten aus [57] erscheinen als die einzige Ausnahme.

In Kapitel 4 dieser Arbeit wird ein Modell für ternäre geordnete Phasen  $(A,C)_mB_n$  vorgestellt. Es werden alle vier möglichen Punktdefekttypen berücksichtigt und das Modell kann auf Daten von Phasen mit unterschiedlicher Kristallstruktur angewendet werden. Es handelt sich um eine allgemeine Methode, die die bereits behandelten Tripel-Defekt- und Dreidefekttyp-Modelle binärer bzw. ternärer B2-Phasen als Spezialfälle enthält.

Es wird gezeigt, daß mit ausreichend genauen experimentellen thermodynamischen Daten (thermodynamische Aktivität und Bildungsenthalpie als Funktion der Zusammensetzung und, falls vorhanden, der Temperatur) die Modellparameter für die Enthalpie- und Entropie-Wechselwirkungsterme von Atompaaaren bestimmt werden können. Dies wird am Beispiel  $B2-Ni_{1-x}Al_x$  und  $B2-(Ni,Co)_{1-x}Al_x$  demonstriert. Im Falle von  $B2-Fe_{1-x}Al_x$  ergeben sich Schwierigkeiten in der Anpassung der Modellparameter, da diese Phase nur zu einer Seite der stöchiometrischen Zusammensetzung existiert. In einem solchen Fall sind mit den vorgeschlagenen Bragg-Williams-Modellen keine eindeutigen Aussagen bzgl. der Defektstruktur zu erreichen.

Die in dieser Arbeit verwendeten Modelle vom Bragg-Williams Typ basieren auf Parametern, die keine wohldefinierte physikalische Bedeutung haben. Es werden Mittelungen über alle Paarwechselwirkungen vorgenommen, da nur die Wechselwirkungen zwischen Atomen in nächster und übernächster Nachbarschaft berücksichtigt werden. Diese Mittelung ist aber auch gleichzeitig ein Vorteil gegenüber Methoden, die mit physikalisch besser definierten Parametern arbeiten (z.B. ab initio Ansatz). Für die Anwendung dieser Methoden ist eine statistische Verteilung der Defekte nötig. Wenn die Defektdichte in einer Phase zu hoch ist, um noch von einer statistischen Verteilung ausgehen zu können, kann eine Beschreibung mit der Bragg-Williams-Methode noch sinnvolle Ergebnisse bringen. Bei Berechnungen im Rahmen der großkanonischen Gesamtheit werden andere Parameter als die im Bragg-Williams-Modell verwendeten benutzt. Man betrachtet hier die Energieunterschiede zwischen dem perfekten Kristallgitter ohne jeden Defekt und dem Gitter mit einem eingebauten Defekt. Diese Energiedifferenzen können mit der ab-initio-elektronentheoretischen

Berechnung bestimmt werden. Dabei hat man mit dem Problem des absoluten Energieniveaus zu kämpfen, das im Rahmen von Bragg-Williams-Modellen nicht auftritt. Ein Energieniveauprobem tritt auch bei statistisch-thermodynamischen Modellen auf, die die Wagner-Schottky Näherung benutzen. Die Parameter sind ähnlich definiert wie in der großkanonischen Gesamtheit, werden jedoch nicht ab-initio berechnet, sondern aus Anpassungen an experimentelle Größen bestimmt. Deshalb können bei der Verwendung von Wagner-Schottky-Modellen nur Größen bezogen auf ihren Wert bei der stöchiometrischen Zusammensetzung verwendet werden (eine detailliertere Analyse findet sich in Kapitel 4.4). Ein Vergleich der mit den verschiedenen Methoden erzielten Ergebnisse ist möglich, wenn man nicht die individuellen Parameter, sondern Parameter höherer Ordnung betrachtet, wie z.B. die berechneten effektiven Bildungsenthalpien von Leerstellen (s.o.).

Der Formalismus der Bragg-Williams-Modelle ist eine einfach anzuwendende Methode, um zu konsistenten Beschreibungen von wichtigen Eigenschaften geordneter intermetallischer Phasen zu gelangen. Es erscheint- wie gezeigt wird- bei angemessener Anwendung auf ausreichend viele und genaue Eingangsdaten sogar möglich, zu Vorhersagen bzgl. nicht gemessener experimenteller Daten zu gelangen.

## Experimentelles

Die für die Modellanpassungen nötigen thermodynamischen Eingangsdaten müssen sehr präzise bestimmt werden. Im Rahmen der vorliegenden Arbeit wurden deshalb die in der Literatur nicht bzw. nicht mit der nötigen Genauigkeit vorhandenen Bildungsenthalpieverläufe in B2-FeAl und B2-(Fe,Ni)Al bestimmt (siehe Kapitel 5 dieser Arbeit). Dazu wurde ein isoperibol arbeitendes Differential-Lösungskalorimeter verwendet [11, 16]. Das Kalorimeter arbeitet bei einer konstanten Umgebungstemperatur (hier: 1073 K) und einer variablen Meßsystemtemperatur. Die Differentialanordnung der in den Meßsystemen eingebauten Thermoelemente (Zwillingsprinzip) bewirkt eine sehr hohe Meßgenauigkeit. Das Differential-Lösungskalorimeter besteht aus vier gleichartigen einzelnen Meßsystemen (Kalorimetern), die in einem großen zylinderförmigen Block aus Nickel angeordnet sind. Jedes einzelne Kalorimeter enthält einen Keramik( $\text{Al}_2\text{O}_3$ )-Tiegel, in dem sich das flüssige Lösungsmittel (hier: Aluminium) befindet. Die Proben sind an dünnen Keramikrührern montiert, die nacheinander in je ein Kalorimeter abgesenkt werden. Die dabei auftretenden Wärmetönungen werden als Temperaturdifferenz-Zeit-Profile zwischen jeweils benachbarten Kalorimetern registriert. Die von den registrierten Kurven beschriebenen Flächen werden mit einer Kalibrierung in Energien umgerechnet. Dazu werden mittels elektrischer Widerstandsheizung Kalibriermessungen durchgeführt, bei der in einer registrierten Zeit eine bekannte Energiemenge dem einzelnen Kalorimeter zugeführt wird. Aufgrund der Anordnung der Kalorimeter wird jede Messung zweimal registriert- die erhaltenen Ergebnisse der einzelnen Messungen sind arithmetische Mittelwerte.

Für die Genauigkeit der Messungen ist die Konstanz der Kalorimeterblock-Temperatur

von entscheidender Bedeutung. Um diese zu gewährleisten, ist das Kalorimeter mit aufwendigen Temperaturreglern ausgestattet, die in insgesamt sechs individuelle, aufeinander abgestimmte Systeme aufgeteilt sind.

Die in dieser Arbeit unternommenen Messungen wurden unter dynamischem Vakuum ( $< 10^{-2}$  Pa) bei einer konstanten Temperatur von 1073 K durchgeführt. Die relative Stabilität der Blocktemperatur lag bei  $\pm 10^{-3}$  K/Tag. Die Bildungsenthalpien konnten mit einer Genauigkeit in der Größenordnung von 1% gemessen werden.

Die Bildungsenthalpie einer festen  $A_{1-x}B_x$ -Legierung,  $\Delta H_{A_{1-x}B_x}$ , aus den festen Elementen A und B ist gegeben durch

$$\Delta H_{A_{1-x}B_x} = (1-x)\Delta H_{L,A}^0 + x\Delta H_{L,B}^0 - \Delta H_{L,A_{1-x}B_x}^0, \quad (6.5)$$

wobei  $\Delta H_{L,i}^0$  ( $i=A,B,A_{1-x}B_x$ ) die Lösungsenthalpien der Elemente A und B bzw. der Legierung  $A_{1-x}B_x$  bei unendlicher Verdünnung bedeuten. In der vorliegenden Arbeit wurde für die experimentelle Bestimmung der Bildungsenthalpien in den Systemen Fe-Al und Fe-Ni-Al Aluminium als Lösungsmittel eingesetzt, so daß die Lösungsenthalpie dieses Elements keine Berücksichtigung findet, wenn man die Bildungsenthalpien bezogen auf flüssiges Aluminium angibt.

Die Ergebnisse der Messungen sind für B2-Fe $_{1-x}$ Al $_x$  in Tabelle 5.3 zusammengestellt und in Abbildung 6.2 im Vergleich mit Bildungsenthalpiendaten von B2-CoAl und B2-NiAl dargestellt.

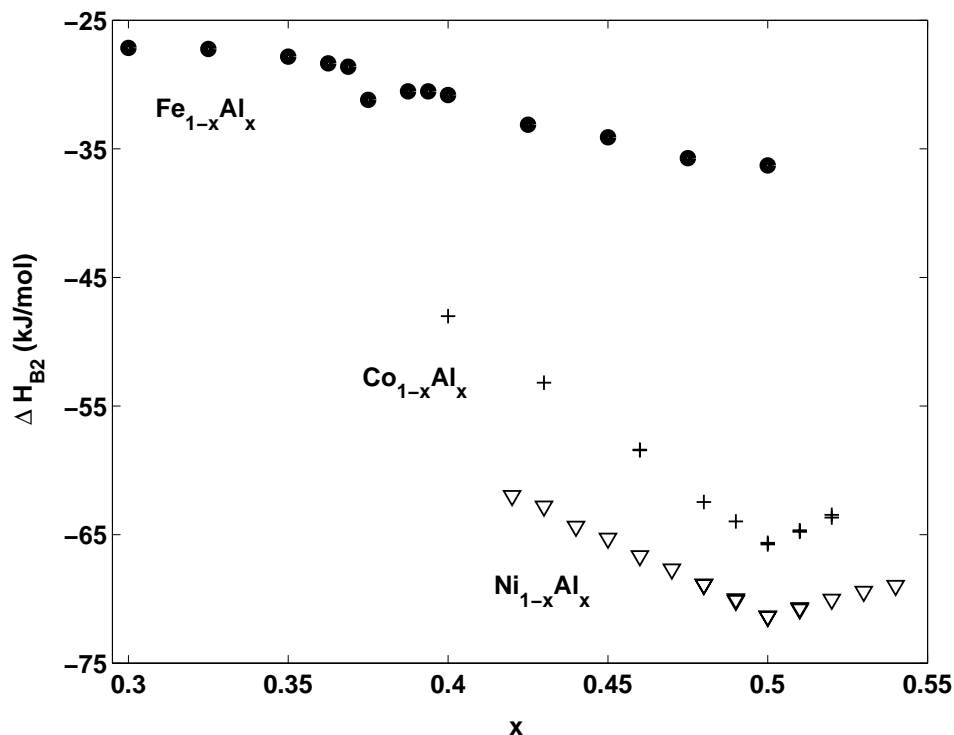


Abbildung 6.2: Bildungsenthalpien binärer Aluminide, im jeweiligen Homogenitätsbereich der B2-Phasen, als Funktion des Molenbruchs, bezogen auf festes Fe, Co und Ni und flüssiges Al: ● Ergebnisse der vorliegenden Arbeit für B2-Fe<sub>1-x</sub>Al<sub>x</sub> ( $T = 1073\text{ K}$ ), + Ergebnisse nach [13] für B2-Co<sub>1-x</sub>Al<sub>x</sub> ( $T = 1100\text{ K}$ ), ▽ Ergebnisse nach [11] für B2-Ni<sub>1-x</sub>Al<sub>x</sub> ( $T = 1100\text{ K}$ ).

Die Bildungsenthalpiendaten von B2-FeAl weisen die geringsten Absolutwerte der drei gezeigten Phasen auf. Dabei ist der Wert der stöchiometrischen Verbindung Fe<sub>0,50</sub>Al<sub>0,50</sub> mit  $-36,29 \pm 0,32\text{ kJ/mol}$  der größte exotherme Wert für B2-FeAl. Mit abnehmendem Al-Gehalt werden die Bildungsenthalpienwerte von B2-FeAl weniger negativ. Auffallend ist, daß bei etwa 38 at.% eine Diskontinuität im Bildungsenthalpienverlauf als Funktion der Zusammensetzung gemessen wurde. Einen solchen Bruch im Bildungsenthalpie-Zusammensetzungsverlauf findet sich bei B2-CoAl und B2-NiAl nicht. Die Ursache des abweichenden Verhaltens von B2-FeAl ist z.Zt. nicht geklärt. Möglicherweise deutet sich durch die Diskontinuität eine im Phasendiagramm nach [70] notierte Unterteilung des zur Fe-reichen Seite ausgedehnten Homogenitätsbereichs von B2-FeAl an.

Die experimentell ermittelten Bildungsenthalpiendaten für B2-(Fe,Ni)<sub>1-x</sub>Al<sub>x</sub> sind in Tabelle 5.4 aufgelistet und in Abbildung 6.3 gezeigt.

Ersetzt man ausgehend von binärem B2-Fe<sub>1-x</sub>Al<sub>x</sub> Eisen durch Nickel bei konstan-

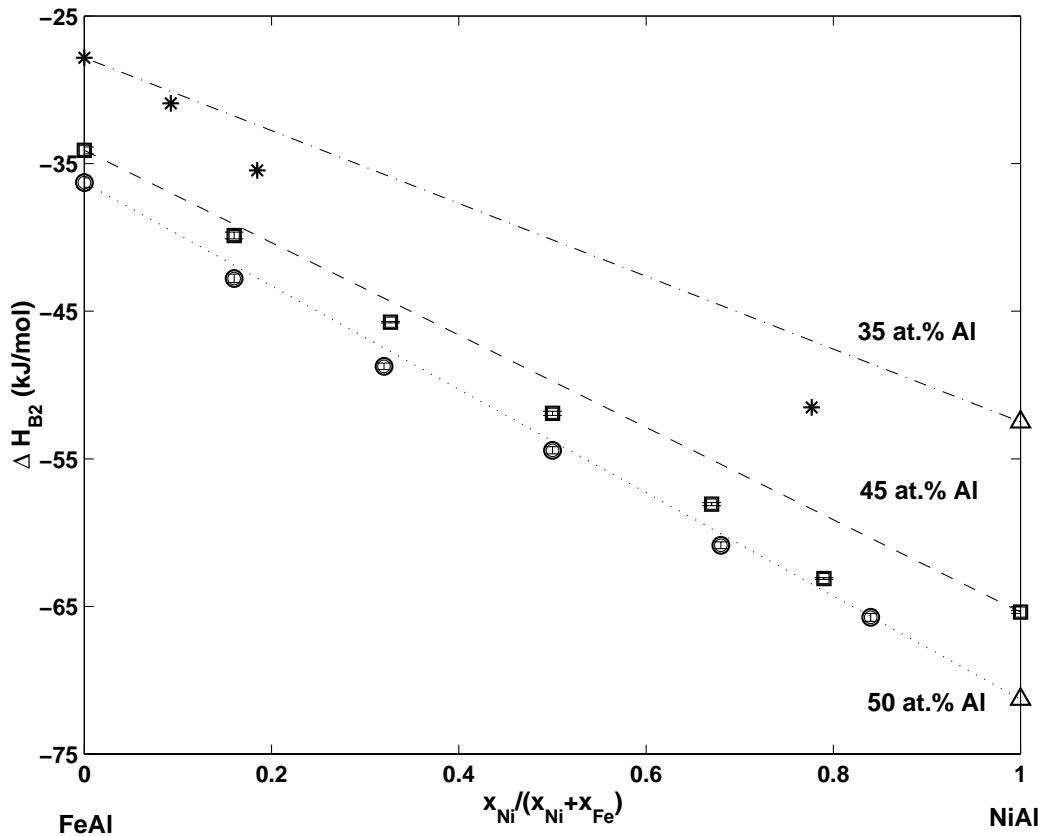


Abbildung 6.3: Bildungsenthalpie von festem B2-(Fe,Ni)<sub>1-x</sub>Al<sub>x</sub> als Funktion des relativen Ni-Gehaltes, bezogen auf festes Ni und Al und flüssiges Al ( $x_{Ni}$  und  $x_{Fe}$  bedeuten die Molenbrüche von Ni und Fe, für verschiedene Molenbrüche von Al;  $x = 0.50$ : ○, ...;  $x = 0.45$ : □, ---;  $x = 0.35$ : \*, -.-.-; △ repräsentiert Daten nach [16] ( $x = 0.50$ ) und Daten extrapoliert nach Daten von [11] ( $x = 0.35$ ). Die Fehlerbalken liegen im Bereich der verwendeten Symbole. Die eingezeichneten Kurven markieren das mechanische Gemenge der beiden binären Randphasen.

tem Aluminiumgehalt, wird der Wert der Bildungsenthalpie exothermer. Hält man den (Fe,Ni)-Gehalt konstant werden die Bildungsenthalpiewerte mit abnehmendem Al-Gehalt weniger exotherm. Die Abweichungen vom mechanischen Gemenge der binären Randphasen B2-NiAl und B2-FeAl sind für alle untersuchten ternären Phasen negativ und sind am ausgeprägtesten, je weniger Aluminium in den Legierungen vorhanden ist.



# References

- [1] Y.A. Chang. *Thermodynamics and lattice disorder in binary ordered intermetallic phases*. In H. Herman, editor, *Treatise on Materials Science and Technology*, volume 4, 173–259. Academic Press, New York and London, 1974.
- [2] R.J. Wasilewski. *Structure defects in CsCl intermetallic compounds-I. Theory*. J. Phys. Chem. Solids, 29:39–49, 1968.
- [3] J. Mayer and M. Fähnle. *On the meaning of effective formation energies, entropies and volumes for atomic defects in ordered compounds*. Acta Mater., 45(5):2207–2211, 1997.
- [4] C. Wagner and W. Schottky. *Theorie der geordneten Mischphasen*. Z. Physik. Chem., 11:163–209, 1931.
- [5] W.L. Bragg and E.J. Williams. *The effect of thermal agitation on atomic arrangement in alloys*. Proc. R. Soc., A 145:699–730, 1934.
- [6] J. Mayer, C. Elsässer, and M. Fähnle. *Concentrations of atomic defects in B2- $Fe_xAl_{1-x}$  - an ab-initio study*. Phys. Stat. Sol., B 191(2):283–298, 1995.
- [7] Y.A. Chang and J.P. Neumann. *Thermodynamics and defect structure of intermetallic phases with the B2 (CsCl) structure*. Progress in Solid State Chemistry, 14:221–301, 1982.
- [8] C. Wagner. *Thermodynamics of Alloys*. Addison-Wesley Press, Inc., 1952.
- [9] J.P. Neumann. *On the occurrence of substitutional and triple defects in intermetallic phases with B2 structure*. Acta Metall., 28:1165–1170, 1980.
- [10] J.H. Westbrook and R.L. Fleischer. *Intermetallic Compounds: Principles and Practice*. Wiley, New York, 1995.

- [11] E.-T. Henig and H.L. Lukas. *Kalorimetrische Bestimmung der Bildungsenthalpie und die Beschreibung der Fehlordnung der geordneten  $\beta$ -Phase (Ni,Cu)Al*. Z. Metallkd., 66(2):98–108, 1975.
- [12] A. Steiner and K.L. Komarek. *Thermodynamic activities of solid nickel-aluminium alloys*. Trans. TMS-AIME, 230:786–790, 1964.
- [13] E.-T. Henig, H.L. Lukas and G. Petzow. *Enthalpy of formation and description of the defect structure of the ordered  $\beta$ -phase in Co-Al*. Z. Metallkd., 71(6):398–402, 1980.
- [14] M. Ettenberg, K.L. Komarek and E. Miller. *Thermodynamic properties and ordering in CoAl*. Trans. TMS-AIME, 242:1802–1807, 1968.
- [15] J.P. Neumann, Y.A. Chang and C.M. Lee. *Thermodynamics of intermetallic phases with the triple-defect B2 structure*. Acta Metall., 24(7):593–604, 1976.
- [16] A. Grün, E.-T. Henig and F. Sommer. *Calorimetric determination of the enthalpy of formation and the description of the constitutional defects of the ordered (Ni,Co)<sub>(1-y)</sub>Al<sub>y</sub> phase*. Z. Metallkd., 89(9):591–597, 1998.
- [17] H. Ipsen, D.-C. Hu and Y.A. Chang. *Thermodynamic properties of ternary B2-phases with triple-defects I: Theoretical model*. Z. Metallkd., 78(2):131–136, 1987.
- [18] R. Krachler and H. Ipsen. *Application of the grand canonical ensemble to the study of equilibrium point defect concentrations in binary intermetallic phases with the B2-structure*. Intermetallics, 7(2):141–151, 1999.
- [19] M. Fähnle, G. Bester and B. Meyer. *On the meaning of effective formation entropies for atomic defects in ordered compounds*. Scr. Mater., 39(8):1071–1075, 1998.
- [20] C.R. Kao, L.M. Pike, S.L. Chen and Y.A. Chang. *Site preference of substitutional additions to triple-defect B2 intermetallic compounds*. Intermetallics, 2(4):235–247, 1994.
- [21] O.A. Bannykh, K.B. Povarova, V.V. Sumin, N.K. Kazanskaya, N.V. Fadeeva and M.D. Bespalova. *Neutron-diffraction study of atomic ordering in the alloys of pseudobinary section of NiAl- FeAl and NiAl- CoAl systems*. Russ. Metall., (3):64–68, 1995.
- [22] A.T. Dinsdale. *SGTE data for pure elements*. Calphad, 15(4):317–425, 1991.
- [23] A. Grün. *Kalorimetrische Untersuchung der Bildungsenthalpie von Überstrukturphasen in den Systemen Nickel-Aluminium-Eisen und Nickel-Aluminium-Kobalt*. Ph.D. thesis, University of Stuttgart, 1996.



- [24] L. Perring, J.J. Kuntz, F. Bussy and J.C. Gachon. *Heat capacity measurements on the equiatomic compounds in Ni-X (X =Al, In, Si, Ge and Bi) and M-Sb (with M = Ni, Co and Fe) systems*. Intermetallics, 7(11):1235–1239, 1999.
- [25] W.H. Press, B.P. Flannery, S.A. Teucholsky and W.T. Vetterling. *Numerical Recipes*. Cambridge University Press, Cambridge, 1986.
- [26] T. Gödecke, M. Scheffer, R. Lück, S. Ritsch and C. Beeli. *Isothermal sections of phase equilibria in the Al-AlCo-AlNi system*. Z. Metallkd., 89(10):687–698, 1998.
- [27] H. Xiao and I. Baker. *Long-range order and defect concentrations in NiAl and CoAl*. Acta Metall., 42(5):1535–1540, 1994.
- [28] X. B. Ren, K. Otsuka, and M. Kogachi. *Do "constitutional vacancies" in intermetallic compounds exist?* Scr. Mater., 41(9):907–913, 1999.
- [29] J. Breuer, F. Sommer and E.J. Mittemeijer. *Thermodynamics of B2 intermetallic compounds with triple defects: a Bragg-Williams model for (Ni,Co)Al*. Met. & Mat. Trans. A, in press, chapter 2 of this thesis.
- [30] L.M. Pike, Y.A. Chang and C.T. Liu. *Solid-solution hardening and softening by Fe additions to NiAl*. Acta Metall., 5:601–608, 1997.
- [31] F. Zobel. *Thermische Fehlordnung der intermetallischen Phasen  $\gamma'$ -Ni<sub>3</sub>Al und  $\beta'$ -NiAl*. Ph.D. thesis, TU Berlin, 1994.
- [32] M. Kogachi, T. Tanahashi, Y. Shirai and M. Yamaguchi. *Determination of vacancy concentration and defect structure in the B2 type NiAl  $\beta$ -phase alloys*. Scr. Mater., 34(2):243–248, 1996.
- [33] H. E. Schaefer, K. Frenner and R. Würschum. *High-temperature atomic defect properties and diffusion processes in intermetallic compounds*. Intermetallics, 7(3-4):277–287, 1999.
- [34] M. Kogachi and T. Tanahashi. *Point defect behavior in the B2 type intermetallic compounds CoAl*. Scr. Mater., 35(7):849–854, 1996.
- [35] E. Wachtel, V. Linse and V. Gerold. *Defect structure and magnetic-moments in beta-phases of CoAl and CoGa*. J. Phys. Chem. Solids, 34(9):1461–1466, 1973.
- [36] B. Meyer and M. Fähnle. *Atomic defects in the ordered compound B2-NiAl: A combination of ab initio electron theory and statistical mechanics*. Phys. Rev., B 59(9):6072–6082, 1999.
- [37] G. Bester, B. Meyer and M. Fähnle. *Atomic defects in the ordered compound B2-CoAl: A combination of ab initio electron theory and statistical mechanics*. Phys. Rev., B 60(21):14492–14495, 1999.

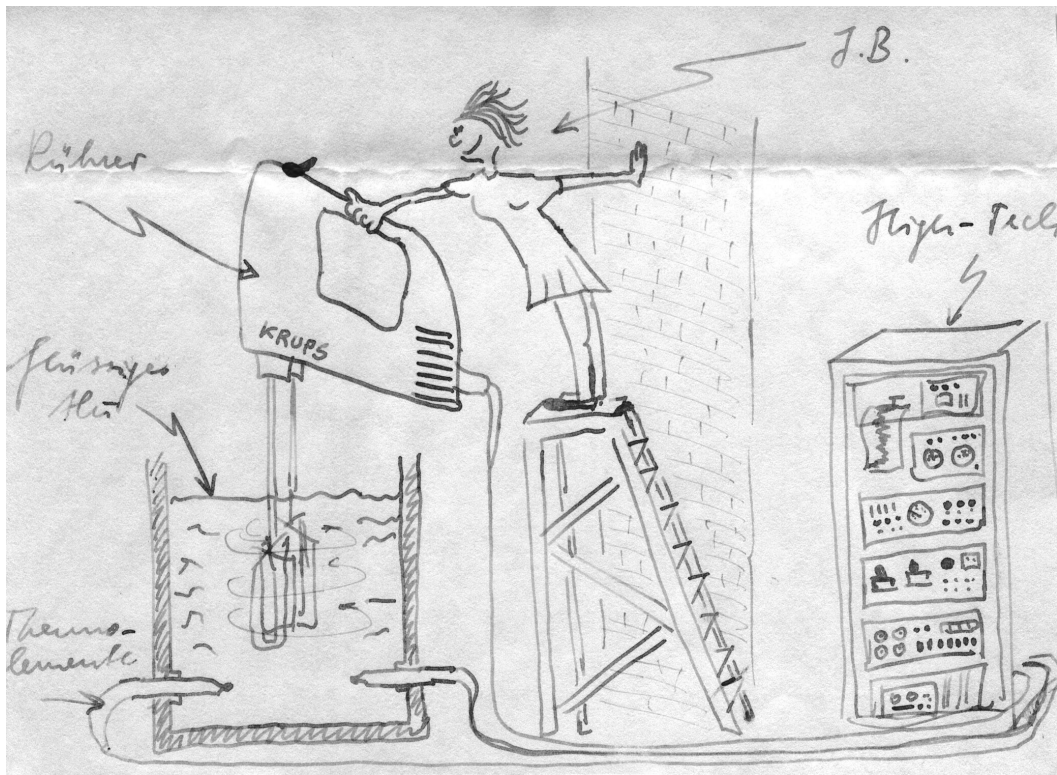
- [38] V. Schott and M. Fähnle. *Concentration of atomic defects in ordered compounds: Canonical and grandcanonical formalism*. Phys. Stat. Sol., B 204(2):617–624, 1997.
- [39] R. Krachler, H. Ipser and K.L. Komarek. *Thermodynamics of intermetallic B2-phases - a generalized-model*. J. Phys. Chem. Solids, 50(11):1127–1135, 1989.
- [40] X.B. Ren and K. Otsuka. *A unified model for point-defect formation in B2 intermetallic compounds*. Phil. Mag., A 80(2):467–491, 2000.
- [41] B. Meyer and M. Fähnle. *Master equations for the concentrations of atomic defects in B2 compounds*. To be published, 2001.
- [42] M. Kogachi, Y. Takeda and T. Tanahashi. *Defect structure in Al-rich composition region in the  $\beta$ -NiAl intermetallic compound phase*. Intermetallics, 3(2):129–136, 1995.
- [43] E.W. Weisstein. *Descartes' sign rule*. Eric Weisstein's World of Mathematics, <http://mathworld.wolfram.com/DescartesSignRule.html>, 20. Sept. 2000.
- [44] *Matlab*. Registered trademark of The MathWorks Inc., 3 Apple Hill Drive, Natick, MA 01760, USA.
- [45] *Maple*. Registered trademark of Waterloo Maple Inc., 57 Erb Street W., Waterloo, Ontario, Canada N2L 6C2.
- [46] A. Seeger. *The study of point defects in metals in thermal equilibrium*. Crystal lattice defects, 4:221–253, 1973.
- [47] R.O. Simmons and R.W. Balluffi. *Measurements of equilibrium vacancy concentrations in aluminum*. Phys. Rev., 117:52–61, 1960.
- [48] R. Kerl, J. Wolff and T. Hehenkamp. *Equilibrium vacancy concentrations in FeAl and FeSi investigated with an absolute technique*. Intermetallics, 7(3-4):301–308, 1999.
- [49] R. Würschum, K. Badura-Gergen, E. A. Kümmerle, C. Grupp and H. E. Schaefer. *Characterization of radiation-induced lattice vacancies in intermetallic compounds by means of positron-lifetime studies*. Phys. Rev., B 54(2):849–856, 1996.
- [50] D. Paris and P. Lesbats. *Vacancies in Fe-Al alloys*. J. Nucl. Mater., 69-7(1-2):628–632, 1978.
- [51] G. Vogl and B. Sepiol. *Elementary diffusion jump of iron atoms in intermetallic phases studied by Mössbauer-spectroscopy .I. Fe-Al close to equiatomic stoichiometry*. Acta Metall. Mater., 42(9):3175–3181, 1994.

- [52] R. Krachler, H. Ipser, B. Sepiol and G. Vogl. *Diffusion mechanism and defect concentrations in  $\beta'$ -FeAl, an intermetallic compound with B2 structure*. Intermetallics, 3(1):83–88, 1995.
- [53] J. Breuer, F. Sommer, and E.J. Mittemeijer. *Thermodynamics of constitutional and thermal point defects in B2-Ni<sub>1-x</sub>Al<sub>x</sub>*. Phil. Mag. A, accepted for publication, chapter 3 of this thesis.
- [54] F. Ducastelle. *Order and phase stability in alloys*. volume 3, *Cohesion and structure*. North-Holland, Amsterdam, 1991.
- [55] S.L. Chen, C.R. Kao and Y.A. Chang. *A generalized quasi-chemical model for ordered multicomponent, multi-sublattice intermetallic compounds with anti structure defects*. Intermetallics, 3(3):233–242, 1995.
- [56] A.J. Bradley and A. Taylor. *An X-ray analysis of the nickel-aluminium system*. Proc. R. Soc., A(159):56–72, 1937.
- [57] M. Kogachi and T. Tanahashi. *Point defect behavior in the B2 type intermetallic compound CoAl*. Scr. Mater., 35(7):849–854, 1996.
- [58] B. Meyer and M. Fähnle. *Atomic defects in the ordered compound B2-NiAl: A combination of ab initio electron theory and statistical mechanics*. Phys. Rev., B 59(9):6072–6082, 1999.
- [59] T.B. Massalski. *Binary Alloy Phase Diagrams 2*. American Society for Metals, Ohio, 1986.
- [60] Y.A. Chang, L.M. Pike, C.T. Liu, A.R. Bilbrey and D.S. Stone. *Correlation of the hardness and vacancy concentration in FeAl*. Intermetallics, 1(2):107–115, 1993.
- [61] J. Breuer, A. Grün, F. Sommer and E.J. Mittemeijer. *Enthalpy of formation of B2-Fe<sub>1-x</sub>Al<sub>x</sub> and B2-(Fe,Ni)<sub>1-x</sub>Al<sub>x</sub>*. Met. & Mat. Trans. B, in press, chapter 5 of this thesis.
- [62] J. Eldridge and K.L. Komarek. *Thermodynamic properties of solid iron-aluminum alloys*. Trans. Met. Soc.-AIME, 230(1):226, 1964.
- [63] M. Kogachi and T. Haraguchi. *Quenched-in vacancies in B2-structured intermetallic compound FeAl*. Mater. Sci. Eng., A 230:124–131, 1997.
- [64] H.D. Dannöhl and H.L. Lukas. *Calorimetric determination of enthalpies of formation of some intermetallic compounds*. Z. Metallkd., 65(10):642–649, 1974.
- [65] A.A. Zubkov. *Dissolution enthalpies of 3d transition metals in liquid aluminium*. J. Chem. Therm., 26:1267–1274, 1994.

- [66] J.C. Mathieu, B. Jounel, P. Desré and E. Bonnier. Chaleurs de dissolution de l'étain, de l'argent, du silicium et du fer dans l'aluminium liquide. In: *Thermodynamics of Nuclear Materials*, 767–773, Wien, 1967.
- [67] M.P. Antony, R. Babu, C.K. Mathews and U.V. Varada Raju. *Enthalpies of formation of UNi<sub>5</sub>, UNi<sub>2</sub> and UFe<sub>2</sub> by solution calorimetry*. *J. Nucl. Mater.*, 223:213–217, 1995.
- [68] J.J. Lee and F. Sommer. *The determination of the partial enthalpies of mixing of aluminum-rich alloy melts by solution calorimetry*. *Z. Metallkd.*, 76(11):750–754, 1985.
- [69] M.S. Petrushevskiy, Y.O. Esin, P.V. Gel'd and V.M. Sandakov. *Concentration-dependence of enthalpy of formation of liquid iron-aluminium alloys*. *Russ. Metall.*, (6):149–153, 1972.
- [70] O. Kubaschewski. *Iron- Binary Phase Diagrams*. Springer-Verlag, Berlin, Heidelberg, New York, 1982.
- [71] W. Köster and T. Gödecke. *Physical measurements on iron-aluminum-alloys between 10 and 50 at percent Al. 1. Confirmation of and additional contribution to the iron-aluminum phase-diagram*. *Z. Metallkd.*, 71(12):765–769, 1980.
- [72] G. Petzow and G. Effenberg. *Ternary Alloys*. VCH Verlagsgesellschaft, volume 5, Weinheim, 1992.

# *Curriculum Vitae*

Name	Jutta Breuer
Date of birth	January 28, 1973
Place of birth	Münster (Westf.)
School	1979 - 1983 Bonhoeffer-Grundschule in Senden
	1983 - 1989 Marienschule in Münster
	1989 - 1990 Topeka High School in Topeka, Kansas, USA
	1990 - 1992 Marienschule in Münster
Higher education	1992 - 1997 Physics at Westfälische Wilhelms-Universität, Münster Degree dissertation: " <i>Investigations on volume diffusion in the intermetallic compound <math>Ti_3Al</math></i> "
	since 1998 PhD at Max-Planck-Institut für Metallforschung and Institut für Metallkunde of Stuttgart university, Stuttgart



Die vorliegende Arbeit wurde am Institut für Metallkunde der Universität Stuttgart und am Max-Planck-Institut für Metallforschung, Stuttgart, angefertigt.

Mein besonderer Dank gilt Herrn Prof. Dr. Ir. E.J. Mittemeijer für die ausgezeichnete Betreuung und das große Interesse am Fortgang der Arbeit. Seine unermüdliche Bereitschaft zum Diskutieren und zum Redigieren von Manuskripten war eine äußerst wertvolle Hilfe.

Bei Herrn Prof. Dr. H.-E. Schaefer vom Institut für Theoretische und Angewandte Physik der Universität Stuttgart bedanke ich mich für hilfreiche Diskussionen und für die Übernahme des Mitberichts dieser Arbeit.

Sehr herzlich danke ich Herrn Prof. Dr. F. Sommer. Seine nie endende Hilfsbereitschaft und seine Beiträge zu einer sehr angenehmen Arbeitsatmosphäre waren einmalig.

Ik wil mijn collega Ir. A. Kempen allerhartelijkst bedanken voor alle, zeer welkome hulp met modelleer- en programmeerproblemen. Het heeft met hem dikwijls "zonnestralen geregend" in onze kamer. Dank je wel, Antoine!

Den Mitarbeitern des Max-Planck-Institutes für Metallforschung und des Instituts für Metallkunde der Universität danke ich für die hilfreiche Zusammenarbeit. Für die gute Kameradschaft bedanke ich mich besonders bei allen Doktoranden und Postdocs der Abteilung Mittemeijer.

Mein innigster Dank gilt nicht zuletzt meinen Eltern.